BIOENGINEERED MESENCHYMAL CELL SHEETS AS AN ALTERNATE TO LIMBAL STEM CELLS FOR OCULAR SURFACE RECONSTRUCTION

A THESIS PRESENTED BY
BALU V GOPAL

TO

THE SREE CHITRA TIRUNAL INSTITUTE FOR MEDICAL SCIENCES AND TECHNOLOGY, TRIVANDRUM
Thiruvananthapuram

IN PARTIAL FULFILMENT OF THE REQUIREMENTS
FOR THE AWARD OF
DOCTOR OF PHILOSOPHY

2018

CERTIFICATE

I, Balu .V. Gopal, hereby certify that I had personally carried out the work depicted in the thesis entitled, "Bioengineered Mesenchymal Cell Sheet as an alternate to Limbal Stem Cells for Ocular Surface Reconstruction", except where external help is sought, it is duly acknowledged. No part of the thesis has been submitted for the award of any other degree or diploma prior to this date.

Signature :

Name : Balu V Gopal

Reg. No : 2014/PhD/09

Date: 07/02/2018

SREE CHITRA TIRUNAL INSTITUTE FOR MEDICAL SCIENCES & TECHNOLOGY, TRIVANDRUM
Thiruvananthapuram – 695011, INDIA
(An Institute of National Importance under Govt.of India)

Dr. T.V. Kumary
Scientist G, Division of Tissue Culture
Department of Applied Biology,
BMT wing, SCTIMST, Trivandrum.

This is to certify that **Mr. Balu .V. Gopal**, in the division of Tissue Culture, of this Institute has fulfilled the requirements prescribed for the Ph. D. degree of the Sree Chitra Tirunal Institute for Medical Sciences and Technology, Trivandrum. The thesis entitled, "Bioengineered mesenchymal cell sheet as an alternate to limbal stem cells for ocular surface reconstruction" was carried out under my direct supervision. No part of the thesis was submitted for the award of any degree or diploma prior to this date.

I declare that this study was conducted with the clearance obtained from the Institutional Animal Ethics Committee for adipose tissue collection and subsequent *in vivo* experiments using rabbit model. Adipose derived stem cells were used in this study with the approval from the Institutional Committee for Stem Cell Research and Therapy. All studies using human amniotic membrane and human corneal tissue were demonstrated after attaining necessary approval from the local ethics research committee (NRES Committee East Midlands-Nottingham) and in accordance with the tenets of the Declaration of Helsinki, upon attaining consent from the donors and/or their relatives.

Dr. T.V Kumary
(Research Guide)

Date:

The thesis entitled

BIOENGINEERED MESENCHYMAL CELL SHEETS AS AN ALTERNATE TO LIMBAL STEM CELLS FOR OCULAR SURFACE RECONSTRUCTION

Submitted by

BALU .V. GOPAL

for the degree of

Doctor of Philosophy

of

SREE CHITRA TIRUNAL INSTITUTE
FOR MEDICAL SCIENCES AND TECHNOLOGY,
TRIVANDRUM - 695011

Is evaluated and approved by

Dr. T. V Kumary	……..…….
(Research Guide)	(Thesis Examiner)

DEDICATED TO MY FAMILY, TEACHERS AND FRIENDS

ACKNOWLEDGEMENT

It is with deep sense of gratitude, satisfaction and with the divine blessings of God that I submit this dissertation. I take this opportunity with much pleasure to thank all who contributed in many ways for the success of this study.

I express my deep gratitude to my supervisor, Dr. T. V Kumary. Her approach enabled me to develop independent thinking. It was only due to her great help, understanding, support, and patience that I could complete my thesis work in time. She was always accessible and willing to help with her suggestions and sound advice.

I thank my Doctoral Advisory Committee members Dr. Sreenivasan K, Dr. Annie John and Dr. Anil Kumar PR for their valuable suggestions, ideas and encouragement that has helped me improve the quality of my work right from the beginning.

I thank Department of Atomic Energy, Board of research in Nuclear Sciences (BRNS), for the fellowship during my PhD tenure. I would like to thank Department of Science and Technology for funding the project pertaining to this study. I am indebted to DST – UKIERI, UK-India Education and Research Initiative, for providing me with the travel grant to University of Nottingham for conducting studies pertaining to the collaborative project between Division of Tissue Culture, SCTIMST and Academic Ophthalmology, University of Nottingham. I am also thank full to Govt. of India, Department of

Biotechnology and Indian council of medical research for providing me the international travel grants to attend ISSCR Annual meeting at Stockholm Sweden, 2015 and TERMIS EU, Switzerland 2017 respectively.

I would like to thank the Director, SCTIMST and the Head BMT wing for providing me the facilities to carry out this research work. I will be always obliged to Prof Nair and Dr. V Kalliyana Krishnan, the Dean, Dr. T V Kumary, Dr. Roy Joseph, the Associate Deans PhD, SCTIMST, for their support both in academic and administrative level. I express my deep gratitude towards Dr. Jayasingh and Dr. Santosh for their administrative support throughout my PhD. I would like to thank all the administrative staff working at Directors, Deans and Deputy Registrar's office for their kind support and help.

I thank Dr. Harikrishnan VS for providing facilities for small animal experiments. My sincere thanks to Dr. Sachin J Shenoy for his help with surgical procedures and for management of experimental animals. I would like to thank Mr. Manoj, Mr. Sunil Kumar, Mr. Sharath and Mrs. Sreeja for their support and help in animal handling and care during my experiments.

I am obliged to Prof. Harminder singh Dua, Dr. Andrew Hopkinson, Dr. Laura Sidney, Dr. Imran Muhammed for their support and help during my tenure in University of Nottingham. I would also like to thank Prof. Jyotsna Dhawan (CCMB), Dr. Abhijit Majumdar (IIT Bombay), Dr. Ramkumar Sambashivan (INSTEM), Dr. Chandrasekhar

(CCMB) and Dr, Santhosh (RGCB) for their help, support and kind advises throughout my work

I express my whole hearted gratitude to Dr Sabareeshwaran, Dr. Sachin J Shenoy, Ms. Sumitha Mohan, Ms. Shabeena for their critical care and support throughout my work.

I extend my sincere thanks to all members of tissue culture lab, Mrs. Usha Vasudev, Mrs Deepa K Raj, Mr. Vinod, Mrs. Lekshmi R Nair, Mrs. Shabeena, Dr. Bernadette, Mrs. Aswathy, Mrs Aswathy Bhaskaran, Mr. Roopesh, Dr, Eva C Das, Dr.Praveen, Dr.Naresh, Ms. Shilpa, Mr. Subash and Mrs. Manjusha for their and support and prayers throughout my tenure.

I would like to thank Dr. Francis, Mrs, Susan, Dr. Beena G Mohan, Dr. Mir Muhammed Dr. Sunitha, and Mr. Joseph for their continuous support encouragement and follow up throughout my tenure. I am thankful to Dr. Suresh babu, Dr. Radha Kumari, Mr. Willi Paul, Mr. Hari PR, Mr. Nishad, Mrs Renu, Mrs Shuba, Mr,. Merlin, Dr. Shanthi Krishna and Mrs. Sreelekshmi for their timely support in completing my work successfully

I would like to express my sincere thanks to all my colleagues in SCTIMST and friends outside the campus for their direct or indirect help during the course of my work and stay at Trivandrum and for making my years a memorable time in my life.

I sincerely thank all, my seniors and well-wishers for their guidance in work ethics, culture and life in SCTIMST.

I have no words to express the gratitude to my family members who provided the most precious support. I am always indebted to my parents, especially to my father, mother and my wife for their endless support, encouragement, love, and prayers, which provided me all the success. I thank my daughter Chaitra for being my bundle of joy in my hardships

With great pleasure, I hope the kindness showered to me will return to you in the same beautiful way it was offered.

Thank God above all!

TABLE OF CONTENTS

LIST OF FIGURES

LIST OF TABLES

ABBREVATIONS

AM	:	Amniotic membrane
AMpro	:	Amniotic membrane protein
ASC	:	Adipose derived mesenchymal stem cells
ATR	:	Attenuated total reflectance
CD	:	Clustur of Differentiation
CK	:	Cyto keratin
CSSC	:	cornea stromal stem cells
DMEM LG	:	Dulbacos modified eagle's medium low glucose
DKSFM	:	Defined keratinocyte serum free medium
FBS	:	Fetal bovine serum
FT –IR	:	Fourier Transform Infrared Spectroscopy
GMA	:	Glycidyl methacrylate
H&E:	:	Haematoxylin and Eosin
Kg	:	Kilogram
LCST	:	Lower Critical solution temperature

LIF	:	leukemia inhibitory factor
LSCD	:	Limbal Stem cell deficiency
MEM	:	Menimum essential medium
Mg:	:	Miligram
Mm	:	Milli meter
MSCs	:	Mesenchymal stem cells
NGMA	:	N-isopropylacrylamide-co-glycidyl methacrylate
NIPAAm	:	N-isopropylacrylamide
PAS	:	Periodic acid Schiff stain
SCM	:	Stem cell medium
TCPS	:	Tissue culture poly styrene
UCST	:	Upper critical solution temperature
UV	:	Ultra Violet

ANNOTATIONS

cm	:	Centimetre
ml	:	Millilitre
µg	:	Microgram
µm	:	Micrometre
mg	:	Milligram
Kg	:	Kilogram
nM	:	Nanomolar
°C	:	Degree Celsius
mm	:	Millimetre
h	:	Hour
M	:	Molar
min	:	Minute
g	:	Gram

SYNOPSIS

According to the global data of visual impairments from World Health Organization (2015), 253 million people around the globe are suffering from some degree of vision loss. There are 36 million bind people across the world and 10 million in India. Among the 10 million bind people, it is reported that 6.8 million people in India are affected by blindness due to the damage to the surface of the eye, known as the cornea, and the majority of the cases are due to a loss of stem cells that reside at the surface of the eye.

Under normal healthy circumstances, damage to the epithelial cells covering the outer surface of the eye is swiftly repaired or replenished by replacement cells. These cells originate from stem cells residing in the region of the corneal-scleral interface, known as the limbus; hence these stem cells are known as limbal stem cells. However, when limbal stem cells are lost through injury or various diseases, a condition known as limbal stem cell deficiency is caused, which prevents the eye from repairing itself. This results in extensive damage to the cornea resulting in visual impairment and eventually 'corneal blindness'. Corneal blindness is considered an avoidable and treatable condition because the cornea can normally be replaced or regenerated to restore vision. This is currently achieved by transplanting donor corneas to replace the damaged tissue and this is achieved by transplanting the patient's own cells from the good eye (autologous transplantation), or from a donor tissue (allogeneic transplantation). Transplantation can be performed directly from tissue to tissue allowing regeneration *in*

vivo. Alternatively, stem cells can be taken from tissue and grown in the laboratory into a transplantable number, which is then transferred to patient. Unfortunately, there are several limiting factors with the use of limbal transplants. In autologous transplants, a limbal biopsy from the contralateral healthy eye is performed, but patients prefer not to have a surgical intervention on their healthy contralateral eye. Allogeneic transplantation ends up in immune rejection and also patients' immune system has to be suppressed for long duration.

In this scenario it would be promising to search for an alternate cell sources other than limbal stem cells for ocular surface reconstruction. Mesenchymal stem cells are widely accepted in tissue engineering protocols and the expression of MSC markers like ABCG2 and ability to differentiate into epithelial cell lineages makes MSCs an ideal alternate source to limbal stem cells. MSCs can be trans differentiated to corneal epithelial lineage by using growth factor cocktails or by using limbal explant medium for conditioning the cells. This work emphasis not only on projecting an alternate stem cell source but also streamline these cells with a technology which will allow efficient transplantation of these cells. Herewith the concept of carrier free cell sheet transplantation was put forward as a methodology towards effective transplantation of cells for ocular reconstruction, which has not yet been attempted with MSCs. Cell sheet technology using thermo responsive culture surface can provide in vitro carrier free corneal constructs qualified for transplantation. Cell sheet technology has gained importance in regenerative medicine by enabling transplanted cells to be engrafted into

damaged tissues without external carrier allowing the transplanted cells to be engrafted for a long time, with greater donor cell presence.

Here we developed an in house thermo responsive polymer N-isopropyl acrylamide-co-glycidyl methacrylate (NGMA), for carrier free cell sheet development. Cell monolayer on thermo responsive surface detaches when incubated below the lower critical solution temperature (LCST) of the polymer, ie: around 32°C. Trans differentiated mesenchymal cell sheets are intended to replace injured tissue and compensate for impaired function. Attempts were made to bio functionalize the polymer NGMA with amniotic membrane proteins envisaging a better platform for cell sheet formation when aiming at corneal surface reconstruction. Identifying an alternative cell source along with developing a stable platform for its transplantation procedures will help corneal surface reconstruction, an easy go procedure from a surgeon's point of view. This will also address the major limitations of modern day corneal transplantation surgery including paucity of donor tissue, graft rejection and failure. Combining these concepts the hyposthysesis was derived and stated as "Stromal derived Mesenchymal Stem Cells as an alternate to limbal stem cells combined with cell sheet technology will be an effective therapeutic mode in the treatment of corneal surface damages and limbal deficiency conditions there by addressing major limitations in the field of corneal reconstruction including paucity of donor tissue and graft rejection."

The main objectives of the work include

Phase I: Synthesis and characterization and modification of the thermo responsive polymer N-isopropyl acrylamide-co-glycidyl methacrylate (NGMA).

Phase II: Isolation and characterization of stromal mesenchymal stem cells, trans differentiation and engineering them to cell sheets. Two types of cells were used (1) Rabbit adipose mesenchymal stem cells (MSC) (2) Human corneal stromal stem cells (CSSC).

Phase III: Proof of concept study: In vivo evaluation of trans differentiated adipose mesenchymal cell sheets in rabbit limbal stem cell deficient models and their histology.

Thesis is divided into following chapters – Introduction (Chapter 1), Literature review (Chapter 2), Materials and Methods (Chapter 3), Results (Chapter 4, 5, 6), Discussion (Chapter 7) and Summary and Conclusion (chapter 8).

The introduction chapter provides an up to date details in the field of corneal tissue engineering - current challenges, treatment modalities & limitations. The importance of identifying alternate cell sources and the incorporation of cell sheet technology is addressed and substantiated. The introduction also details about thermo responsive polymers context of corneal tissue engineering, importance of amniotic membrane proteins with respect to corneal regeneration, benefits by bio functionalizing NGMA with amniotic membrane proteins and cell sources used in this study

Chapter 2, the literature review addresses the field in general at the beginning, tracing out the origin and intractable nature of corneal injuries. The

development of current technologies and the emergence of novel tissue engineering methods are highlighted. The use of thermo responsive polymers and history of cell sheet engineering is addressed. The need for alternate replacement of limbal stem cells and various alternates sources attempted in literature is well reviewed with special emphasis on their lineage plasticity as well as suitability to the therapy at hand. Use of amniotic membrane for corneal therapies and the logic in conjugating it to the polymer is also reviewed to the possible extend.

Chapter 3 – Materials and Methods, spans over the experimental design including a detailed depiction of protocols, materials and equipment. Phase I includes the synthesis and physicochemical characterization of thermo responsive polymer N-isopropyl acrylamide-co-glycidyl methacrylate (NGMA). Bio functionalization of polymer NGMA with amniotic membrane proteins and its evaluation. Phase II in this session details the cell sources used including rabbit adipose derived Mesenchymal Stem Cells and Human corneal stromal stem cell (CSSCs). Both the cell populations were isolated and characterized. Limbal explants were also obtained from rabbit eyes for collection of conditioned medium. MSC's were then differentiated into corneal epithelial lineage by using limbal explant conditioned medium. Differentiated cells were evaluated using cytokeratin 3/12 staining, flow cytometry and qPCR analysis The cell sheet on NGMA was reterived by virtue of its thermo responsive property and the Cell sheet was transferred to a new dish using PVDF membrane as a transfer tool. CSSCs were cultured on amniotic membrane bio functionalized NGMA and was retrieved as a sheet later transferred to a new substrate using gelatin as a tool to transfer. Phase III details the in

vivo experiments evaluating the efficacy of trans differentiated adipose mesenchymal cell sheets in a rabbit limbal stem cell deficiency model. Models were generated through mild alkali burn using n-heptanol along with excision of limbus. The damage was graded by various methods and suitable models were taken for transplantation. The detached cell sheet was then transferred to the corneal damage model by placing the cell sheet on the cornea and spreading it over the cornea. The transplanted animals were observed for a period of one month and was then euthanized to evaluate the structural integrity of the transplanted cell sheet and its efficacy in vivo. Histological analysis with Hematoxylin and Eosin was carried out to see how well the cell sheet has integrated with the host environment.

Results is divided in to three different chapters (Chapter 4, 5 6). Chapter 4 deals with the synthesis, characterization and modification of the thermo responsive polymer. ATR–FTIR spectrum showed functional groups representing individual monomers of NGMA polymer. The thermo gram showed a dip at 32.5ºC which corresponded to the LCST of pNIPAAm as the polymer property changes. The weight average molecular weight (M_w) of the polymer was determined to be 183787 and the water contact angle was around 70º. Amniotic membrane proteins were conjugated to NGMA by epoxy ring opening mechanism. SDS PAGE and western blot analysis showed that the conjugate is trapped in the well due to increase in molecular weight while control protein run down the lane in the wells. Decorin and Mimican were the proteins analyzed by western blot and was shown to have trapped in the well in comparison to the control. Chapter 5 includes mesenchymal stem cell characterization

and engineering them to cell sheet. MSCs isolated were characterized for their stemness using flow cytometry showed more than 85% positivity for CD 105 and CD 90, showed negative for CD 34. MTT assay and test on extract showed NGMA was cyto compatible for cell culture studies and it doesn't alter the any MSC properties. MSCs differentiated to corneal epithelial linage were stained positive for CK 3/12 supported by qPCR data. The cell sheet detached from NGMA was transferred to a new dish using PVDF membrane and was evaluated after 24h.

CSSCs were characterized for mesenchymal stem cells markers CD 73, CD 90, CD 105 and CD 34. These characterized cells were then cultured on NGMA-AM pro modified substrate and cell sheet detachment was achieved by using 10% gelatin gel cell sheet retrieval system. Chapter 6 includes the In vivo demonstration of Cell sheet in rabbit models. Fluorescein staining demonstrated excised limbal region and also debrided epithelium. The sham models showed conjunctival ingrowth over cornea and presence of goblet evident confirming epithelial damage. In non-transplanted control, a scar tissue was formed over the cornea while in the cell sheet transplanted model cornea was more or less clear, but not comparable to the normal eye. Histology observation showed a layer of cell sheet over the corneal stroma, well adhered to the corneal surface.

Chapter 7 discusses the results obtained in details and emphasis on the fact that MSCs as an alternate to limbal stem cells combined with cell sheet technology will prove a more stable system for corneal transplantation studies. Cells as a sheet will enhance the number of cells per damaged area and there by the effect of cell sheet will

be much more than cell suspensions or other cell transplantation methods and this concept was evaluated in vivo with success in rabbit models.

Chapter 8 summarises the thesis. NGMA was demonstrated to be an effective substrate for cell sheet engineering and can also be bio-functionalized by epoxy ring opening mechanism. The use of mesenchymal stem cells for cell sheet technology opens up avenues in the field of tissue engineering and regenerative medicine. Human derived stromal cell sheet formation was also standardized in amniotic membrane proteins conjugated NGMA polymer surface for guided cell sheet engineering. Mesenchymal stem cells derived Corneal epithelial cell sheet is a novel attempt towards corneal surface reconstruction. Achieving corneal epithelial differentiation from adipose MSCs and a combined use of NGMA for cell sheet retrieval may help in addressing limbal stem cell deficiency conditions and other corneal surface disorders. These trans differentiated sheet was evaluated in vivo in rabbit LSCD models and have promising results in the pilot study, guiding to the avenues in future on human applications.

CHAPTER - I

1. INTRODUCTION

1.1. Eye – structure and function

The human eye serves as one of the most important sensory organs and is also the most complex organ in human body. Eyes along with its other functional composites enable people to see things, providing them with a complex mechanism called vision. Eyes are placed safely within a bony socket called orbit in the front part of the skull. There are six muscles within the orbit that are attached to the eye, which help to move the eyes upwards, downwards, sideways and to rotate.

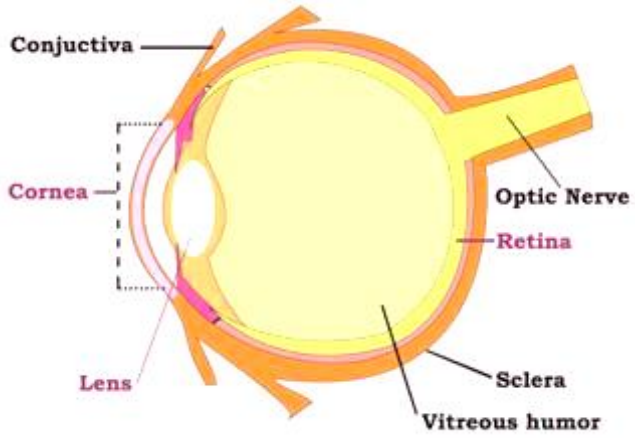

Figure 1: Anatomical Structure of Human Eye

(http://www.hybridcornea.org/aboutcornea.htm)

The eye is made up of multiple layers and can be functionally divided into two segments – anterior and posterior. Anterior region is specialized in light perception while the posterior region is specialized in light sensing. Structurally, eye

can be divided further into three parts: the cornea and sclera; the iris, choroid and ciliary body; and the retina

Stimuli to vision are initiated when light rays from an object enter eye via cornea. The cornea is often mentioned as the clear front "window" of the eyeball. The cornea is capable of bending the light in such a way that the light passes freely through the pupil and reaches the iris. Iris controls the amount of light entering the lens. The light rays passing through the lens is further focused to the retina. The retina situated at the back of the eye contains millions of light-sensitive nerve cells or light receptors. These receptors are the rod and cone cells. These light receptors convert the cells into electric impulses which are then transmitted to the vision processing region of the brain converting the impulses to an image. The vision processing centre of the brain is the visual cortex located in the occipital lobe at the back of the brain

1.2. Statistics of vision impairment

The global number of visually disabled is increasing day by day making visual impairment an alarming scenario across the world. According to the global data of visual impairments (2015), 253 million people around the globe are suffering from some degree of vision loss (Bourne et al.,) There are 36 million blind people across the world and 10 million in India. A little more than 20% of the world's blind population belongs to India, while 13.2% belong to European countries. Recent reports in 2015 highlight that India has the highest number of blind population. WHO in their 2010 report states that about 80% visual impairment is curable or preventable if identified at the right time (Universal eye health: a global action plan

2014-2019. WHO, 2013). A visual loss by any reason will have a profound effect on the patients, based on their psychological, financial and social situations. According to the statistics about 90% of the world's visually impaired live in low-income settings and around 56% are females (Bourne *et al.,* 2017).

Vision impairment refers to a condition in where we lose the ability to see things around us with clarity. Visual impairment is classified into 4 different categories according to the International Classification of Diseases - normal vision, moderate vision impairment, severe vision impairment and Blindness. Moderate and severe vision impairment is generally referred to the term "low vision": Low vision and the last group "blindness "represents all vision impairment. Visual loss can be due to various reasons that include the following and is ranked in the below-mentioned order in terms of its incidence,

- Cataract
- Glaucoma
- Age-related macular degeneration
- Corneal opacities
- Childhood blindness
- Refractive errors and low vision
- Diabetic retinopathy
- Genetic eye diseases

1.3. Cornea and corneal surface disorders

Corneal surface disorders are is the fourth leading causes of blindness in the world. Among the 10 million blind people in India, It is reported that 6.8 million people are affected by blindness due to the damage of the surface of the eye (Vashist et al., 2013) known as the cornea, and majority of these cases are due to a loss of stem cells that reside at the surface of the eye. Corneal surface disorders are the second largest cause of blindness in India next to cataract.

The cornea is the transparent dome-shaped outermost part of the eye, which is mainly protective in function. It should be structurally and functionally intact for clear and correct vision. Cornea also contributes to the refractive power of eye (Karring et al., 2004). It helps to filter out harmful ultraviolet radiations, prevents entry of foreign objects, traps foreign organisms and protects the inner eye from various external stimuli. The cornea measures approximately 12mm vertically, and 11mm horizontally in case of humans. The steepest part is in the centre and then flattens out towards the periphery. The cornea receives its nutrient supply via tears and aqueous humour, as the cornea is avascular and does not contain blood to nourish the corneal tissue or protect it against infection (Sweeney et al., 1998). The avascular cornea gets its oxygen supply directly from the air. The atmospheric oxygen gets dissolved in the tears which then diffuses throughout the cornea via the tears (Holden and Mertz, 1984). When the cornea is of normal shape and curvature, it bends or refracts light on the retina with precision.

Light passes through the cornea before reaching the retina in the back of the eye, and thus it is mandatory that the cornea must remain clear for the incoming

light to pass through. The cornea is made up of five different layers and all these layers play an important role in maintaining corneal transparency for vision (DelMonte and Kim, 2011). The corneal transparency is very important so as to refract light properly, and the presence of even small blood vessels, cloudiness and opacity can affect the refraction of the incoming light rays interfering with proper vision. Corneal disorders that result in minor irritation to vision problems or even blindness due to scarring or clouding of the cornea falls in the group corneal opacity disorders. Corneal epithelium is the outer most layer is very prone to various kinds of damages including thermal or chemical injuries.

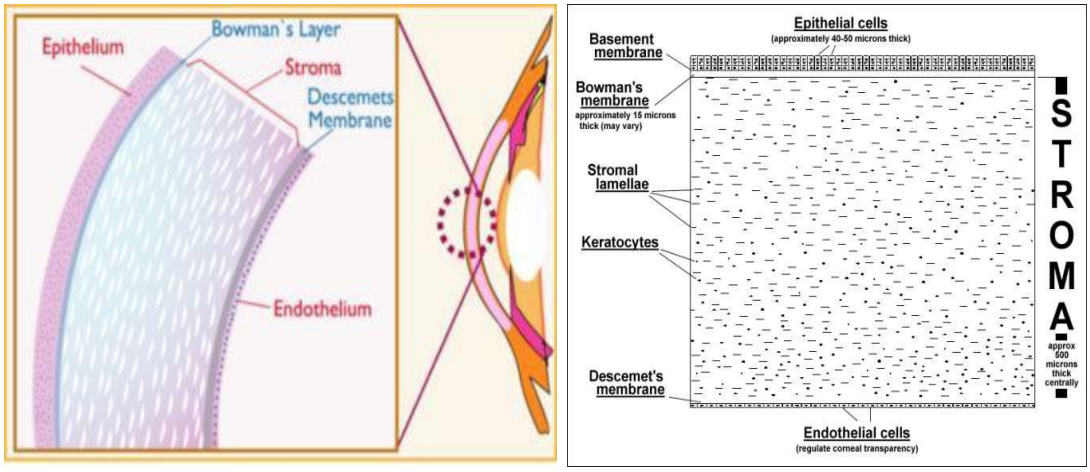

Figure 2: Structure of Cornea; a Cross-sectional view showing corneal layers. (http://www.hybridcornea.org/aboutcornea.htm,http://www.lasikdisaster.com)

1.4. Corneal Anatomy - Layers of cornea

1.4.1. Corneal epithelium

The epithelium is the outermost layer which serves as an effective barrier against foreign entry. It is composed of layers of non-keratinized stratified epithelium and is constantly replaced (DelMonte and Kim, 2011). The corneal

epithelium comprises 10% of the corneal thickness. The outer layer of corneal epithelium is 2-3 layer thick terminally differentiated squamous epithelial cells with effective tight junctions making it impervious to a foreign body and also prevent loss of fluid (Klyce, 1972). These cells also have surface microvilli that help to increase the surface area of the cornea (Hoffmann and Schweichel, 1972). Below the terminally differentiated cells are the supra basal cells or the wing cells followed by the basal or stem-like cells (Agrawal and Tsai, 2003). The supra basal cells are polyhedral in shape representing a transitional stage between basal cells and superficial epithelial cells. The basal cells mediate cell migration during epithelial injury, by regulating the organization of hemidesmosomes and local complexes, in turn, helping attachment of a cell to the underlying basement membrane (Pajoohesh-Ganji and Stepp, 2005). The basement membrane acts as a foundation or anchorage on which these epithelial cells grow and organize themselves. The epithelium of human is around 51µm in thickness.

1.4.2. Bowman's layer

Bowman's layer is an irregularly arranged acellular region constituting mainly of collagen fibres. This layer acts as a separating layer between epithelium and underlying stroma. It also protects the stromal layers from injury and harmful external stimuli. This layer is around 8-14µm in thickness.

1.4.3. Stroma

Stroma is an avascular layer lying beneath Bowman's layer and is the thickest layer of the cornea. This layer mainly contains water (78%), regularly organized collagen fibrils (16%) and stromal keratocytes. These collagen fibrils

form flat bundles of lamellae arranged in a regular lattice-like pattern. This structure allows light to pass through without getting absorbed and also accounts for corneal transparency (Meek and Knupp, 2015). Any damage to this pattern can result in cloudiness of cornea. Collagen also provides the cornea with its strength, elasticity and form. Stromal keratocytes mediate the synthesis and organization of collagen and proteoglycans. Corneal crystallins in the cytoplasm of keratocytes contribute to their transparency (Jester et al., 1999)**.**

1.4.4. Descemet's membrane

Descemet's membrane is a thin but strong sheet of tissue that serves as the basement membrane of corneal endothelium. It is a rapidly regenerating layer that serves as a protective barrier against infections and injuries. It is mainly composed of collagen type IV, VIII and is acellular in nature (Pajoohesh-Ganji and Stepp, 2005).

1.4.5. Endothelium

Endothelium consists of a single layer of cuboidal cells that are actively involved in regulating fluid balance. It is extremely thin and is the innermost layer of the cornea. This layer helps to maintain the fluid content of cornea. The homeostatic fluid balance in the cornea is maintained by the inflow and outflow of fluid within corneal stroma. Endothelial cells pump out the fluid from the stroma through the endothelial cells (Waring et al., 1982). If there is a fluid imbalance, the corneal stroma will swell, become hazy and opaque. Extensive endothelial damage by disease or trauma usually results in corneal oedema and blindness due to poor

regeneration potential. Corneal transplantation is the only available therapy in case of endothelial damage.

1.5. Limbus and Limbal Stem Cell Deficiency conditions

Corneal epithelium has a great potential to regenerate and under normal healthy circumstances, damage to the epithelial cells covering the surface of the eye is swiftly repaired or replenished by replacement cells. These cells originate from stem cells residing in the region of the corneal-scleral interface, known as the limbus; hence these stem cells are known as limbal stem cells (Boulton and Albon, 2004). However, loss of limbal stem cells results in limbal stem cell deficiency (LSCD), which prevents the eye from repairing itself (Chen and Tseng, 1991). The deficiency in functional limbal stem cells and the damage of limbal stem cell niche impairs the normal homeostasis of corneal epithelial regeneration (Dua et al., 2000). Damage or dysfunction of the limbal stem cell population can occur due to inherited (Ocular cicatricial pemphigoid, Stevens-Johnson syndrome) or acquired conditions (chemical and thermal injuries, corneal dystrophies, recurrent surgeries). The LSCD can compromise ocular surface integrity resulting in scarring, opacification and extensive damage to the cornea, which is the clear window of the eye, resulting in visual impairment and eventually permanent loss of vision known as ‘corneal blindness’.

1.6. Current therapies and associated problems

Corneal blindness due to LSCD is considered as an avoidable and treatable condition (Vashist et al., 2013) because the corneal surface can normally be restored or regenerated to regain vision. This is currently achieved by transplanting tissue biopsies from the corneo-limbal region to replace the damaged tissue. To

allow this, the lost stem cells of the recipient must first be replenished, and this is achieved by transplanting the patient's own tissue graft/cells from the good eye (autologous transplantation), or from a donor tissue (allogeneic transplantation) (Ghezzi et al., 2015) in case of bilateral limbal damage. Transplantation can be performed directly from tissue to tissue allowing regeneration *in vivo*. One of the successfully used therapeutic strategies for treating corneal blindness is the transplantation of limbal biopsies taken from donors or cadavers (Tan et al., 1996). Allogeneic transplantation methodologies face problems associated with scarcity of donor tissue, graft rejection due to the presence of abundant vasculature, recurrent infections and long-term immunosuppression treatments (de Araujo, 2015). Cultivated limbal epithelial transplantation is yet another method with ex vivo expansion of limbal stem cells from very small explant pieces. This solves the issue of donor site morbidity but poses threat of having xenogeneic components while ex vivo expansion of limbal stem cells ((Pellegrini et al., 1997). Simple limbal epithelial transplantation (SLET) was introduced as a modified surgical technique addressing the limitations associated with the previous techniques in cornea surface therapies. This procedure was able to remove the complications that may arise due to the ex vivo expansion of stem cells including interaction with xenogeneic components (Sangwan et al., 2012). But this still does not address the issue of bilateral limbal damage conditions. Currently, in India, there is an annually estimated need for 100,000 corneas, but there are only 17,000 eyes procured annually, of which 50% to 60% are utilized (Press Information Bureau, GoI, MoHFW, 2014). Therefore the need for an alternate treatment strategy stands significant. Stem cell transplantation and corneal surface reconstruction hence becomes a promising approach over limbal

grafts. Stem cell transplantation can be considered the first essential step over corneal grafting, as the graft may be rejected as a foreign tissue due to the presence of abundant vasculature. Stem cells can be harvested from various tissues and expanded in laboratory conditions for transplantation to the corneal surface for immediate effective relief (Pellegrini et al., 1997).

1.7. Alternate approaches and use of non-ocular cell sources

Alternate approaches to overcome the aforementioned limitations is to adopt tissue engineering strategies utilizing ex vivo expansion of ocular and non-ocular stem cells supported by various matrices including amniotic membrane, using amniotic membrane (AM) transplantation and *ex vivo* expanded autologous stem cells taken from the contralateral healthy eye (Tseng, 2001). In cases where transplantation is unavoidable, the current treatment regime is the ex vivo expansion of limbal cell on amniotic membrane and transplantation to restore corneal surface. But in the case of bilateral LSCD, lack of host limbal stem cells demand allogeneic stem cell sources, wherein all the aforementioned problems exist. In this scenario, it would be promising to search for an alternate autologous cell source other than limbal stem cells for ocular surface reconstruction. Cotsarelis *et al*., were the first to show the presence of label-retaining cells in the limbal epithelium by labelling with 3H- thymidine (Cotsarelis et al., 1989) and since then various cell sources have been tried for ocular surface reconstruction including corneal stromal stem cells (Hashmani et al., 2013), oral mucosal epithelial cells, hair follicle stem cells, embryonic stem cells and other mesenchymal cell sources (Sehic et al., 2015).

1.8. Mesenchymal stem cells

Mesenchymal Stem Cells (MSCs) are one among the most prominent and easily available cell source that is widely used in the field of regenerative medicine (Hima Bindu and Srilatha, 2011). More over MSCs exhibit multi lineage differentiation potential, self-renewal and immune modulatory properties (Gao et al., 2016) which make them, the most suitable stem cell source for use in tissue engineering. Since MSCs can be isolated from a variety of sources, a patient can always rely on autologous mesenchymal stem cell for any regenerative therapeutic interventions**.** MSCs can secrete a wide array of growth factors, cytokines, matrix proteins and also recruit other endogenous stem cells to the site of injury, thereby playing a major role in wound healing (Park et al., 2009). Role of MSCs in promoting wound healing and reconstruction of the cornea is also reported. The expression of markers like ABCG2 (Ebrahimi et al., 2009) and ability to differentiate into epithelial cell lineages makes it an alternate source to limbal stem cells (Li and Zhao, 2014) for ocular surface regeneration in the treatment of bilateral limbal stem cell deficiency. Mesenchymal stem cells (MSC) from bone marrow were reported to be successful for the reconstruction of the corneal surface because of their plasticity and expansion potential (Reinshagen et al., 2011). Previous studies have attempted transdifferentiation of MSCs and few studies have tried out transplantation with limited success (Gu et al., 2009).

1.9. Delivery of stem cells as cell sheets

Current applications of MSCs in wound healing use intravenous injection of MSC expecting them to home at the site of injury (Wang et al., 2012) along with

the direct application of cells on to the wounded surface (Kirby et al., 2015). Reports suggest that homing of MSCs to target organs or sites is below 5% in case of systemic infusions (Kang et al., 2012). For cell therapy to be effective, it has to be successfully delivered to the patient ensuring maximum donor cell interaction at the wound microenvironment. Engineered matrices usually serve this purpose, by holding cells to a definite area, and are widely used in various fields of regenerative medicine like bone regeneration, cosmetic therapies etc. These matrices or scaffolds also provide structural integrity to the repair site and help to harbour and deliver growth factors (Manning et al., 2013). However, identifying a suitable non-toxic, non-immunogenic and biocompatible scaffold is the main hurdle in this field. Scaffold-free cell sheet engineering eliminates the use of a scaffold, stabilizing the cells within a sheet as reported (Matsuura et al., 2014). Cell sheets maintain their structural integrity by retaining intact cell-cell and cell-extracellular matrix architecture, thereby making them an independent unit for use in tissue engineering therapies (Yamato and Okano, 2004).

In this study, apart from using mesenchymal stem cells as an alternate to limbal stem cells, we have attempted to engineer them to a sheet in order to streamline this concept with an effective technology aiming at enhanced therapeutic benefits during transplantation. Cell sheets are successfully engineered using temperature-responsive matrices, whose properties alter with a change in temperature (Tang et al., 2012), (Joseph et al., 2010). Enhanced therapeutic effects by the cell sheet technique have been reported in comparison with other cell delivery methods, as the cell sheets can achieve greater donor cell presence after transplantation (Narita et al., 2013). MSCs as a sheet will have an enormous number of medical applications

due to their aforementioned properties. MSC sheets have been attempted in the field of bone tissue engineering using magnetic nanoparticles, treatment of periosteal defects and myocardial infarction using PNIPAAm (Shimizu et al., 2007), (Long et al., 2014), (Augustin et al., 2013).

CHAPTER – II

2. REVIEW OF LITERATURE

2.1 Homeostasis of corneal epithelial regeneration

The outermost layer of the corneal epithelium shed away and is replaced at regular intervals. In case of humans, a stable process of renewal and regeneration happens in regular intervals where the cells in the superficial layers are continuously sloughed off from the surface and replaced by proliferating cells from the basal layer (Yazdanpanah et al., 2017). These basal cells reside in the lower layers of the corneal epithelium on the basement membrane called the limbus. These cells undergo mitotic division while the cells in the upper suprabasal layer become postmitotic and differentiate into superficial squamous cells (Kruse, 1994). The maintenance or self-renewal of the corneal epithelial cells is achieved by vertical and horizontal movement of cells. The proliferative pressure due to division of cells in the basal cell layer causes the vertical movement of the basal cells towards the top layers (Lavker et al., 1991) while the corneal epithelial cells migrate in horizontal direction from peripheral cornea to central cornea in response to wound healing (Kuwabara et al., 1976)(Buck, 1979). Centripetal movement of corneal epithelial cells takes place under physiological conditions in murine, rabbit and human corneas as well (Kinoshita et al., 1981), (Buck, 1985), (Dua and Forrester, 1990), (Kaye, 1980), (Lemp and Mathers, 1989). The dogma in corneal epithelial homeostasis indicates

that the total epithelial cell mass remains constant, or the total loss of cells by shedding is equal to the total gain of cells by mitotic division and migration (Sharma and Coles, 1989).

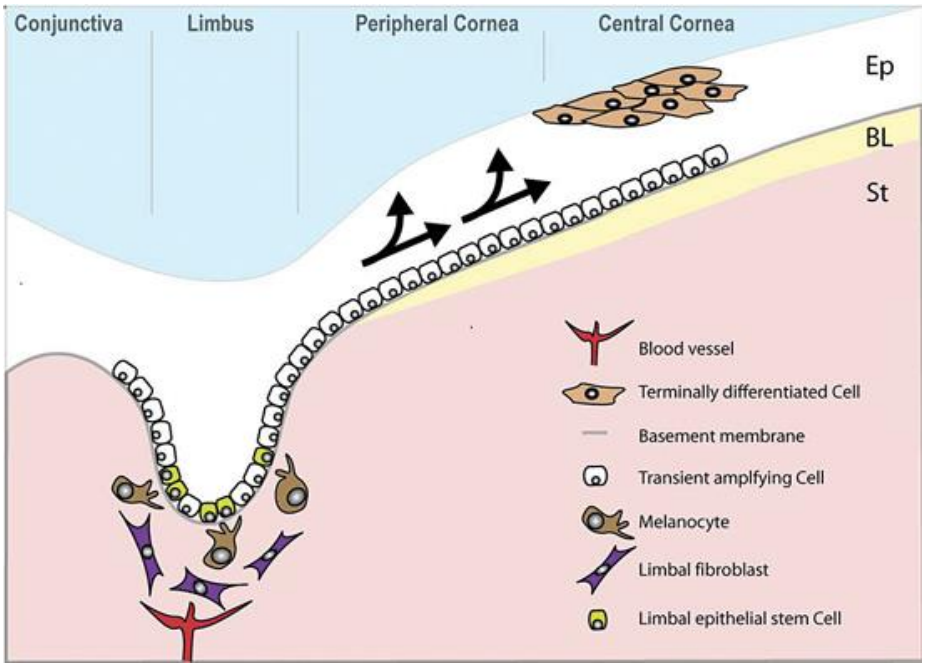

Figure 3: Homeostasis of Corneal epithelial regeneration

Genevieve et al, Limbal epithelial Stem cells in Cornea, StemBook, 2009

The XYZ hypothesis of corneal epithelial maintenance put forward by Thoft and Friend (1983) describes that the limbus serves as a reservoir of stem cells (SCs) (Thoft and Friend, 1983). These SCs undergo asymmetric division producing a stem-like daughter cell and a transient-amplifying cell (TAC). TACs multiply and migrate anteriorly to post-mitotic suprabasal wing cells which later become terminally differentiated superficial squamous cells. The superficial cells are lost from the surface by normal exfoliation. Thus, migration of basal cells anteriorly (X) and centripetal migration from the limbus (Y) equals sloughing off of the superficial

cells from the surface (Z). However, this theory has been challenged by clinical observations and animal studies, which together propose that not only the limbal region but the central cornea may also contain these stem cells (Majo et al., 2008; Dua et al., 2009).

2.2 Corneal stem cell niche

Stem cells reside within the body in a nest and are preserved till a stimulus activates them, generally termed as stem cell niche. A stem cell niche provides the cell with a wide array of intrinsic and extrinsic factors supporting maintenance of a stem cell population within the niche (Klenkler and Sheardown, 2004). This includes the interaction of cells with niche surface, availability of survival factors and cytokines along with a variety of signalling molecules supporting stem cell functions.

In one of the first studies towards understanding the corneal epithelial niche factors, Davanger and Evensen in their studies with guinea pigs showed that limbal region in the eye has a role in epithelial self-renewal (Davanger and Evensen, 1971). Later in 1981, Shapiro *et al.,* suggested conjunctival epithelium as the source from which corneal epithelial cells were formed (Shapiro et al., 1981). In 1986, it has been proven experimentally using cytokeratin 3 staining of corneal surface, that corneal stem cells reside at the basal layer of the limbal epithelium (Schermer et al., 1986). It was then reconfirmed that the limbal region does not contain cytokeratin 3 and cytokeratin 12 positive cells, instead, they had label-retaining cells at this location (Cotsarelis et al., 1989), which are considered stem cells. The study on label-retaining cells evidently suggested that stem cells remain within the limbal

region and are slow cycling or quiescent in nature (Cotsarelis et al., 1989). These cells, named limbal epithelial stem cells displayed a greater tendency to grow in colonies (Pellegrini et al., 1999), a property of stem cells.

Over the past decade, research had been driven towards understanding the corneal stem cell niche. These have brought in to light several hypothetical niches for the peripheral cornea including palisades of Vogt, limbal epithelial crypts and focal stromal projections (Yoon, 2014). These structures are characterized by rete folds, melanocytes, nerve endings and underlying blood vessels (Ordonez and Di Girolamo, 2012). These niche structures are thought to support and facilitate adhesion, the supply of growth factors and nutrients, provide a barrier from external forces, UV rays and oxidative damage (Bessou-Touya et al., 1998), (Echevarria and Di Girolamo, 2011). Limbus has a unique anatomical structure that provides it with micro-environmental characteristics required for stem cell niche known as Limbal Epithelial Crypt (LEC) or Limbal Crypt (LC). These form finger-like invaginations into the limbal stroma from the rete ridges extending to conjunctival stroma (Shortt et al., 2007), (Dua et al., 2005). The presence of cytokeratin 14, ABCG2 and P63 were added as evidence to suggest that corneal stem cells reside in limbal crypts ((Dua et al., 2005).

Limbal niche and the cells within are also associated with various signalling pathways. Sonic hedgehog, Wnt/β-catenin, TGF-β and Notch signalling pathways are important signalling pathways associated with niche control of limbal stem cells (Li et al., 2007). Wnt and Notch signalling pathways modulate cell cycling and self-renewal regulation of limbal stem cells, while Wnt/β-catenin signalling also

plays a role in limbal SC differentiation during morphogenesis (Kulkarni et al., 2010), (Mukhopadhyay et al., 2006).

Within the limbal niche, the limbal stem cells divide asymmetrically to provide one stem cell daughter and one transient amplifying cell. The transient amplified cells can be called as committed stem cells, which will divide multiple times giving daughter cells. From the limbal niche, these cells travel to the corneal periphery and will then move centripetally over the corneal surface and mature into corneal epithelial cells forming the 5-7 layered epithelium (Sun and Lavker, 2004). Furthermore, the limbus also prevents the conjunctival over-running to the corneal surface.

2.3 Problems associated with damage to limbal niche

Corneal epithelial renewal is associated with proliferation and differentiation of limbal stem cells situated in the limbal niche along with their peripheral and centripetal movement to reach the central corneal surface forming corneal epithelial cells. This also checks and prevents the conjunctival out-growth over cornea resulting in blurred vision (Tseng, 1996). Any damage or deficiency of the stem cells at the limbus would result in disturbing the normal homeostasis of corneal epithelial regeneration and prevent self-renewing corneal epithelium from forming the new epithelial layer (Tseng, 1989). The absence of corneal epithelium will result in conjunctival over - growth on to the cornea resulting in blurred vision. This condition where the limbal stem cells are lost or damaged due to the environment, UV exposure, thermal and chemical burns, is called limbal stem cell deficiency (LSCD) (Dua et al., 2000). Apart from LSCD, there are several other

conditions that can result in limbal damage or tiger LSCD conditions, which include chemical and thermal burns, corneal infections and foreign body entry to the eye which are detailed in the next session.

2.4 Limbal Stem Cell Deficiency Condition (LSCD)

Limbal stem cell deficiency can be related to any case where there is a loss of availability of limbal stem cells or loss of function of these cells due to hereditary or acquired reasons. The causes include aniridia (Skeens et al., 2011), keratitis (Puangsricharern and Tseng, 1995), a condition where limbal stem cells may be congenitally absent or dysfunctional. Acquired conditions include diseases like Stevens-Johnson syndrome, ocular cicatricial pemphigoid, neurotrophic keratopathy, peripheral ulcerative keratitis and accidental conditions like chemical injuries, burn wounds, contact lens-induced keratopathy and repeated surgical interventions (Deng et al., 2013) Most of the clinical scenarios reported are due to acquired disorders. LSCD is manifested mainly by reduced vision, sensitivity to light, vascularization and conjunctival growth in the corneal surface causing cloudiness to the cornea, chronic inflammation of the ocular surface, loss of corneal clarity and increased opacification (Dua et al., 2000).

LSCD may be partial or complete. In partial LSCD, the limbal niche is partially damaged while the rest of the limbal region is unaffected and still harbours the limbal stem cells for corneal epithelial regeneration. Conjunctivalisation is restricted to damaged regions. In total LSCD conditions, the entire limbal niche is damaged and thereby corneal surface replenishment by corneal epithelial cells is inhibited. Conjunctival cells outgrow corneal surface and are also presented by heavy

neovascularization, corneal opacity and epithelial defect. Identify the extent of damage is crucial in determining treatment methodologies as this varies from topical medication to surgical transplantation procedures. The main symptoms include blurred vision, tear discharge, swelling, sensitivity to light and vision loss (Deng et al., 2013).

2.5 Treatments towards corneal surface damage conditions

Corneal surface treatments or therapies is tailored to the type of diseases and the individual patients (Dua, 2001). Treatments can vary from minor medications to complex surgeries, depending on the condition. Few infections of the eyes can be treated with medicated eye drops (for example, antibiotics), in some cases, oral medication and at times with anti-inflammatory steroid eye drops. The best treatment method differs depending on the specific type of corneal surface damage or disease. The treatment strategy for a corneal surface damage depends on the cause and extent of the injury. An abrasion or damage might require minor treatments like a temporary patching/bandage contact lens to complex transplantation surgeries for making cornea clear and allowing to perform its function. Partial damage to the corneal surface with conjunctivalisation may not require intervention. Corneal and conjunctival epithelial cells co-exist without significant overgrowth of conjunctival epithelium into cells of corneal epithelial phenotype (Dua et al., 1994), Coster et al., 1995). Conjunctivalisation over visual axis may require mechanical debridement of conjunctival epithelium for adequate corneal epithelial healing promoted by the remaining intact limbus with or without amniotic membrane transplantation (Tseng, 1998) In patients with total limbal damage limbal auto- or allotransplantation are

suitable for corneal surface reconstruction. Kenyon and Tseng proposed the current treatment strategy (Kenyon and Tseng, 1989) with several modifications reported over time. In short, a donor epithelium is transplanted replacing the diseased corneal surface after removing the epithelium and pannus.

Risk of immune rejection associated with allografts, lead to modifications in existing methods of corneal reconstruction therapies. This lead to attempt ex vivo expansion of limbal epithelial stem cells enabling to generate the required number of stem cells for corneal surface reconstruction. The scope of using ex vivo expanded limbal stem cells were exploited by Pelligrini *et al*., and this group also demonstrated the transplantation of *ex vivo* expanded autologous limbal stem cells in LSCD conditions due to unilateral alkaline injury (Pellegrini et al., 1997). followed by this another group demonstrated *ex vivo* expanded autologous stem cells in LSCD conditions due to chemical burn by using amniotic membrane as a carrier membrane. Cultivated limbal epithelial transplantation (CLET) was able to address the issue of donor site morbidity in autologous therapies as a very small 1-2 mm tissue was dissected from the healthy fellow eye of the patient for ex vivo expansion in controlled culture systems raises safety concerns including immune rejection when used for transplantation purpose and is yet to be addressed

Simple limbal epithelial transplantation (SLET) was introduced as a modified surgical technique addressing the limitations associated with the previous techniques in cornea surface therapies. This procedure was able to remove the complications that may arise due to the ex vivo expansion of stem cells including interaction with xenogenic components. This was demonstrated by Sangwan et al., and they reported successful reconstruction in 6 patients who underwent SLET for

unilateral or bilateral limbal damage (Sangwan et al., 2012). This technique utilizes a small 2x2 mm donor limbal tissue and is then dissected into still smaller pieces which is then placed over the damaged corneal surface with an amniotic membrane placed over it.

Thermal and chemical damages induce conditions where limbal stem cells can be partially or totally damaged depending on extent of the burn. If the damage is partial, the host cornea itself has the potential to recover from the damage and this is determined either by "Roper-Hall classification for the severity of ocular surface burns" (Roper-Hall, 1965) or by "Clock hour limbal involvement classification by Prof Harminder Dua (Dua, 2001). Roper-Hall classification was based on the extent of epithelial damage and limbal ischemia.

2.5.1 Determining the extent of corneal surface damage - Classification based on Clock hour limbal involvement

The method of treatment is decided depending on the extent of the damage. The cornea has the capacity to cope very well with minor injuries or damages. In case of a scratch in the cornea, the healthy cells can slide in quickly and heal the injury. Healing process depends on the depth of the injury, if the scratch penetrates deep into cornea, it slows down the healing process. This delay can result in the aforementioned symptoms including pain and blurred vision. These conditions may require treatment to enhance healing and prevent inflammation. Deeper scratches or injuries may result in severe damage and impair vision which may require a corneal transplant to rectify the damaged cornea. The prognosis is detailed by Dua et al., describing the extent of damage based on limbal involvement. The

extent of damage determines the treatment modality from simple eye drops to corneal transplant surgeries.

Grade	Prognosis	Clinical findings	Conjunctival involvement	Analogue scale (%)
I	Very Good	0 clock h of limbal involvement	0	0/0
II	Good	<3 clock h of limbal involvement	< 30	0.1-3/1-29.9
III	Good	> 3 – 6 clock h of limbal involvement	> 30 - 50	3.1- 6/31-50
IV	Good to Guarded	> 6 – 9 clock h of limbal involvement	> 50 - 75	6.1- 9/51-75
V	Guarded to Poor	> 6 – < 9 clock h of limbal involvement	> 75 - < 100	9.1-11.9/75.1-99.9
VI	Very Poor	Total limbus (12 clock h) involved	100	12/100

Table 1: Classification based on Clock hour limbal involvement (Dua et al., 2001)

2.5.2 Laser Therapy

A computer-controlled excimer laser is used to treat the majority of infections where the damage is not severe. This technique is called phototherapeutic keratectomy (PTK) (Rathi et al., 2012) and in few cases this would be enough to regain vision and eliminate the need for transplantation. The laser is used to remove the diseased or damaged corneal surface including irregular corneal tissues and scars formed thereby promoting the cornea to heal or regenerate on itself. Laser therapy is successful when the damage is limited to corneal surface and limbus is mostly not

involved. In case of unilateral or bilateral limbal deficiency conditions, PTK is followed by corneal transplantation to regain vision.

2.5.3 Corneal transplantation

A corneal transplant surgery is intended to replace an injured or diseased cornea with a donor one. The central corneal region is removed and replaced by a donor cornea usually from the eye bank. Corneal transplants are very common in this new era and have saved sights of many suffering from corneal injury, infection, or inherited corneal disease or degeneration. Donor corneal transplants is preferred for treatment of various corneal diseases like keratopathy, corneal dystrophy and corneal scar. However, Donor corneal transplants will be successful in cases where, limbus is not usually affected and not so beneficial in case of limbal stem cell deficiency (LSCD). Corneal transplantation was also modified over time. Earlier the technique was called penetrating keratoplasty; this is a full thickness graft where the entire cornea is replaced with a donor cornea (Tan et al., 2012). Recently this procedure was modified and is called lamellar keratoplasty which is a partial thickness graft herein only the diseased layer in the cornea is replaced instead of an entire cornea (Espandar and Carlson, 2013). Replacing only the diseased portion keeps the host cornea intact and minimises the foreign donor portions to the minimum thereby reducing post-transplantation complications.

Lamellar keratoplasty is of different types depending upon what part of the cornea is removed in the procedure. Anterior lamellar keratoplasty is designed to remove the anterior cornea leaving behind the posterior cornea intact. This procedure is less invasive than a penetrating keratoplasty (Yeung et al., 2012). In deep anterior

lamellar keratoplasty (DALK), the patient's normal endothelium is preserved whereas stroma and epithelium are replaced by the donor tissue (Terry, 2000). Endothelial lamellar keratoplasty replaces damaged or degenerated endothelial tissue with a donor healthy endothelial layer. Descemet Stripping Automated Endothelial Keratoplasty (DSAEK) is a partial thickness corneal transplant (Price and Price, 2005). This procedure involves the removal of Descemet's membrane and endothelium which is then replaced by a donor counterpart. All this methods relay on allogenic corneal sources which always pose a threat of rejection on the recipient.

2.5.4 Artificial Cornea

Boston Keratoprosthesis (B-KPro) is a complete artificial cornea. B-KPro may be the only option for end-stage tissue failure and graft rejection cases. Boston type 1 keratoprosthesis is one well used prosthetic device (Al Arfaj and Hantera, 2012). It consists of three parts with donor cornea tissue clamped between front and back plates resembling a collar button. Successful clinical use of B-KPros is being reported from various studies, even though, financial challenges, lack of trained surgeons, shortage of donor corneas are still limitations in using this artificial cornea (Al Arfaj, 2015).

2.5.5 Treatment for LSCD

In partial damage conditions, improving ocular surface health is one effective means to provide a better environment which may help the remaining LSCs to survive. If visual axis gets affected, then sequential sector conjunctival epithelialectomy is the preferred mode of treatment (Dua, 1998). This procedure removes conjunctival epithelium that has invaded the cornea thereby improving

vision by promoting epithelialisation. This procedure can also be combined with amniotic membrane patch on the corneal surface for enhanced epithelialisation and corneal wound healing. Transplantation of amniotic membrane to damaged cornea prevent recurrent epithelial erosion and promotes epithelialisation and visual rehabilitation (Anderson, 2001). Another alternative approach towards treating partial LSCD is ipsilateral limbal translocation. In this case, the undamaged limbus from the eye is used to treat a damaged limbal region in the same eye. This helps in repopulation of limbal cells and thus enhancing normal healing (Nishiwaki-Dantas et al., 2001).

Total LSCD can be either unilateral or bilateral. An autograft from the contra lateral eye is opted and is considered gold standard, while in case of bilateral conditions, the allograft is the only available option. Autograft technique involves harvesting of a small limbal biopsy from the contralateral eye and is transplanted to the injured eye (Kenyon and Tseng, 1989). Autografts avoid chances of graft rejection and immunosuppression and favour improved healing, increased vision and regression of LSCD. But at the same time, surgical intervention of the contralateral eye is not preferred by most patients as it can also cause limbal erosion in the normal eye. In bilateral LSCD conditions where both the eyes are involved and limbus is completely damaged, allograft remains the only feasible option. Limbal biopsies were obtained from the cadaveric eye or HLA matched donors by superficial lamellar dissection after central cornea trephining (Dua et al., 2000) and are then transplanted to the diseased eye. Since these grafts are from a donor tissue, these procedures have to be followed by long-term immunosuppressive therapies and also involves a high risk of graft rejection. In case of allogeneic transplantation,

acceptance of graft by the host tissue dramatically increases when tissues from HLA matched individuals are used in combination with amniotic membrane during transplantation (Gomes et al., 2003). But in comparison with autograft transplantation the failure rates of allogenic transplants are quite high (Solomon et al., 2002). Apart from issues associated with allografts, the availability of donor allografts itself is a major issue that limits above methods of treatment. To highlight the severity of the scenario in India, only 25000 corneas are collected for transplants against the annual demand of 2, 50,000. Alternate methods have to be attempted to reconstruct the damaged cornea and restore vision. Tissue engineering approaches are the one being in focus which aims at corneal reconstruction through cell-based, lab-developed corneal layers supported by various scaffolds to artificial synthetic corneas.

2.6 Use of Amniotic membrane in corneal surface damage conditions

There is increasing evidence on the use of an amniotic membrane as a tool in the treatment of various ophthalmic conditions that affect the ocular surface. Amniotic membrane is the innermost layer of the placenta consisting of a single layer of cuboidal to columnar epithelium that is attached to the basement membrane and an avascular stroma (Malhotra and Jain, 2014). Davis in 1910, first reported the use of AM in therapeutic purpose for skin transplantation (Davis, 1910). Subsequently, AM was demonstrated in ocular surface damages by de Roth in 1940 for treatment of the ocular surface with chemical burn (de ROTTH, 1940). The epithelium and stroma harbour within it a lot of cytokines and growth factors

including transforming growth factor beta, fibroblast growth factor 6 and epidermal growth factor (Koob et al., 2013).

Amniotic membrane is used in various means for ocular surface reconstruction. In few cases, AM is used as a graft where the amniotic membrane is intended to act as a substrate support to mobilize host epithelial cells (Zhang et al., 2016a). Amniotic membrane is also used as a patch where these are essentially used as a biological bandage (Gruss and Jirsch, 1978). The main function is to support the underlying cells or tissues to grow and perform their function. These patches are removed over time from the host tissue.

Amniotic membrane is used alone or in combinations with stem cell transplantation for ocular surface therapies depending on the extent any kind of damage (Du et al., 2003). AM has been applied successfully in clinical settings for various ocular surface disorders like Stevens-Johnson syndrome, chemical or thermal burns and ocular cicatricial pemphigoid (OCP) (Rahman et al., 2009). Tsubota et al., first attempted the use of AM in patients with OCP (Tsubota et al., 1996) while Sangwan et al. demonstrated the successful application of AM membranes on patients with partial LSCD (Sangwan et al., 2004). In the case of total LSCD, 60-70% of people successfully responded to AM transplantation. The success rate was variable on a patient to patient basis depending on the conjunctival involvement in the damage.

Unfortunately, there are several limiting factors with the use of the amniotic membrane. The first is the supply of the raw materials to meet demand, associated processing, cold chain storage and distribution conditions. The second is that amniotic membrane is a biologically variable tissue (Malhotra and Jain, 2014)

which limits the ability to manufacture a truly standardized and reproducible ‘off the shelf’ product with no batch to batch variations. The need for cold storage, risk of cryptic infections and thorough screening of donors further limits its usage (Rahman et al., 2009). Therefore, the search for an alternative material, preferably synthetic in origin, is of great interest to replace the use of the amniotic membrane. The challenge is to recreate the properties of the amniotic membrane without compromising on its functional relevance in supporting cell growth. Though a standardized, reproducible and generic amniotic membrane alternative is highly desirable, unfortunately, no available substrate, to date, has been able to fully recapitulate the ability of the amniotic membrane to support cell growth and stem cell survival. However, development in the field of tissue engineering has indicated the use of novel biomaterials and scaffold-free transplantation concepts for corneal reconstruction therapies.

2.7 Tissue engineering approaches towards corneal repair

"Tissue engineering (TE) is an interdisciplinary field that applies the principles of engineering and life sciences towards the development of biological substitutes that restore, maintain or improve tissue function (Langer and Vacanti, 1993). Tissue engineering aims at addressing issues in human health care combining the interdisciplinary fields of engineering and biology. Recent advances in this field focus on regenerating or reconstructing organs addressing the issues of organ donor shortage. The main components in this field include cells, matrix, conditional signals and growth factors (O’Brien, 2011). Tissue engineering has far-reaching applications in the field of ophthalmology and it focuses issues addressing corneal and retinal

degeneration. Various techniques using different cell types with or without scaffold have been evolved for the effective ocular surface reconstruction.

2.7.1 Cell choices for ocular surface reconstruction

The limbal stem cells located deep within the palisade of Vogt at the corneoscleral junction is the major cell source attempted for use in tissue engineering strategies (Pellegrini et al., 1997). Allogeneic and autologous cells are attempted depending on the extent of damage and type of deficiency. Limbal stem cells being a pre-committed group of stem cells has a limited lifespan and undergo quick differentiation to corneal epithelial cells. In partial and unilateral conditions, limbal stem cells are still considered the gold standard. In case of bilateral deficiencies, other cells sources have to be explored to address issues with graft rejection and immune suppression. In order to overcome these problems, alternative autologous sources with potential for ocular surface reconstruction have to be explored. Various cell sources from epithelial, mesenchymal and embryonic lineages were attempted for use in the ocular surface reconstruction (Sehic et al., 2015). Oral mucosal cells are one best-suggested alternate to limbal stem cells. Carrier-free cell sheets using autologous oral mucosal epithelial cells has been used as an alternative to limbal stem cells and was demonstrated in patients with severe bilateral disorders of the ocular surface (Nishida et al., 2004).

There have been reports of differentiation of human embryonic stem cells to epithelial-like cells when cultured on collagen IV in limbal fibroblast conditioned medium (Ahmad et al., 2007)). Another group reported differentiation of murine embryonic into corneal epithelial cells *in vitro*. These differentiated cells expressed

cytokeratin 3, ABCG2 and P63 (Zhang et al., 2017). Reports also suggest that adult hair follicular epithelial stem cells differentiated to corneal epithelial-like cells in *vitro* and was demonstrated to restore visual function in patients with ocular surface disorders (Blazejewska et al., 2009). Saichanma et al., successfully demonstrated the use of skin-derived stem cells for restoring a normal corneal surface when expanded in vitro (Saichanma et al., 2012).

Mesenchymal stem cells (MSC) is another group of stem cells well established in the field of regenerative therapies. These are isolated from a variety of sources from the body. MSCs are also reported for use in ocular surface reconstruction. Ma *et al.,* used MSCs from bone marrow for the reconstruction of corneal surface to promote corneal wound healing (Ma et al., 2006). The presence of MSC like cell within cornea expressing MSC properties (Yoshida et al., 2006)), presence of ABCG2 marker pertaining to limbal epithelial stem cells (Poleshko and Volotovski, 2016), (de Paiva et al., 2005) , multilineage differentiation potential of MSCs (Alhadlaq and Mao, 2004) and extra mesenchymal differentiation potential to epithelial lineage (Sueblinvong et al., 2008) make MSCs an ideal candidate and an alternate autologous cell source to limbal stem cells for ocular surface regeneration.

2.7.2 Adult stem cells

Mesenchymal stem cells belong to the most promising group of adult stem cells in the human body with proven potential in the field of tissue engineering and regenerative medicine. Recently, there are reports of using mesenchymal stem cells (MSCs) for corneal surface reconstruction. *In vitro* and *in vivo* data generated from MSCs in corneal surface reconstruction provided ample evidence to

substantiate the role of MSCs in modifying the microenvironment and playing a role in corneal wound repair(Zhang et al., 2015).

MSCs are said to self-renew as stem cells and can differentiate into various lineages including bone, cartilage, fat, muscle neurons, cardiac muscle cells and epithelial cells (Sottile et al., 2007). These are multipotent progenitor cells easily isolated from various anatomical locations like the bone marrow, adipose tissue, Wharton's jelly, dental pulp, peripheral blood, cord blood (Law and Chaudhuri, 2013) and limbal stroma of the human eye (Hashmani et al., 2013). MSC became potential candidates in regenerative medicine studies because of lack of expression or minimal expression of major histocompatibility class II (MHC II) and other co-stimulatory CD markers under normal conditions allowing them to escape the host response system upon infusion to an allogenic host environment (Gao et al., 2016). Moreover, the anti-inflammatory and angiogenic effects of MSCs make them the best candidate for use in regenerative medicine therapies.

MSCs are now widely attempted in corneal repair research too (Li and Zhao, 2014). MSCs are either administered directly to the cornea (Yao et al., 2012) or by carriers, such as the amniotic membrane (Ma et al., 2006) or fibrin gels (Gu et al., 2009). There are reports on trans differentiation potential of MSCs as they can differentiate to corneal epithelial cells when given appropriate cues. Various reports suggest that MSCs can express CK3/12, a corneal differentiation marker, under suitable differentiation environment. Gu et al. demonstrated that MSCs can differentiate into corneal epithelial-like cells *in vivo* and *in vitro* (Gu et al., 2009). Either differentiated or undifferentiated MSC sheets are said to be beneficial, as both have been shown to play a role in corneal wound healing (Zhang et al., 2015).

2.7.3 Adipose-derived mesenchymal stem cells

The term "adipose-derived stem cell" (ASC) refers to the unique population of MSCs and more-committed progenitor cells present within the stroma of adipose tissue. (Flynn and Woodhouse, 2008). Zuk *et al.* identified this putative stem cell population from a lipo-aspirate and termed it as processed lipoaspirate (PLA) (Zuk et al., 2002). These isolated cells were shown to have multilineage differentiation potential as they differentiated to osteogenic, adipogenic, chondrogenic, myogenic and neurogenic lineages (Zuk et al., 2002). ASCs displayed striking similarities with marrow-derived stem cells in morphology and phenotype both these group of stem cells express multi-differentiation potential and also express a similar array of CD markers which are supposed to be present on the surface of MSCs (Gomillion and Burg, 2006). The advantage of ASCs over marrow-derived stem cells is that adipose tissue is readily accessible, abundant and usually removed as a waste in the lipo-aspiration procedure. ASCs isolated from adipose tissue may be a better candidate for cell therapy and tissue engineering as lipo aspirates are a good source of human ASCs (Lin et al., 2008). Cells being from the patient's own fat, lead to an autologous therapy eliminating issues of immune rejection. In short adipose tissue represents an abundant, practical, feasible source of donor tissue for autologous cell replacement therapies where stem cells within the stromal-vascular fraction provide us with a potential cell source with therapeutic potential.

2.7.3.1 Nomenclature of Adipose-derived Mesenchymal stem cells

Soon after Zuk et al., identified adipose-derived stem cells (Zuk et al., 2002), different groups reported the presence of these stem cells in various

anatomical locations and named them differently. Different nomenclatures include terms like adipose-derived stem/stromal cells (ASCs), adipose-derived adult stem (ADAS) cells, adipose-derived adult stromal cells, adipose-derived stromal cells (ADSCs), adipose stromal cells (ASCs), adipose mesenchymal stem cells (ASCs), lipoblast, pericyte, pre-adipocyte and processed lipoaspirate (PLA) cells. The International Fat Applied Technology Society reached a consensus to adopt the term "adipose-derived stem cells" (ASC) to stem cells isolated from adipose tissue (Gimble et al., 2007)

2.7.3.2 Identification of Mesenchymal stem cells

To confirm that the isolated cells can be considered as mesenchymal stem cells, the main criteria to be followed are

- They should be plastic adherent
- They should be able to be differentiated to all the three lineages to prove its multilineage differentiation potential.
- Presence of a series of CD markers to be expressed by the isolated cells

A brief list of surface markers expressed by mesenchymal stem cell which is also applicable for adipose-derived mesenchymal stem cells are given below (Zuk et al., 2002) (Flynn and Woodhouse, 2008). Table 2 gives the list of surface positive and negative markers for mesenchymal stem cells**.**

MSC Markers	Effect	MSC Markers	Effect
CD9 (tetraspan)	+	CD54 (ICAM-1)	+
CD10 (CALLA)	+	CD90 (Thy-1)	+
CD11 (α-integrin)	-	CD105 (Endoglin)	+
CD13 (aminoepetidase)	+	CD106 (VCAM)	+/-
CD31 (PECAM-1)	-	CD117 (c-kit)	+
CD34	+/-	α-smooth muscle actin	+
CD44 (hyaluronate receptor)	+	Collagen type I	+
CD45 (LCA)	-	Collagen type II	+
Stro -1	+/-	Vimentin	+

Table 2: Common stem cell markers (Gomillion and Burg, 2006)

2.7.4 Carriers used in ocular surface reconstruction

Various attempts to use multiple cell carriers to transfer cells on to ocular surface are in practice. The most effective among them is amniotic membrane based transplantation (Gomes et al., 2003). One of the most extensively used natural material to grow and transplant stem cells is an amniotic membrane (AM) (Anderson, 2001), a component of the sac surrounding the developing fetus, which is usually discarded at birth. .The amniotic membrane acts as a carrier as well as an effective wound dressing that can be used alone without cells for ocular surface therapies (Gruss and Jirsch, 1978; Tseng, 1998). Amniotic membrane has proven to be an ideal and effective substrate for growing and supporting cells for transplantation. There are reports of using alternative cell carriers based on collagen,

fibrin, siloxane hydrogel contact lenses, poly (ε-caprolactone), gelatin-chitosan, silk fibroin, human anterior lens capsule, keratin, poly(lactide-co-glycolide), polymethacrylate, hydroxyethyl methacrylate and poly(ethylene glycol) for their potential use in corneal surface reconstruction. Scaffold-free transplantation of cell sheets was also attempted avoiding the use of foreign carrier platforms (Tang and Okano, 2014). Gu et al. has used fibrin successfully as a carrier for transplantation of bone marrow MSC into rabbit models (Gu et al., 2009). Non-mulberry silk fibroin was also reported as a carrier for corneal surface reconstruction (Hazra et al., 2016). Scaffold-free cell sheets provide an advantage not only by avoiding foreign transfer materials but also enhance the therapeutic benefits by providing cell as a sheet rather than in suspension (Narita et al., 2013).

2.7.5 Cell sheet Technology

Cell sheets are successfully engineered using temperature-responsive matrices, whose properties alter with a change in temperature (Matsuura et al., 2014). Cell sheet engineering is now demonstrated with a variety of cell types for various regenerative therapies and at least few of these concepts are promising and enable development of tissues and organs. Some of the regenerative therapies using monolayer cell sheets are in clinical trials addressing cornea, oesophagus, skeletal muscle, periodontal and myocardium (Miyagawa et al., 2017), (Iwata et al., 2015), (Nishida et al., 2004). Cell sheet engineering is assumed to develop and address the issue of organ transplantation to an extent.

The concept of ‘cell sheet engineering’, is based on harvesting intact cell sheets using stimuli-responsive cell culture surfaces. When cells are grown as a

monolayer on thermoresponsive surfaces, it enables us to harvest back these cells as sheets without the use of proteolytic enzymes, such as trypsin or dispase, thereby reducing cell damage and loss of function (da Silva et al., 2007). Since cells are detached as a sheet without much application of enzymatic or mechanical force, the extracellular matrix (ECM) secreted by the cells are also trapped or harboured within these cell clusters which is an added advantage of cell sheet engineering. The cell sheets being an independent unit, with intact cell-cell, cell- ECM can be transferred or transplanted directly to tissue beds or even overlapped to make 3D structures (Chen et al., 2015). This approach of transplanting cell sheets appears to have numerous advantages over conventional tissue engineering strategies including cell injections and use of biodegradable scaffolds. Reports suggest that homing of MSCs to target organs or sites is below 5% in case of systemic infusions (Kang et al., 2012). Enhanced therapeutic effects by the cell sheet technique have been reported in comparison with other cell delivery methods, as the cell sheets achieve greater donor cell presence (Narita et al., 2013). Injected cells even though exist as a population, interact with the damaged host microenvironment as independent cells and thus are difficult to survive and perform its function in the damaged microenvironment. While the cell sheet behaves as a unit of cell cluster where each cell is mechanically supported by the other. Along with the deposited ECM, cell sheets can attach to host tissues and will add more therapeutic benefit to the damaged region in comparison of injected cell suspensions (Narita et al., 2013). Cell sheet engineering has been demonstrated successfully in various tissues including cornea. Oral mucosal tissue derived cultured epithelial cell sheets have been successfully developed using thermoresponsive polymer surfaces. A pre-clinical study was carried out with rabbit

LSCD model (Hayashida et al., 2005) and also was demonstrated to be successful in human patients (Nishida et al., 2004) which was the first clinical trial using cell sheets for medical application.

Additionally, induced pluripotent stem (iPS) cell and embryonic stem cell (ESC) derived cell sheets have been proposed and attempted for tissue regeneration (Sehic et al., 2015). Current applications of MSCs in wound healing use intramuscular or intravenous injection of MSC expecting them to home at the site of injury (Wang et al., 2012) along with the direct application of cells on to the wounded surface. MSCs as a sheet will have an enormous number of medical applications due to their aforementioned properties. MSC cell sheets have been attempted in the field of bone tissue engineering using magnetic nanoparticles, treatment of periosteal defects and myocardial infarction using PNIPAAm (Augustin et al., 2013; Long et al., 2014; Shimizu et al., 2007). Since MSCs can be isolated from a variety of sources, a patient can always rely on his autologous mesenchymal stem cell for regenerative therapeutic interventions.

2.7.6 Thermoresponsive polymers

Thermoresponsive polymers fall into the class of "smart" materials with the ability to respond to change in temperature. This temperature sensitiveness was made use of in a wide range of medical applications and attracts huge scientific interest. These group of polymers are used for biomedical applications including drug delivery, tissue engineering and gene delivery(Shimizu et al., 2010; Stile and Healy, 2001; Twaites et al., 2005). These polymers exhibit a phase transition at a particular temperature. This is due to change in the solvation state of the polymers

caused by changes in inter and intramolecular hydrogen bonding. Polymers which become insoluble upon heating are called Lower critical solution temperature systems, while those systems which become soluble upon heating are said to have an upper critical solution temperature (Feil et al., 1993), (Gandhi et al., 2015).Poly(N-alkylacrylamide)s is one class of thermos responsive polymer. Poly (N-isopropylacrylamide) (PNIPAAm) is the most prominent candidate in this class along with PDEAM (poly(N,N-diethylacrylamide)). Both these polymers have been efficiently used and demonstrated for tissue engineering and cell culture applications (Schild, 1992), (Fujishige et al., 1989). Changing the temperature to below lower critical solution temperature (LCST), PNIPAAm will become hydrophilic, enabling the easy detachment of cell sheet with intact cell-cell and cell-extracellular matrix (ECM) contacts. Below LCST, the polymer changes its surface behaviour from hydrophobic to hydrophilic thereby allowing the cells to detach from the polymer surface as a sheet without applying any mechanical pressure on the cells (da Silva et al., 2007). Even though Poly(N-vinyl caprolactam) (PVC) possess thermoresponsive behaviour with a transition temperature around 33°C, has not been utilized intensively as PNIPAAm (Makhaeva et al., 1998) for tissue engineering applications. Poly(N-ethyl oxazoline) (PEtOx) have a transition temperature around 62°C, which is too high for any biomedical applications (Rueda et al., 2005). Poly (methyl vinyl ether) (PMVE) has a transition temperature exactly at 37 °C, which makes it very interesting for biomedical application. PMVE is sensitive to alcohol or amino groups and this limits its potential use as a thermos sensitive polymer (Gandhi et al., 2015). An interpenetrating network of poly (acrylic acid) and polyacrylamide is one system with UCST behaviour within the biomedical setting. The transition temperature is at

25 °C (Aoki et al., 1994). Elastin Polypeptides can also show LCST behaviour when hydrophilic and hydrophobic residues are balanced well. The LCST behaviour of these polymers is tailored in a way that the slightly higher change in temperature is enough to undergo a phase transition (Gandhi et al., 2015).

2.7.7 Biofunctionalization of thermoresponsive polymers

Thermoresponsive polymers can be modified to increase the bio-functionality of the polymer by incorporating various biomolecules, protein and growth factors. One of the methods attempted was to immobilize biomolecules into the polymer. Most of the attempts were made with PNIPAAm backbone as this was widely used in biomedical settings. Copolymers of PNIPAAm was made with acrylic acid (AAc) to incorporate a reactive carboxyl group to polymer backbone (Stile and Healy, 2001). This modification increased the LSCT of the copolymer formed and also hindered cell spreading (Chen and Hoffman, 1995). To prevent a change in LCST, a 2-carboxyisopropylacrilamide (CIPAAm) polymer was synthesised with a functional carboxylate group and a similar chain structure that of PNIPAAm (Aoyagi et al., 2000). CIPAAm copolymer-grafted surfaces had an accelerated cell detachment rate compared to PNIPAAm surfaces (Ebara et al., 2003). Arg-Gly-Asp-Ser (RGDS) peptides were covalently immobilized onto poly (IPAAm-co-CIPAAm)-grafted TCPS dishes which resulted in enhanced cell spreading and adhesion without affecting cell sheet detachment (Ebara et al., 2004). Co-immobilization of RGDS and Pro-His-Ser-Arg-Asn (PHSRN) sequences onto poly (IPAAm-co-CIPAAm)-grafted dishes were also attempted to enhance cell detachment (Ebara et al., 2008). Joseph et al attempted to incorporate a Glycidyl group into PNIPAAm backbone, which can

provide a reactive epoxy group available for biofunctionalization (Joseph et al., 2010). This may enable peptide linking to polymers which are reported to give more control over cell attachment and detachment enabling more control over the required application (Ebara et al., 2008).

2.7.8 Animal models for corneal surface reconstruction

Preclinical evaluation for corneal repair was attempted in various animal models for evaluating the efficacy of the therapy before clinical experiments. Rabbit, goat and rat models were widely attempted for corneal reconstruction studies. Gomes *et al.* has created LSCD models using alkali burn by sodium hydroxide (NaOH) and was treated using tissue-engineered cell sheets composed of human immature dental pulp stem cells (Gomes et al., 2010). Gu *et al.* has attempted differentiation of rabbit bone marrow mesenchymal stem cells into corneal epithelial cells and evaluated in vivo in rabbit injury models developed by alkali damage (Gu et al., 2009). Omoto *et al.* attempted bone marrow human mesenchymal stem cells as feeder for epithelial cell sheets in rabbit alkali damage models and reported corneal surface reconstruction (Omoto et al., 2009). Similar report was published by Reinshagen *et al.*, using bone marrow mesenchymal stem cells for corneal surface reconstruction in rabbit models created by chemical damage with n-heptanol and surgical incision of limbus (Reinshagen et al., 2011). Multiple groups have attempted MSCs on rat models for corneal surface reconstruction (Jiang et al., 2010; Rohaina et al., 2014). Mouse cornea was treated with n-heptanol for creating a chemical damage and was then treated with mouse embryonic stem cells (Homma et al., 2004). Most of the

animal models reported success in short-term and few have reported long-term success in corneal surface reconstruction.

2.8 Lacuna in current scenario and rationale for the present study

In most of the corneal surface damages, the corneal epithelial regeneration will be affected if limbus is damaged partially or completely. Normal homeostasis of the corneal epithelial regeneration depends on the extent of damage and availability of limbal stem cells in the limbal niche. Incomplete damage, limbus is not available and in partial damage, the extent of damage determines normal healing process (Dua, 2001). In unilateral damages (one eye is affected), an autologous limbal transplant from the contralateral eye is an option. In case of bilateral damage when both eyes are damaged, allogenic therapies are the only available options. The main disadvantage projected in autologous limbal transplant, is the surgical intervention in the healthy eye, while allogenic transplantation reports high chances of immune rejection and long-term failures.

Identifying an autologous cell population with the potential to replace and perform limbal stem cell function would be an ideal solution to address the aforementioned scenario. There are a lot of cell sources in literature attempted for corneal surface reconstruction from ocular and non-ocular cell sources which include, induced pluripotent stem cells, embryonic stem cells, epithelial and mesenchymal cell sources (Sehic et al., 2015). Oral mucosal progenitor cells are currently stated as the best available non-ocular source to date (Nishida et al., 2004). Mesenchymal stem cells are also attempted due to their enhanced therapeutic effect when compared to other cell sources (Kim and Cho, 2013; Kim and Park, 2017).

Moreover using MSCs allow us to harvest these cells from multiple locations of the body unlike oral mucosal cells (El, 2011).

Even if an ideal cell candidate was identified within the patient's own body, it has to be streamlined in a way that maximum therapeutic benefits are achieved. Multiple cell carriers for transplantation are in practice, of which the most effective among them is amniotic membrane based transplantation (Gomes et al., 2003). There are reports of using alternative cell carriers based on collagen, fibrin, siloxane hydrogel contact lenses, poly (ε-caprolactone), gelatin-chitosan, silk fibroin, human anterior lens capsule, keratin, poly(lactide-co-glycolide), polymethacrylate, hydroxyethyl methacrylate and poly(ethylene glycol) for their potential use corneal surface reconstruction. Scaffold-free transplantation of cell sheets was also attempted avoiding the use of foreign carrier platforms (Tang and Okano, 2014). Using cell sheets provide an advantage not only by avoiding foreign transfer materials but also enhance the therapeutic benefits when compared to cells in suspension (Narita et al., 2013).

Herein the suitability of an in-house developed thermoresponsive polymer NGMA was evaluated (N-isopropylacrylamide-co-glycidyl methacrylate), for mesenchymal cell sheet engineering. The focus was on creating corneal epithelial differentiated MSC sheet using thermoresponsive polymer NGMA as an effective mode of a therapeutic system for corneal surface reconstruction. This work demonstrated adipose MSCs as an alternative cell source to limbal stem cells. In terms of its application, autologous MSCs along with cell sheet engineering eliminate the use of allogeneic cells thereby ensuring a complete autologous

bioengineered graft avoiding immune suppression and immune rejection. Firstly attempts were made to differentiate ASCs into corneal epithelial lineage so as to assess whether ASC can be used as an alternative to limbal stem cells and then transformed into a sheet. Efficacy of the cell sheet was then evaluated in a rabbit corneal injury model in a one-month study.

As a small detour from the mainframe, this work was taken to the next level by bio functionalizing NGMA with Amniotic membrane (AM) protein as the amniotic membrane is routinely used as a wound dressing and a carrier support in corneal surface damages. AM proteins were conjugated to NGMA by making use of the epoxy ring opening mechanism in GMA group of the NGMA copolymer. The idea was to develop a bio-functionalized transplantable amniotic membrane alternative for use in enhanced corneal regenerative studies. Modifying NGMA with AM proteins helps the NGMA surface to mimic the substrate properties of amniotic membrane for the development of an innovative, carrier free strategy for expanding and transplanting human corneal stromal derived stem cells. AM conjugation and corneal cell sheet retrieval was successfully attempted, demonstrating the possibility of innumerable avenues towards guided cell sheet engineering with conjugating proteins and other components required for guided selection and differentiation of cells

Herewith, this work put forward a carrier free cell sheet transplantation which has not been attempted with ASCs. Cell sheet technology using thermoresponsive culture surface can provide *in vitro* carrier free corneal epithelial constructs qualified for transplantation. *In vitro* evaluated mesenchymal cell sheet

with corneal epithelial differentiation potential was evaluated for its efficacy *in vivo* in a rabbit LSCD model for a period of one month. Simultaneously, human corneal stromal cell sheets developed on AM protein conjugated NGMA could be a bio-functionalized transplantable amniotic membrane alternative for use in corneal regenerative studies.

2.9 Strategizing the Hypothesis

1. The concept leading to the hypothesis include the need to identify an easily accessible alternate autologous cell source to limbal stem cells in case of total limbal damage conditions.
2. To streamline the above concept with a technology that will ease the transplantation procedure with beneficial therapeutic effects, thereby addressing the major limitations of modern day corneal epithelial transplantation including the paucity of donor tissue, graft rejection and failure.

The hypothesis statement can be thus formulated as

"***Stromal-derived Mesenchymal Stem Cells as an alternate to limbal stem cells combined with cell sheet technology will be an effective therapeutic mode in the treatment of corneal surface damages and limbal deficiency conditions thereby addressing other major limitations including the paucity of donor tissue and graft rejection***".

2.10 Aim and Methodology

The goal is to restore a normal ocular surface using bioengineered mesenchymal cell sheets in rabbit corneal injury models.

Methodology adopted

- Development of the thermoresponsive surface (poly(N-isopropylacrylamide-co-glycidyl methacrylate) NGMA
- Biofunctionalization of NGMA with Amniotic derived proteins (Ampro)
- Isolation, culture and characterization of Adipose-derived Mesenchymal stem cells (ASC)
- Evaluation of Adipose stem cells sheets on NGMA
- Differentiation of Adipose MSC to corneal epithelial lineage and cell sheet retrieval.
- Isolation and cell sheet formation of human-derived corneal stromal stem cells on AM protein biofunctionalized NGMA (Ampro-NGMA)
- *In vivo* efficacy evaluation of trans differentiated ASC cell sheet using rabbit corneal injury model.

2.11 Schematic Work Plan

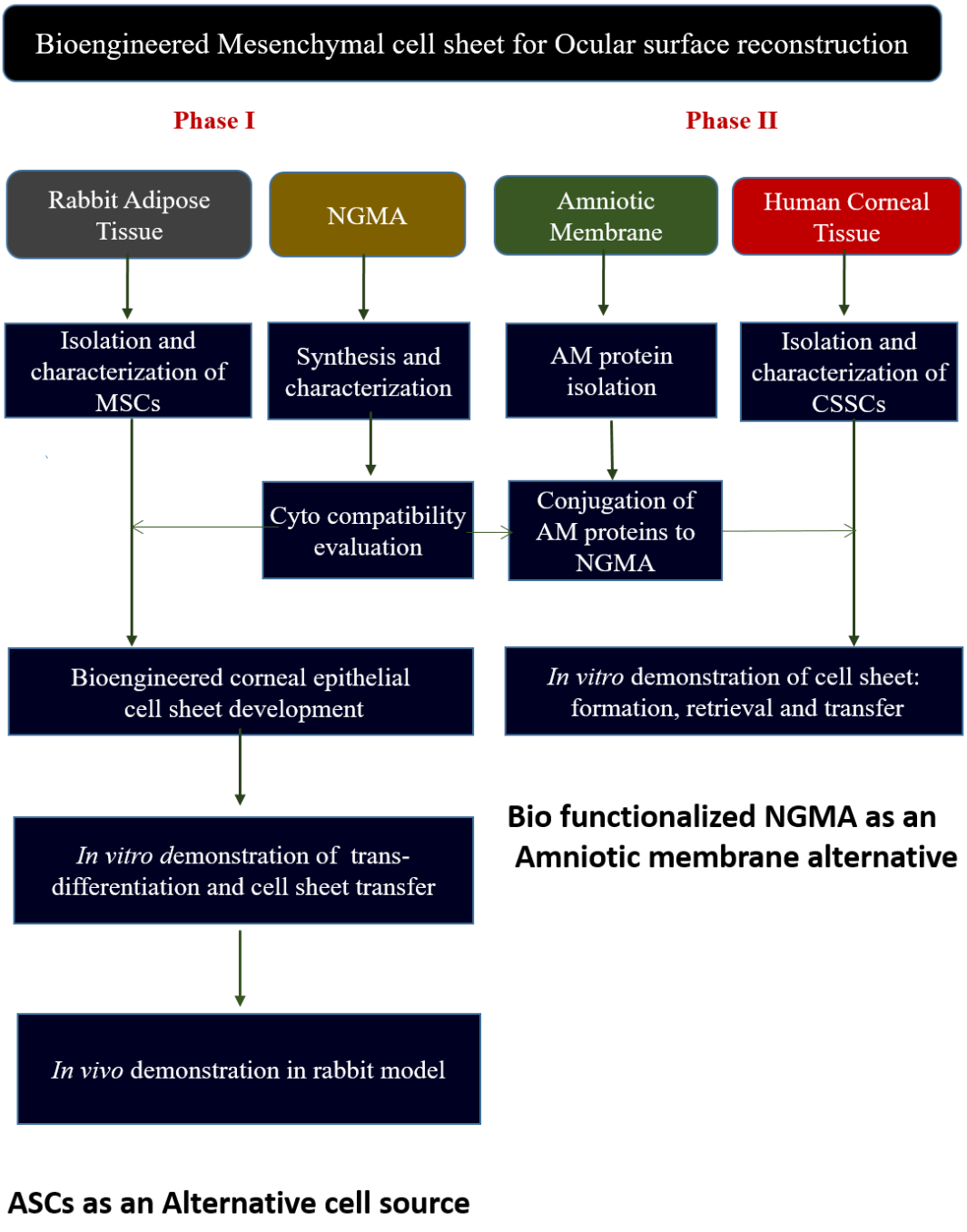

CHAPTER - III

3 MATERIALS AND METHODS

3.1 NGMA Synthesis

Co-polymer NGMA was synthesized in-house by free radical random copolymerization of NIPAAm (Sigma-Aldrich) with GMA (Sigma-Aldrich) in 10:1 ratio based on the procedure of Joseph et al., (Joseph et al., 2010). The reaction was carried out in methanol (Merck), in presence of nitrogen with Azo-bis-isobutyronitrile (AIBN) (Spectrochem) as initiator at 60^{o}C with gentle stirring. The reaction was continued for 6h. The copolymer was obtained as a viscous solution that was dissolved in Tetrahydrofuran (THF) (Merck). The copolymer was precipitated using water/ THF multiple times to remove unreacted monomers and dried in an oven. The dried copolymer was dissolved in isopropanol to make a 4% NGMA solution. This 4% NGMA solution was used to hand-coat 35 mm culture dishes (Nunc).

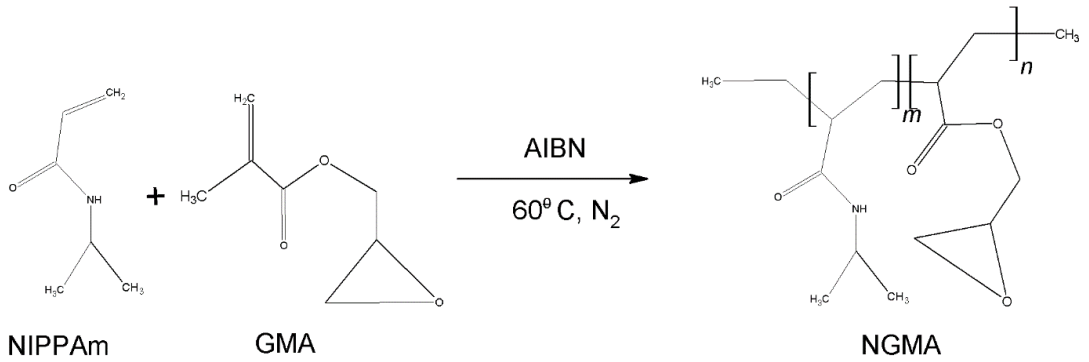

Figure 4: Schematic representation of NGMA Synthesis

The solution was dropped on to the dish, swirled and the remaining solution was collected by tilting the dish to one side. The culture dish was allowed to dry at 55°C overnight and then rinsed with cold distilled water to remove impurities and unbound NGMA. Later the dish was air dried, packed and sterilized using ethylene oxide.

3.2 Physico-chemical Characterization

The copolymer formed was then characterized and confirmed for its various physicochemical properties including functional group evaluation, phase transition, surface wettability and thermal analysis.

3.2.1 Attenuated Total Reflectance–Fourier Transform Infrared Spectroscopy

Functional groups were evaluated by reading the FT-IR spectrum with a horizontal attenuated total reflectance (ATR) (Thermo Nicolet 5700 model, Thermo Electron Scientific Instruments Corp., Madison, WI USA). Spectra were taken in the wavelength region from 600 cm^{-1} to 4000 cm^{-1} from 64 scans. The coating of NGMA on the culture dishes was also evaluated to determine the coating behaviour. The NGMA coated culture dishes were compared with pure NGMA to determine the effective coating of the dishes.

3.2.2 Differential Scanning Calorimetry

The phase transition property of NGMA was identified using differential scanning calorimetry (DSC). The lower critical solution temperature (LCST) value for NGMA was determined by allowing the sample to swell in distilled water. About 10 mg of equilibrium swollen sample was sealed in hermetic pans and thermal

analysis was performed from 0ºC to 60ºC at a heating rate of 3ºC/min in a nitrogen atmosphere. (DSC Q 100, TA Instruments Inc, USA).

3.2.3 Water Contact Angle

The surface wettability of NGMA coated culture dishes was determined by water contact angle (WCA) measurement using sessile drop method (NRL Contact Angle Goniometry). The contact angle was measured with OCA 15 plus (DataPhysics, Germany), a video-based contact angle measuring device and was imaged using imaging software (SCA 20). For statistically significant data, 3 different NGMA dishes were analyzed. Data are expressed as a mean ± standard deviation.

3.2.4 Gel Permeation Chromatography

The average molecular weight of the polymer was determined by gel permeation chromatography using Waters HPLC system 600 series pump with styragel HR series columns (Waters, Canada). The molecular weight was estimated from 1% polymer solution in THF. Polystyrene standards for peak molecular weight (Mp) of 100000, 34300 and 3250 were used for relative calibration.

3.2.5 Thermo Gravimetric Analysis

Thermogravimetric analysis (TGA) was done to determine the thermal stability of polymer NGMA using SDT Q600, simultaneous DTA-TGA system (TA Instruments, USA). The test method is based on ASTM E 1131-08 (Krishna et al., 2015). Before starting the experiment, the mass of the sample and reference pans are tared using the software. 10mg of the freeze-dried sample was taken in a platinum

cup and heated under nitrogen atmosphere at a heating rate of 10°C/min. The temperature range for the particular experiment was from room temperature to 800°C. The reference material used was calcined Alumina.

3.3 *In-vitro* Cytotoxicity assay of NGMA

In vitro cytotoxicity of NGMA was evaluated by test on extract method and MTT assay based on ISO 10993/5 standard. The mouse fibroblast cell line [L929] was used for the cytotoxicity assay as per the prescribed standard. The NGMA was hand coated into 35 mm dishes. Cytotoxicity of NGMA was carried out based on the protocol from Joseph et al., 2010.

3.3.1 Test on extract

NGMA coated culture dishes were incubated with MEM containing 5% FBS for 24h at 37ºC for preparation of extract. The extract medium [Test] was then placed on a monolayer of L929 cells for 24 h at 37ºC. Ultra high molecular weight polyethene was used as negative control and phenol as a positive control. The cell monolayer was examined under a microscope for the cellular response around the test samples. The experiment was repeated with ASCs and imaged using Nikon TS 100 phase contrast microscope.

3.3.2 MTT assay

MTT assay was performed on L929 cells after incubating these cells with the extract medium for 48h to measure the metabolic activity of cells. Metabolically active cells reduce yellow coloured tetrazolium salt 3-(4, 5-Dimethyl thiazol -2-yl)-2,5- diphenyltetrazolium bromide to purple coloured formazan. After 48 ± 2h

incubation of cells with extract medium [Test], the extract medium was replaced with 200µl MTT solution (1mg/ml in medium without supplements) and incubated at 37± 2°C for 2h. The MTT solution was then dicarded and replaced by isopropanol, the plates were shaken well and the absorbance was read at 570 nm using a spectrophotometer (Biotek Powerwave XS). Cells incubated with medium alone was considered as negative control and cells in phenol was used as positive control.The data obtained are expressed as a mean ± standard deviation and is from two independent experiments. Metabolic activity was calculated for the concentrated extract or 100% extract and expressed as percent of control, calculated as

Metabolic activity = OD of test/OD of control x 100.

3.4 Evaluation of thermoresponsive property

L929 cells were cultured on NGMA dishes to confluency and cell detachment was evaluated with a change in temperature. Cell detachment from NGMA surface due to thermoresponsive behaviour of the polymer was imaged using TS100, Nikon, Japan and these detached cells were transferred on to a new cell culture dish using PVDF membrane (Kushida A, et al., 2001). The cells at confluence on the NGMA coated dish were incubated at a temperature below 20ºC with PVDF membrane on it. Later the PVDF membrane was transferred to a new dish with the cell sheet adhered to it. The sheet attached to the new dish was analysed for viability using Calcein AM (Invitrogen). Cells were stained with Calcein AM at 1:1000 dilution in PBS and incubated for 15 min which was imaged using inverted fluorescence microscope.

3.5 Biofunctionalization of NGMA

Biofunctionalization of NGMA was attempted with amniotic membrane proteins to demonstrate the efficiency of NGMA as a tunable matrix in supporting cell growth and enhanced cellular functions.

3.5.1 Amniotic membrane Processing

Placenta was obtained after prior consent from patients undergoing elective caesarean, approved and monitored by the ethics committee at the University of Nottingham. The amniotic sac was separated from the placenta using scissors and rest of the procedures were performed in a class II biosafety cabinet. AM sac was cleaned using saline for 30min. Chorion was then removed from the AM layer manually and the AM layer is given multiple washes to be free of blood stains. After washing, the spongy layer was also removed from the amniotic membrane using a blunt scalpel and is further washed with saline. AM was processed using a modified protocol of Hopkinson et al., 2008.

3.5.2 Denuding Amniotic membrane

Denuding of the AM was performed to remove the cellular components using a previously optimised thermolysin treatment. AM was treated with 12.5% thermolysin for 10 minutes (Hopkinson et al., 2008). After thermolysin treatment, the surface of the amniotic membrane is scraped off and thoroughly washed in phosphate buffer saline. The AM is later stored at -80 ºC until use. To evaluate the efficiency of denuding, the AM was fixed in 10% neutral buffered formalin, dehydrated in graded ascending series of acetone (30 – 90%); infiltrated in xylene and embedded in

paraffin wax. Thin sections of 5µm to 7µm were made using microtome. For Hematoxylin and Eosin staining the paraffin-embedded sections were deparaffinised with xylene, rehydrated in descending grade of ethanol; washed in tap water and stained with Harris's Hematoxylin for 15 min; differentiated in 1% acid alcohol for 30sec and blued with 0.2% ammonia water for 2sec. It was then rinsed with tap water for 5min and counterstained with 1% eosin for 5min; dehydrated in ethanol cleared in xylene mounted in DPX and viewed under a Light microscope (TS 100 Nikon).

3.5.3 Isolation and purification of AM-derived proteins

The denuded amniotic membrane was snap frozen using liquid nitrogen, and then extracted in Urea-thiourea buffer. This was later exchanged to PBS at pH 5 for conjugation with NGMA. The AM proteins (Ampro) were isolated from the denuded membrane and were quantified using 2D Quant Kit (GE Health Care). The protein was then conjugated to NGMA.

3.5.3.1 Extraction of AM protein through Urea -Thio Urea buffer

The Amniotic membrane was weighed after blotting in a Whatman filter paper and protein was extracted with urea-thiourea buffer at a weight/volume ratio of 150ug/ml.

Urea – Thio Urea buffer

7M Urea

2M Thio Urea

2% W/V CHAPS

Protease Inhibitor

The weighed AM was ground with liquid nitrogen in a motor and pestle. This was powdered and resuspended with urea – thiourea buffer. The sample was then vortexed for around 45 minutes and then centrifuged at a maximum speed of 12000 rpm. The supernatant was stored and the pellet was suspended in 5 ml of buffer by vortexing and later was centrifuged. The supernatant was then used for buffer exchange.

3.5.3.2 Buffer exchange with PBS using Vivaspin 6 concentrators

The protein in Urea-thiourea buffer was buffer exchanged to Phosphate buffer saline (pH 5) and concentrated to 20-30 fold using viva spin protein concentrator with 3000 MWCO (GE Healthcare). The protein solution in Urea - thiourea buffer was loaded to the viva spin column and centrifuged in a swing bucket rotor at 4000g for 30min. After 30min, if the suspension still remains in the tube due to clogging of the filter by proteins, the remaining solution was resuspended and the centrifugation step was repeated. This step was repeated till the Urea thiourea buffer was completely filtered out and then the tube was washed with PBS. Once the tube was washed three times with 2 to 3 ml of PBS and filtered out, 1 ml of PBS is added to the tube. The assembly is removed and the sample is recovered from the bottom of the concentrate pocket by resuspending the protein in PBS with a pipette. The protein in PBS was quantified using 2-D quantitation assay kit (GE Healthcare), according to manufacturer's recommendation. Standards were prepared from bovine serum albumin provided with the kit. The optical density was measured at 490 nm in a spectrophotometer plate reader (CLARIOstar – BMG Labtech).

3.5.4 Conjugation of AM protein with polymer

Conjugation of the protein with the polymer is through a simple epoxy ring opening mechanism. NGMA in isopropanol was mixed with AM protein in PBS in a ratio of 2:1 v/v. The mixture initially precipitated and later the solution turned colourless. The conjugate solution was hand coated by swirling in 35 mm dishes (Nunc). The dishes were allowed to dry at 37°C, washed with cold water and dried. This was UV sterilized for 15 minutes and was used for further experiments.

3.5.4.1 FT- IR analysis of the polymer – protein conjugation

The FT-IR spectra for NGMA, AMpro and the AMpro-NGMA conjugated system was recorded in the IR range between 600cm^{-1} to 4000cm^{-1} using Nicolet 5700 FT-IR spectrometer (Madison WI) with Diamond ATR accessory. The conjugated protein polymer solution was placed on the diamond ATR crystal and was allowed to dry. The spectrum was read at a resolution of 4cm^{-1}.

3.5.4.2 SDS PAGE Analysis of Conjugated Protein

AMpro-NGMA, AM protein and PNIPAAm was analysed on SDS PAGE using NuPAGE® Bis-tris Mini Gel electrophoresis system (Novex, Life technologies). NuPAGE® Bis-Tris Gels (NP0335BOX) are precast polyacrylamide gels for separation of small- to medium-sized proteins under denaturing gel electrophoresis conditions. Samples were prepared as per Table 3 and heated at 70˚C for 10 minutes. 50 mL of 20X NuPAGE® MES - SDS Running Buffer is diluted to 1000 ml using deionized water to prepare 1X SDS Running Buffer. For reduced samples, add 500µl of NuPAGE® Antioxidant to 200 mL 1X SDS Running Buffer.

Sample	3 - 5 µL
NuPAGE® LDS Sample Buffer	2.5 µL
NuPAGE® Reducing Agent (10X)	1 µL
Deionized Water	Up to 6.5 µL
Total Volume	10 µL

Table 3: Sample preparation: SDS PAGE

The protein samples were electrophoresed at 200V for 35 min in the XCell *SureLock*® Mini-Cell gel running tank. After electrophoresis, the gels were stained by a simply blue safe stain (Thermo Scientific) for visualization of bands. The gels were removed carefully from the cassettes and were placed in distilled water. The proteins were fixed in the gel by microwaving the gel at 950 - 1100 W for 1 min with intermittent shaking on an orbital shaker. The above step was repeated twice after discarding the water. The simple blue safe stain is added to the gels and microwaved for around 45sec to 1min. The gel was then washed with ultra-pure water by shaking on an orbital shaker. Later the gel was incubated with 10% NaCl and the visualised bands were imaged using a high-resolution camera.

3.5.4.3 Determination of proteins in the conjugate by Western blot

Western blot (WB) was carried out according to the established technique. The protein lysates were resolved on NuPAGE 12% Bis-Tris gel (Invitrogen) and were transferred onto polyvinylidene difluoride (PVDF) membranes (Millipore). The membranes were blocked for 1h at room temperature using Tris-

buffered saline, pH 8.0 (Sigma), 0.05% v/v Tween 20 (Promega) and 5% w/v non-fat dried milk powder followed by incubation with the primary monoclonal Ab overnight at 4°C to detect total proteins. The blots were then incubated with alkaline phosphatase-conjugated secondary Ab to detect the primary Ab and then developed with premixed alkaline phosphatase chromogen kit (BCIP/NBT; Sigma). AMpro-NGMA was compared with AMpro alone to determine conjugation and the type of protein conjugated. A total of 10µg protein was run for both conjugated and control AMpro. The primary antibodies used were Mimican (Goat polyclonal AF2846- R&D Systems), Lumican (Goat Polyclonal AF2846) and Decorin (mouse monoclonal - AF1060).

3.6 Cell Culture Studies

3.6.1 Isolation, culture and characterization of rabbit adipose mesenchymal stem cells

Adipose-derived mesenchymal stem cells (ASCs) were isolated from the subcutaneous fat pad of male New Zealand white rabbit (1 year of age and 1.5-2 kg body weight) by collagenase digestion method following protocol from Venugopal et al., 2012. Briefly, the subcutaneous fat pad was collected aseptically in phosphate buffered saline (PBS) containing 2X antibiotic (penicillin /streptomycin, Gibco, Invitrogen). The fat was minced and digested with collagenase (Gibco, Invitrogen) for 1 h at 37^{o}C; filtered with a 180µm filter (Millipore). The filtrate was centrifuged and the pellet was resuspended in DMEM High Glucose (Gibco, Invitrogen) with 10% fetal bovine serum (Gibco, Invitrogen) and 1% Antibiotics (Gibco, Invitrogen), hereafter referred to as growth medium (Venugopal et al., 2012). Isolated cells were

cultured in 25cm^2 culture flask (Nunc) and were passaged using trypsin EDTA (Gibco, Invitrogen) at 80% confluence and maintained at 37°C, 5% CO_2 in an incubator (Sanyo, Japan). Experiments were done with approval from Institute Animal Ethics Committee.

3.6.2 Characterization of rabbit ASCs

The cell population isolated from rabbit subcutaneous fat pad was screened for CD markers using flow cytometry and multilineage differentiation potential.

3.6.2.1 Flow cytometry analysis of Mesenchymal Cell Markers

Rabbit ASCs were cultured in T-25 flasks (Nunc). Passage 3 and 4 were taken for flow cytometry analysis. The cells at 70 - 80% confluence were taken, washed with PBS; trypsinized with 0.25% trypsin (Invitrogen) for 2-3 minutes and centrifuged (Hermele, Germany) at 1500 rpm for 6min. The pellet was equally divided into 1.5 ml micro centrifuge tubes and fixed with 500µl 3.7% paraformaldehyde for 15 min; centrifuged at 1500rpm for 6 minutes. The pellet was washed with PBS, blocked with 1% bovine serum albumin and incubated with primary antibodies of respective CD markers. Isolated mesenchymal stem cells were characterized by their markers CD105, CD 90, CD 44 and CD 34 using flow cytometry (BD FACS Aria) (Mathews et al., 2017). Later incubated with Alexa Fluor secondary antibodies (Molecular Probes, Invitrogen). One of the microcentrifuge tubes were kept unstained as control and then another set was stained with respective secondary antibodies to negate nonspecific binding of the secondary antibody.

ABCG2 a marker co-existing in both limbal stem cells and ASCs were also evaluated. Details of the Antibodies used are mentioned in table below

CD 90	ab225, Abcam, USA	Goat anti-mouse Alexa Fluor® 488
CD105	SC-71042, Santa Cruz Biotechnology, USA	Goat anti-rat Alexa Fluor® 488
CD 44	ab157107, Abcam USA	Goat anti-rabbit Alexa Fluor® 546
CD 34	ab6330, Abcam USA	Goat anti-mouse Alexa Fluor® 488
ABCG2	ab3380, Abcam USA	Goat anti-mouse Alexa Fluor® 488

Table 4: Details of Flow Cytometry Antibodies used.

3.6.2.2 Multilineage differentiation of ASCs

Induction of ASC to osteogenic lineage

Rabbit ASCs (cells in passage 3) cultured in growth medium were trypsinized, pelleted and seeded on to the coverslips (Blue star). It was maintained for 24h in order to facilitate the cell adhesion and spreading. After 24h the cells were induced to osteogenic lineage by maintaining the cells in osteogenic induction medium (Stem pro, Gibco, Invitrogen). After 28 days, the induced cells were fixed in 3.7% paraformaldehyde and later washed with PBS. The osteogenic differentiation was confirmed by Alizarin red staining and silver nitrate staining. The fixed cells were stained with 1% Alizarin red (Sigma Chemicals) to determine calcium

deposition. For silver nitrate staining, the fixed cells on coverslips were stained with 5% silver nitrate (Merck India) in distilled water and exposed to UV light for 5min. Uninduced cells cultured for 28 days were used as a control. The cells are then washed with distilled water, air dried and viewed under a light microscope (TS-100, Nikon Japan).

Induction of ASCs to Adipogenic lineage

Rabbit ASC (cells in passage 3) were cultured in growth medium for 24 h in coverslips in order to facilitate the cell adhesion and spreading. After 24 h the cells were induced to adipogenic lineage by maintaining in Adipogenic induction medium (stem pro, Gibco, Invitrogen). The cells were induced for 21 days and then stained with Oil Red O (Sigma Chemicals) after fixing with 3.7% paraformaldehyde. Oil Red O Stock solution was prepared by dissolving 300mg in 100ml Isopropanol (Nice Chemicals). Oil Red O Working Solution was obtained by diluting 6 parts Oil Red O stock with 4 parts distilled water and filtered. Prior to staining, the cells were treated with 60% isopropanol. The induced rabbit ASC was then stained with oil red O for 10 min and observed under Light Microscope (TS 100, Nikon, Japan).

3.6.3 Culture of Rabbit limbal explants and collection of limbal condition medium

The limbal ring was cut out from the cornea of male New Zealand white rabbits and was then cut into 1-2mm pieces and these explants were expanded. The protocol was modified from Zhang et al., 2005. These cells were cultured in Minimum Essential Medium (MEM Sigma-Aldrich) using 5% fetal bovine serum (Gibco, Invitrogen) and 1% Antibiotics (Gibco, Invitrogen, Thermo Scientific).

When these cells reach 70% confluence, the medium is collected at 48h intervals, filtered and stored at -80°C. This conditioned medium was used in a ratio of 1:1 with DMEM low Glucose (DMEM LG, Gibco, Invitrogen, Thermo Scientific) for corneal epithelial differentiation of ASCs and is further mentioned as a limbal conditioned medium.

3.6.4 Isolation, culture and characterization of human corneal stromal stem cells

Corneal stromal stem cells (CSSC) were isolated from the limbal region of the human cornea. Human donor tissue was obtained from "Manchester or Bristol Eye Bank" with approval from the local ethics research committee (NRES committee, East Midlands, Nottingham) and consent from the donors and/or their relatives. Only those tissues not suitable for the purpose of transplantation were used for research purpose, from which CSSC were isolated. The limbal tissue was minced into small pieces and was digested by collagenase at 37^{o}C. The digested tissue was filtered and then the filtrate was centrifuged and the pellet was resuspended in SCM medium [20% FBS, basic fibroblast growth factor and leukemia inhibitory factor called stem cell medium as reported by Sidney et al., (Sidney et al., 2015)] in 75cm^2 culture flask (Nunc) coated with 0.1 % gelatin. Cells were passaged using trypsin-EDTA (Gibco, Invitrogen) at 80% confluency and maintained at 37°C, 5% CO_2 in the incubator. CSSCs cultured on SCM media will adhere and grow only on to the protein-coated surface and is usually cultured in gelatin-coated culture dishes. CSSCs were grown on gelatin, NGMA and AMpro-NGMA with SCM medium to see the

effect of culture substrate on cells. CSSC isolation followed the protocol of Hashmani et al., 2013.

3.7 Specific Cyto compatibility evaluation of NGMA using ASCs

3.7.1 Cytotoxicity assay for NGMA coated TCPS using ASCs

In vitro cytotoxicity of NGMA was evaluated by Test on extract method and MTT assay using ASCs to evaluate specific cytotoxicity.

3.7.1.1 Test on Extract

NGMA coated culture dishes were incubated with DMEM (Gibco, Invitrogen, Thermo Scientific) growth medium for 24h at 37ºC for preparation of extract at a concentration of 9cm^2/ml, based on ISO 10993-5. The extract medium was then used to incubate a monolayer of ASCs for 24h at 37ºC. Ultra-high molecular weight polyethene was used as negative control and phenol as a positive control. The cell monolayer was examined for the cytotoxic response and imaged using phase contrast microscope (TS 100, Nikon, Japan).

3.7.1.2 MTT assay

MTT assay was performed on ASCs after incubating these cells with the extract medium for 48h to measure the metabolic activity of cells. Metabolically active cells reduce yellow coloured tetrazolium salt 3-(4, 5-Dimethyl thiazol -2-yl)-2,5- diphenyltetrazolium bromide to purple coloured formazan. After 48 ± 2h incubation of cells with extract, the extract medium was replaced with 200µl MTT solution (Sigma-Aldrich) (1mg/ml in medium without supplements) and incubated at 37± 2°C for 2h. The MTT solution was then replaced by isopropanol, the plates were

shaken well and the absorbance was read at 570nm using a spectrophotometer (Biotek Powerwave XS, BioTek Instruments, Inc, USA). The data obtained were expressed as a mean ± standard deviation and was from three independent data sets/experiments. Cells in medium alone were taken as control. Metabolic activity was calculated using the formula

Metabolic activity = OD of test/OD of control X 100.

3.7.2 Evaluation of ASC characteristics on NGMA

ASCs cultured on NGMA dishes using growth medium was evaluated for cell morphology (Actin cytoskeletal staining, Actin Green™ 488 ReadyProbes® Reagent (Thermo Fisher Scientific), viability (Calcein AM, Invitrogen, Thermo Fisher Scientific), and for stemness using CD 90, CD 105 immunostaining. For calcein AM staining the cells were incubated with calcein at a dilution of 1:2000 with growth medium and imaged. For actin staining the cells were fixed with 4% paraformaldehyde, permeabilized with 0.5% Triton-x-100 (Sigma-Aldrich) for 5 min and stained with ActinGreen™ 488 ReadyProbes® Reagent (Thermo Fisher Scientific). For immunostaining, after fixing, the cells were blocked with 1% bovine serum albumin (Sigma-Aldrich), stained with primary antibody CD 90 (ab225, Abcam, UK) and CD 105 (SC-71042, Santa Cruz Biotechnology, USA) for 1h, washed and stained with Alexa Fluor® 488 (Molecular Probes, Thermo Fisher Scientific) secondary antibody for 45min. Goat anti-mouse Alexa Fluor® 488 and goat anti-rat Alexa Fluor® 488 was used as secondary antibodies for CD 90 and CD 105 respectively. The nucleus was counterstained with Hoechst (Sigma-Aldrich),

mounted (fluorescent mounting medium, Dako) and imaged. All fluorescent images were taken using DMI 6000, Leica, Germany.

3.8 Differentiation of ASCs to corneal epithelial lineage

3.8.1 Standardization of Differentiation medium

ASCs were evaluated for corneal epithelial differentiation using two different medium. One is a commercially available defined keratinocyte medium (DSFM) with growth factors (Gibco Invitrogen), while the other is limbal conditioned medium. The limbal conditioned medium was obtained from culturing limbal explant cells in Minimum essential medium (MEM) as described above. ASCs were cultured for 14 days in DSFM and in the limbal conditioned medium.

3.8.1.1. Standardization of medium for corneal epithelial differentiation: by Immunocytochemistry

Differentiated cells were evaluated using cytokeratin 3/12 staining using primary antibodies (ab68260, Abcam, UK). The differentiated cells were fixed with 4% paraformaldehyde, washed, permeabilized with 0.5% Triton-x-100 for 5 min, incubated with 1% BSA; stained with primary antibody for 1h and then with secondary antibody (anti-mouse Alexa Fluor® 488, Thermo Fisher Scientific) for 45min; immunostained cells were mounted with fluor mount (Dako, Agilent Technologies, USA) and imaged using Leica fluorescent microscope (DMI 6000, Leica, Germany).

3.8.1.2. Standardization of medium for corneal epithelial differentiation: by Gene expression studies

Quantitative-PCR (qPCR) analysis was done to compare the efficiency of DSFM and limbal condition medium in inducing corneal epithelial differentiation. ASCs (passage 3) cultured on tissue culture polystyrene (TCPS) were taken for gene expression analysis after 14 days of induction in limbal conditioned medium and DSFM. Total RNA was collected from the induced ASCs (n=3) and the controls using TRIzol® (Ambion^{TM} Invitrogen) as per manufacturer's specifications. The RNA was purified using a conventional method by phenol-chloroform extraction and was quantified using Nanodrop (ND 1000, Thermo Scientific). cDNA was synthesized by reverse transcriptase PCR in a thermocycler (Eppendorf, Germany). 1ug RNA was used in a 20µl of reaction mix with Superscript III reverse transcriptase (11752-050, Invitrogen). The reaction mixture was then incubated at 25°C for 10 minutes and the reverse transcriptase step for 30 min at 50°C. The final incubation for 5 min at 85° C was given to inactivate the Reverse Transcriptase enzyme. The cDNA synthesized was stored at -20°C till use.

The cDNA was amplified by using Roche light cycler® 96 real-time PCR system using Kapa SYBR® Fast qPCR Master mix (Kapa Biosystems). $2^{-\Delta\Delta C(t)}$ Method was used for relative quantification with GAPDH as the housekeeping gene. Amplification was performed using specific primer sequences (IDT, USA) for different markers as given in Table 5. Cycling conditions were as follows. Initial denaturation at 95 ºC for 3 min, denaturation at 95ºC for 10s, the annealing temperature was set at 55 ºC for 20s and extension at 72ºC for 20s followed by plate

reading and the analysis of melting curve. The reaction was set for 45 cycles. The expression of CK3, CK12 and ABCG2 were compared between the ASCs incubated with limbal conditioned medium and DSFM which was normalized with control ASCs incubated in 3:1 MEM and DMEM LG. Differentiation was evaluated after 14 days of the differentiation process. The fold change is represented graphically and the data expressed as the mean ± standard deviation (n=3).

3.8.2. Evaluation of corneal epithelial differentiation by immunocytochemistry and flow cytometry

Differentiated cells were evaluated using cytokeratin 3/12 staining using primary antibodies (ab68260, Abcam, UK) and Connexin 43 (ab11369, Abcam, UK). For flow cytometry analysis, the cells were trypsinized and fixed in suspension. The differentiated cells were fixed with 4% paraformaldehyde, washed, permeabilized with 0.5% Triton-x-100 for 5min, incubated with 1% BSA; stained with primary antibody for 1h and then with secondary antibody (anti-mouse Alexa Fluor® 488, Thermo Fisher Scientific) for 45min; immunostained cells were mounted with fluor mount (Dako, Agilent Technologies, USA) and imaged using Leica fluorescent microscope (DMI 6000, Leica, Germany). For flow cytometry analysis the secondary stained cells were washed and resuspended in PBS which were later analysed using BD FACS ARIA (Becton Dickinson, USA).

3.8.3. Evaluation of corneal epithelial differentiation by molecular phenotyping - Real-Time PCR.

Detailed evaluation of ASCs induced to corneal epithelial lineage was done for the selected differentiation medium. Total RNA isolation, cDNA synthesis

and qPCR were done according to the standardized protocol mentioned in section 3.7.3.3. ASCs (passage 3) cultured on TCPS were taken for gene expression analysis after 14 days of induction in the limbal conditioned medium. The gene expression was compared between the ASCs incubated with limbal conditioned medium (differentiated ASCs) and control ASCs. The gene expression of the differentiated ASC population is normalized with the control ASCs. Differentiation was evaluated for day 7 and day 14 of the differentiation process. The fold change is represented graphically and the data expressed as the mean and standard deviation (n=3). The set of genes used for evaluation and their sequences are mentioned in Table 5.

Gene	Sequence
CK 3 Forward	GACTCGGAGCTGAGAAGCAT
CK 3 Reverse	CAGGGTCCTCAGGAAGTTGA
CK 12 Forward	GAGCTGGCCTACATGAAG
CK 12 Reverse	TTGCTGGACTGAAGCTGCTC
P63 Forward	TGTGTTGGAGGGATGAACCG
P63 Reverse	CACCGTTCTTTGTGCTGTCC
ABCG2 Forward	CTGTTTTCTGATTTACTACCCATGC
ABCG2 Reverse	GCCACGGACACTACACTCTG
PAX 6 Forward	CGGGAAAGACTAGCAGCCAA
PAX6 Reverse	TGGTTGGTAGACACTGGTGC
CK 19 Forward	CTACAGCTATCGCCAGTCGT
CK 19 Reverse	TTGGAGTTCTCAATGGTGGCA
GAPDH Forward	CAACGAATTTGGCTACAGCA
GAPDH Reverse	AAACTGTGAAGAGGGGCAGA

Table 5: Primer Sequence for qPCR analysis of corneal epithelial differentiation

3.9. Culture and retrieval of ASC sheet from NGMA

2 x 10^4 ASCs were seeded on NGMA coated culture dishes and the cell morphology was evaluated using phase contrast microscopy. After 14 days of induction using limbal conditioned media, cell sheet detachment was attempted by a change in temperature. The cell sheet on NGMA at 37^{o}C was brought to a temperature below 20^{o}C and the cell sheet detachment was monitored under an inverted phase contrast microscope (TS 100, Nikon, Japan). Time-lapse images of the cell sheet retrieval were captured using a digital camera (DS-Fi2**,** Nikon) controlled through NIS Elements Software (Nikon).

3.9.1. Transfer of cell sheet

Retrieved cell sheet was transferred to a new dish using PVDF membrane as a transfer tool as described in section 3.4. The confluent cells on the NGMA coated dish were incubated at a temperature below 20^{o}C with PVDF membrane on it. Later the PVDF membrane was transferred to a new dish with the cell sheet adhered to it. The sheet attached to the new dish was analysed for viability using calcein AM and cytoskeletal morphology using ActinGreen^{TM} 488 ReadyProbes$^{®}$ Reagent. The scanning electron micrograph of the cell sheet was taken after fixing the cells with 2% glutaraldehyde; treated with graded series of alcohol, dried at a critical point and then imaged using Scanning Electron Microscope (FEI QUANTA 200, Thermo Fisher Scientific, USA).

3.9.2. *Ex vivo* demonstration of cell sheet transfer

ASCs were cultured to confluence on NGMA and the cells were detached as a sheet by dropping the temperature to 10°C.The viable cell sheet was then transferred to an *ex vivo* excised rabbit eye from a cadaver to standardize cell sheet transfer on to the corneal surface. Corneal surface damage was simulated on the ex vivo eye by using n-heptanol and by mechanical debridement (protocol was modified from Sehic et al., 2015). The corneal surface damage was demonstrated using Fluoro touch fluorescein sodium ophthalmic strip USP (Loyal Medi Optha, India). Excess dye was washed off with saline and was imaged with a digital camera (Cool pix 340L Nikon, Japan). Later the cell sheet was transferred to this damaged corneal surface for a demonstration of the feasibility of cell sheet transplantation.

3.10. Biofunctionalization of NGMA – Cell Culture and Evaluation of Cell Sheet

3.10.1. Coating of AMpro-NGMA on to 35mm dish

4% NGMA in isopropanol was mixed with a definite amount of protein in PBS (pH 5) in a ratio 2: 1 and is coated on to the 35 mm dish, dried at 37^{o}C for 2h; washed with cold water multiple times to remove any unattached debris or remaining. This was again dried at 37^{o}C for 2h and UV sterilized for 15 minutes. The dish was conditioned with SCM media before seeding the cells.

3.10.2. Cell patterning to prove protein conjugation/ presence

CSSCs will adhere only on to protein modified surfaces and not on to normal TCPS dishes. So as to prove that CSSCs can attach and grow on AMpro-

NGMA surfaces and not on NGMA or TCPS, patterned spots of AMpro-NGMA and NGMA alone were made on TCPS dishes. 40ug AM protein was used for conjugation with NGMA. These patterns were stained with SimplyBlue^{TM} to demonstrate the presence of AM proteins on conjugated AMpro-NGMA system. Later CSSCs were seeded on to these patterns and was imaged using phase contrast microscopy to prove cell adherence on AMpro-NGMA while they do not adhere to NGMA. CSSCs grown on gelatin and AMpro dishes served as a positive control to demonstrate adherence and non-patterned areas of the patterned dish served as negative control where the cells fail to adhere. The adhered cells were then fixed and stained with crystal violet to demonstrate cell adherence on to patterns.

3.10.3. Standardization of AM protein concentration for cell sheet detachment

To determine the effective protein concentration to be used for conjugation per 35 mm dish, CSSCs were cultured in dishes with variable protein concentrations. 1µg, 3µg, 6µg, 10µg, 20µg and 40µg concentrations of AM were used per dish to determine cell spreading. 2 x 10^4 cells were seeded on to each dish with variable AM concentration and the spreading was evaluated after 24h. To quantitatively determine the cell adhesion, the initial adhesion of CSSCs on gelatin and amniotic membrane protein in the above-mentioned protein range were compared using presto blue staining. 10X Presto Blue reagent (Life technologies) was diluted 10 times with SCM media and is added on to the culture dish. 1ml Preso Blue working solution was added to a 35 mm dish and was incubated at 37^{o}C for 20 min. The fluorescence was read at 535 nm with an emission window at 615 with

10nm bandwidth. The result is then plotted on to a graph for three independent experiments.

3.10.4. CSSC sheet transfer to new substrate using PVDF membrane

CSSC sheet transfer was attempted from 10μg, 20μg and 40μg AMpro conjugated NGMA using PVDF membrane as explained in section 3.4. The detached cell sheet was transferred to a new AMpro coated substrate.

3.10.5. Modified transfer Protocol- Gelatin based cell sheet transfer

10% gelatin (Sigma) was made using serum-free media and this solution was pre-warmed to 37°C. The medium from the confluent monolayer of CSSC was removed and serum-free medium was added to the CSSC monolayer. The dish was transferred to a temperature at 4^{o}C for 2-3min. Once the cells begin to show signs of detachment, gelatin solution was added and the cells were kept at room temperature for 5min and then transferred to 4^{o}C for another 5min. After cold incubation, gelatin formed a gel which can be detached as a whole from the dish and placed on a new dish. Here, the cells have also detached along with the gel and were transferred to the new dish. The new dish was placed in the incubator where the gelatin liquefies and was removed in 1h. Growth medium was added to the new dish where the transferred cell sheet attaches to the new dish. Protocol modified from Kikuchi et al., 2014 was followed.

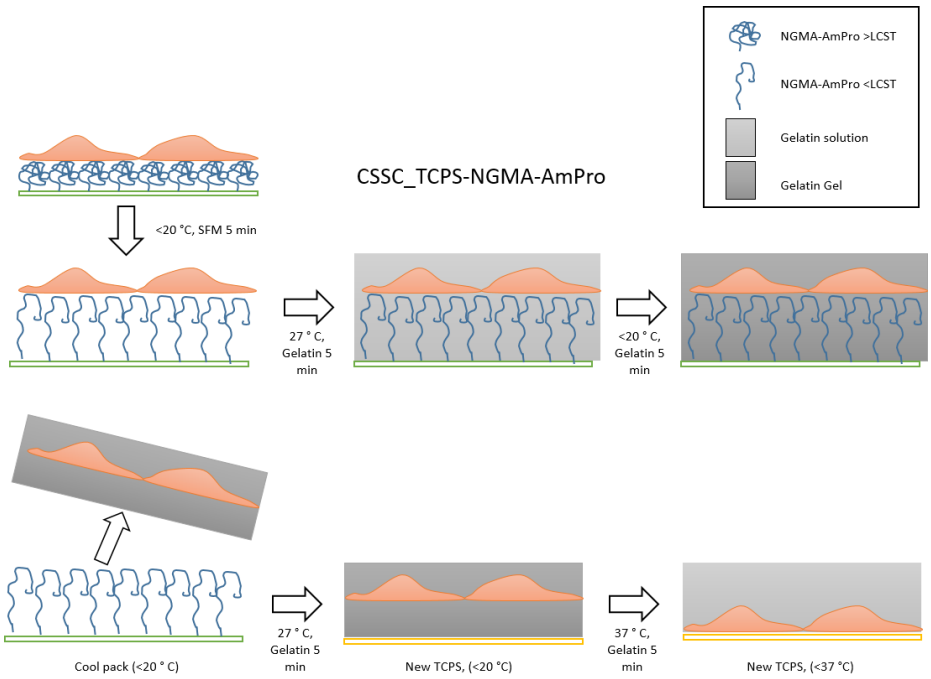

Figure 5: Modified Method of Cell Sheet retrieval using 10% Gelatin Gel

3.10.6. Viability of CSSCs on AMpro-NGMA

5 x 10^4 CSSCs were seeded on AMpro-NGMA and AMpro coated dishes to compare cell growth, viability and cell loss during transfer. Proliferation and viability were assessed using presto blue (Invitrogen) as per manufacturers protocol as mentioned in section 3.10.3. Viability was determined over a period of 7 days and the results were then plotted on to a graph for three independent experiments. CSSCs on AMpro-NGMA was transferred to AM coated dishes on the 3rd day and was evaluated for viability on the new dish for another four days. Cells on AM coated dishes served as control from day 1 to 7 to assess cell loss.

3.11. *In vivo* demonstration of transdifferentiated ASC sheets in Rabbit corneal injury models.

3.11.1. Creation of rabbit corneal injury model

New Zealand white rabbits of 6 months -1 year with 2 - 3 kg body weight were used for the study. All experiments were done with approval from Institute animal ethics committee. All Animals were anesthetized with Ketamine (70 mg/kg body weight) + midazolam (0.3 mg/kg body weight) + Xylazine (5mg/kg body weight) combination intramuscularly. The animals were secured on right lateral recumbence. Periorbital area was clipped, shaved and prepared aseptically. Eyes were swabbed with 0.5% povidone iodine solution. The eyelids were then retracted with an eyelid speculum and the eyeball was fixed with superior, and inferior stay sutures using size 3/0 braided silk. The limbal region and the surface were then scarified with a 2.6 mm crescent angled bevel up a microsurgical full handled knife (Sharpedge Classic line, Ophthalmic Marketing and services, India). This was followed by chemical injury induced by gentle rubbing of N-heptanol (Merck) soaked cotton buds on corneal epithelium for 60s-90s for removing or damaging the corneal epithelium followed by debridement of epithelial surface ensuring complete removal of corneal epithelium. As post-operative care Dexamethasone + gentamycin eye drops were instilled into the eye twice daily for 2 weeks. For analgesia, meloxicam at 0.5mg/Kg body weight was administered for 5 days post-operation. There were two groups of rabbits. The contralateral normal eye in each animal was used as the control. 4 rabbits were used as sham models while 4 animals were treated

with cell sheet on 30 days after induction of corneal injury. Protocol was modified from Helga et al., 2011, Sehic et al., 2015, Sitalakshmi et al., 2009.

3.11.2. Selection of corneal injury models for transplantation studies

Eyes were divided into four quadrants and based on visual examination animals were graded as complete, partial or without LSCD depending upon the severity of the clinical abnormalities mentioned below. Animals which had developed complete LSCD (3+, 4+) were selected for cell sheet transplantation studies. Selection of models for transplantation was based on scoring pattern given by Sitalakshmi et al. 2009.

Scoring pattern was made based on

Corneal Opacity

Neovascularization

Surface irregularity

Conjuctivalization

Epithelial damage

3.11.3. Transplantation of cell sheet in rabbit corneal injury models

Superficial Keratectomy was performed prior to cell transplantation to remove the conjunctival layer with a 2.6 mm Crescent Blade in both the groups. In the transplanted groups, the cell sheet was transferred to the corneal surface by placing the cell sheet on the cornea and spreading it over the cornea. Cell sheet was manually transferred to the corneal surface without external support. A soft bandage

contact lens was then placed over the eye to protect the cell sheet. Partial tarsorrhaphy was then performed to retain the cell sheet and soft contact lens. Ciprofloxacin ophthalmic solution was instilled three times daily after transplantation for one week. In the sham group, all the procedures except cell sheet transplantation were performed. Animals were sacrificed one month after transplantation and the eyeballs were collected in buffered formalin for histology.

3.11.4. Histological evaluation of transplanted cell sheet

After gross evaluation of the eyeball, the cornea was carefully excised and fixed in 10% neutral buffered formalin, washed, dehydrated with acetone (Merck) and infiltrated with xylene (Merck) in automated Leica TP 1020 Histokinette (Germany), later embedded in paraffin wax (SLEE MP3/P1 Paraffin wax embedder). Sections of 5-7 um were cut using the microtome (Leica RM2255, Germany). These sections were deparaffinized with xylene, rehydrated in descending grade of ethanol, stained with Harris' hematoxylin, rinsed with water and counterstained with 1% eosin, dehydrated in ethanol, cleared in xylene, mounted in DPX (Merck), and viewed under a light microscope (Leica DM 6000). For PAS staining deparaffinized section were hydrated in water. Oxidize in 0.5% periodic acid in 5 minutes. Rinse in distilled water, immerse in Schiff reagent for 15 to 20 minutes. Wash with lukewarm water, counterstain with Mayer's haematoxylin for 1 min. Wash, dehydrate and mount with DPX. Image with Leica DM 6000.

3.12. Statistical Analysis

Values are presented as a mean ± standard deviation. Comparison and analysis of significance between experimental groups were evaluated using Student's t-test and considered statistically significant if $p < 0.05$. Graph pad software was used for statistical analysis.

CHAPTER - IV

4. RESULTS: POLYMER CHARACTERIZATION

4.1. NGMA Synthesis and Characterization.

NGMA was synthesized by free radical random co-polymerization of NIPAAm (Sigma-Aldrich) with GMA in 10:1 ratio. The dried co-polymer was dissolved in isopropanol to make a 4% NGMA solution. This 4% NGMA solution was hand coated on to 35 mm culture dishes. These dishes were air dried, packed and sterilized using ethylene oxide or UV sterilization. UV sterilization was given for two cycles of 15 minutes each.

4.1.1. Fourier Transform – Infrared Spectroscopy

The copolymer characterization of NGMA was done using ATR-FTIR spectroscopy. The ATR–FTIR spectrum of the pure NGMA depicted the peaks at 1635 cm^{-1}, 1540 cm^{-1}, and 1458cm^{-1} corresponding to the –NHCO groups in PNIPAAm and the characteristic peaks of epoxy groups of GMA was depicted at around 838 cm^{-1}, 925 cm^{-1} and 978 cm^{-1} (Figure. 6A).

This confirmed the presence of both NIPAAm and GMA in the copolymer. Also, the coating efficiency of NGMA on tissue culture polystyrene (TCPS) dishes were evaluated using ATR-FTIR by analysing the FTIR spectrum of the NGMA. This depicted the same characteristic peaks as in the pure NGMA (Figure.6B).

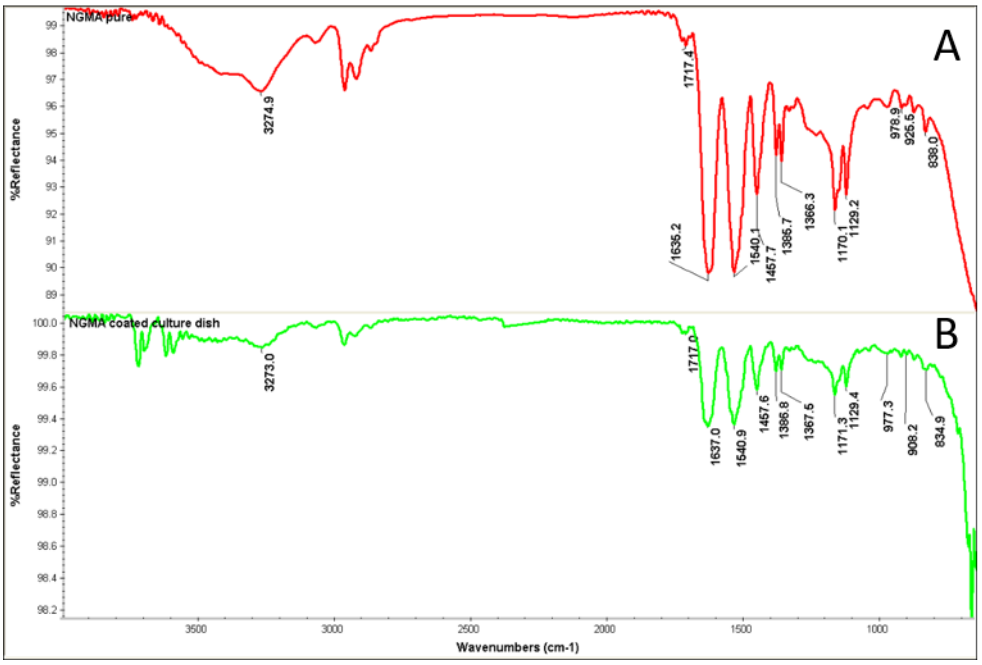

Figure 6: FT-IR spectrum of NGMA: showing peaks at 1635 cm^{-1}, 1540 cm^{-1}, and 1458cm^{-1} corresponding to the –NHCO groups in PNIPAAm and peaks at 838 cm^{-1}, 925 cm^{-1} and 978 cm^{-1} corresponds to an epoxy ring of GMA. (A) The red spectrum depicts the pure NGMA and the (B) green spectrum shows NGMA coated on the culture dish.

4.1.2. Differential Scanning Calorimetry

The LCST of NGMA co-polymer was determined based on the abrupt changes in the polymer based on thermal properties. The observed endothermic peak was due to the breakage of a hydrogen bond between water molecules and the hydrophobic domains, which represented the LCST. The thermogram showed a dip at 32.5ºC (Figure.7A) which corresponded to the temperature at which NGMA alters its property. NGMA appeared as a transparent polymer below LSCT (Figure.7E) and formed white insoluble precipitate above LSCT (Figure.7F).

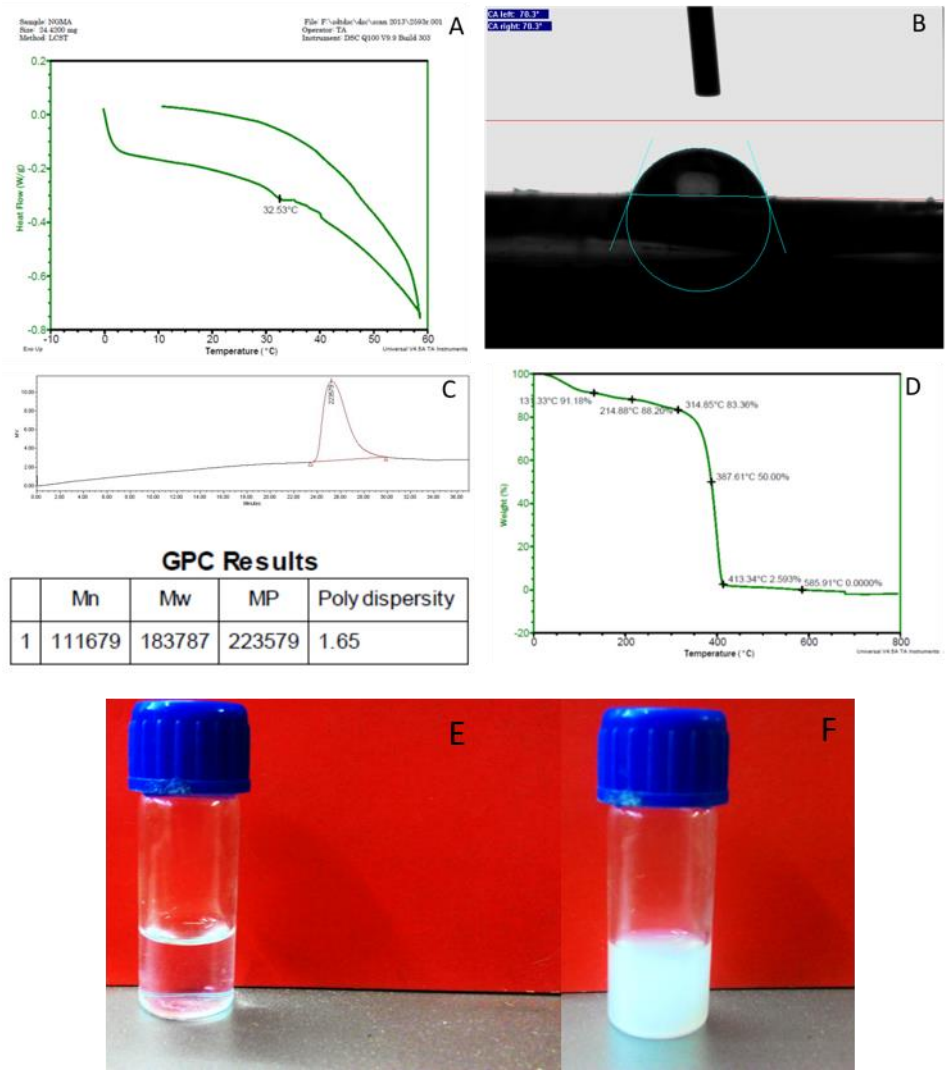

Figure 7: Physico-Chemical properties of NGMA: (A) The DSC thermogram depicts the LCST around 32^0C (B) Water Contact angle measurement using Goniometry showing 70.3^0 contact angle (C) Gas permeation chromatography depicting the molecular weight of the formed polymer (D) TGA analysis depicting the thermal decomposition curve of the polymer (E) 4% NGMA at 20 ºC (F) 4% NGMA at 33ºC.

4.1.3. Water Contact Angle

The contact angle was determined to confirm the suitability of NGMA coated surface for cell culture studies. The contact angle of NGMA was found to be

71.45 ± 2.4 (Figure.7B). The contact angle values of multiples areas of a dish were determined. This was repeated from three different dishes and was calculated and mentioned in terms of mean and standard deviation. Most of the values were very close indicating an evenly coated surface.

4.1.4. Gel Permeation Chromatography (GPC)

Gel permeation chromatography determines the molecular weight of the synthesized polymer. The synthesized NGMA polymer showed a number average molecular weight (M_n) of 111679 and weight average molecular weight (M_w) of 183787. NGMA showed a polydispersity index of 1.65 (Figure. 7C).

4.1.5. Thermal Gravimetric Analysis

In order to study the thermal behaviour of the polymer NGMA, thermal analysis was conducted up to 800^{0}C. Percentage weight loss against temperature curves of NGMA is given in Figure. 7D. Around 10% weight loss was observed below 200^{0}C. The initial decomposition starts at around 314^{0}C and fifty percent weight loss for polymer NGMA was found to be at 387^{0}C. However, at 585^{0}C the polymer completely degrades away (Figure. 7D).

4.2. In vitro cytotoxic evaluation of NGMA

In vitro cytotoxicity evaluation was done according to ISO 10993/5 standard using L929 cells.

4.2.1. Test on extract

The cell monolayer incubated with the NGMA extract for 24h was examined microscopically for cell morphology. No vacuolization, detachment and membrane disintegration was observed in L929 cells treated with the extract. L929

cells maintained their characteristic spindle-shaped morphology (Figure. 8A). the cells on UHMPE exhibited normal morphology while, cells incubated with phenol, detached from the culture surface and showed massive cell death.

4.2.2. MTT Assay

MTT assay was performed with L929 cells after 48h to measure the metabolic activity of cells to reduce yellow coloured tetrazolium salt 3-(4, 5-Dimethyl thiazol -2-yl)-2,5- diphenyltetrazolium bromide to purple coloured formazan. The extract incubated cells were compared with cells incubated with normal growth medium and cells cultured with phenol as a positive control. The extract dilutions showed comparable OD reading with control medium at 570 nm, which corresponded to similar metabolic activity (Figure. 8B).

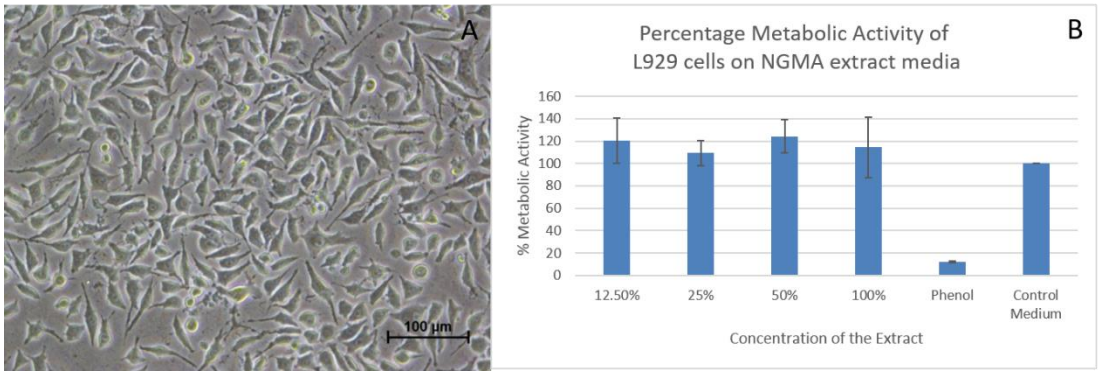

Figure 8: *In vitro* cytotoxicity studies of NGMA: (A) L929 cells maintained their morphological features 24h after incubation with NGMA extract. (B) Metabolic activity evaluation of NGMA extract concentrations on L929 cells by MTT assay.

4.3. Evaluation of Thermoresponsive property of NGMA

Thermoresponsive property of NGMA was evaluated using L929 cells. When L929 cells were cultured to monolayer and the temperature was brought down to 20^{o}C or below, NGMA undergoes phase transition making the cells to detach from

the polymer surface. The phase contrast images of L929 showed a dense monolayer of cells on the NGMA surface (Figure. 9A) at 37^{o}C. Reducing the temperature, lead to a reversal of L929 - NGMA adhesion, the cells adhered to the PVDF membrane placed over the cell monolayer indicated by the arrow mark (Figure.9B). In the mother dish where the monolayer was present, the cells have been detached without mechanical or enzymatic treatment.

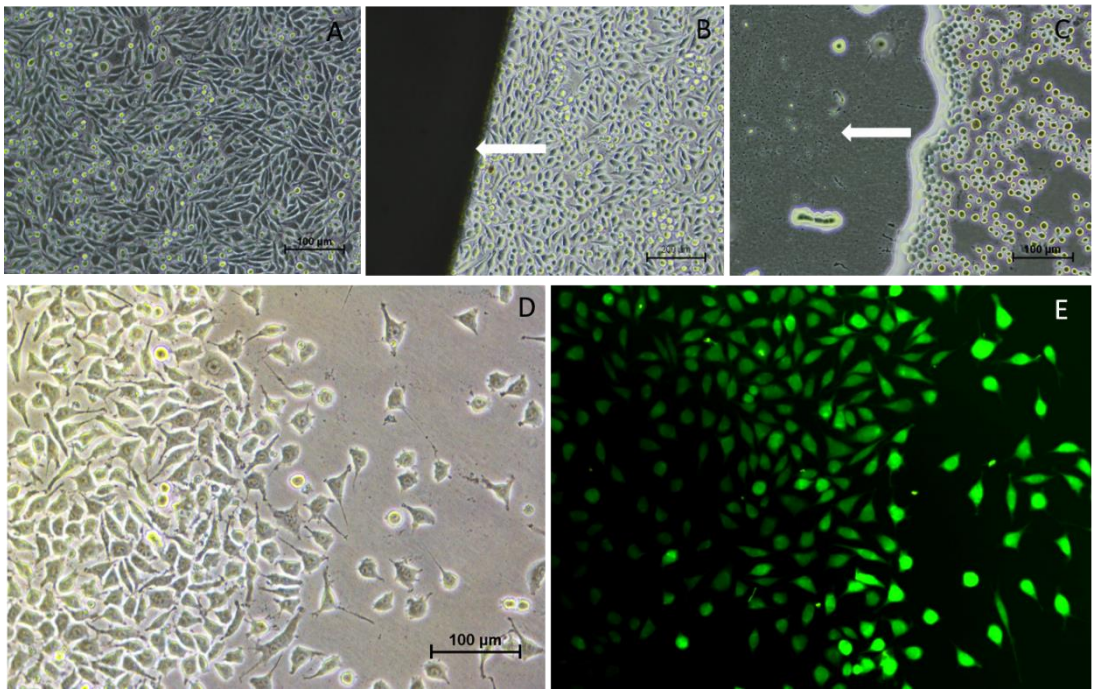

Figure 9: Demonstration of thermoresponsive property by NGMA. (A) a confluent monolayer of L929 cells on NGMA (B) PVDF membrane placed on NGMA (indicated by arrow mark) while incubating at a temperature around 20℃ (C) Image of the NGMA dish after PVDF membrane is removed. Arrow mark indicates the region where PVDF membrane was placed on the cell monolayer (D) phase contrast image of L929 cells on the new dish 24h after transfer (E) Transferred cells stained with calcein AM for viability

The mother dish shows empty areas where the PVDF membrane was earlier placed and then removed (indicated by arrow mark) (Figure.9C). Here the cells detached from NGMA and were transferred to the new substrate via PVDF. After transfer to the new dish, the cells reattached when placed back in an incubator at 37^{o}C (Figure.9D). The cells were transferred to a new dish using PVDF membrane and were imaged post 24h and they showed a viable cluster of calcein AM stained cells (Figure.9E). Transferred cells maintained characteristic L929 morphology as evident from phase contrast microscopy (Figure.9D).

4.4. Modification of NGMA with Amniotic membrane protein

NGMA, as mentioned, is a copolymer of PNIPAAm and glycidyl methacrylate (GMA). The Glycidyl methacrylate group (GMA), group within the copolymer leaves us with an unreacted, epoxy group available within NGMA.

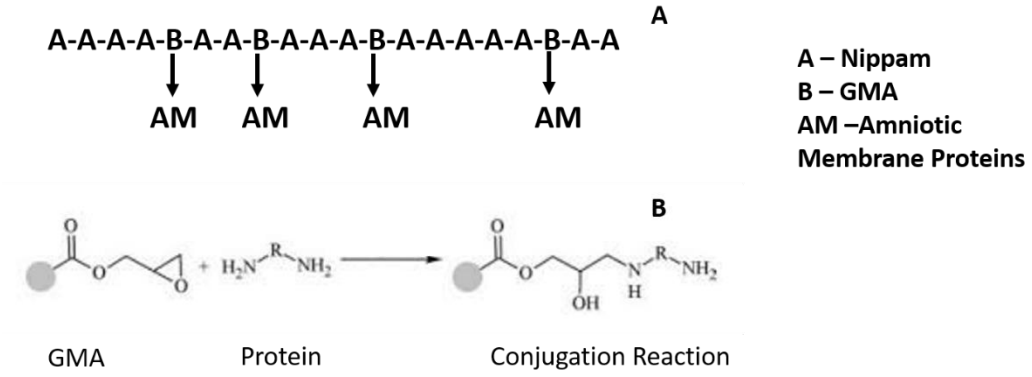

Figure 10: Bio-functionalization of NGMA: (A) Schematic representation of AM conjugation to Glycidyl methacrylate (GMA) group of NGMA (B) Epoxy ring opening mechanism of GMA to incorporate AM proteins with –NH2 group.

The epoxy ring opening in acidic conditions allows incorporating any nucleophile to the polymer chain for enhanced modulation of polymer behaviour. N-isopropyl

acrylamide–co–glycidyl methacrylate (NGMA) polymer was biofunctionalized with amniotic membrane proteins that modified polymer behaviour for guided cell growth, differentiation and cell sheet formation.

4.5. Processing and Denuding of AM membrane.

AM proteins were isolated from placental amniotic sac obtained after C-section. The amniotic membrane was processed for use after removing the chorion (Figure. 11A & B) and spongy layer (Figure. 11E & F).

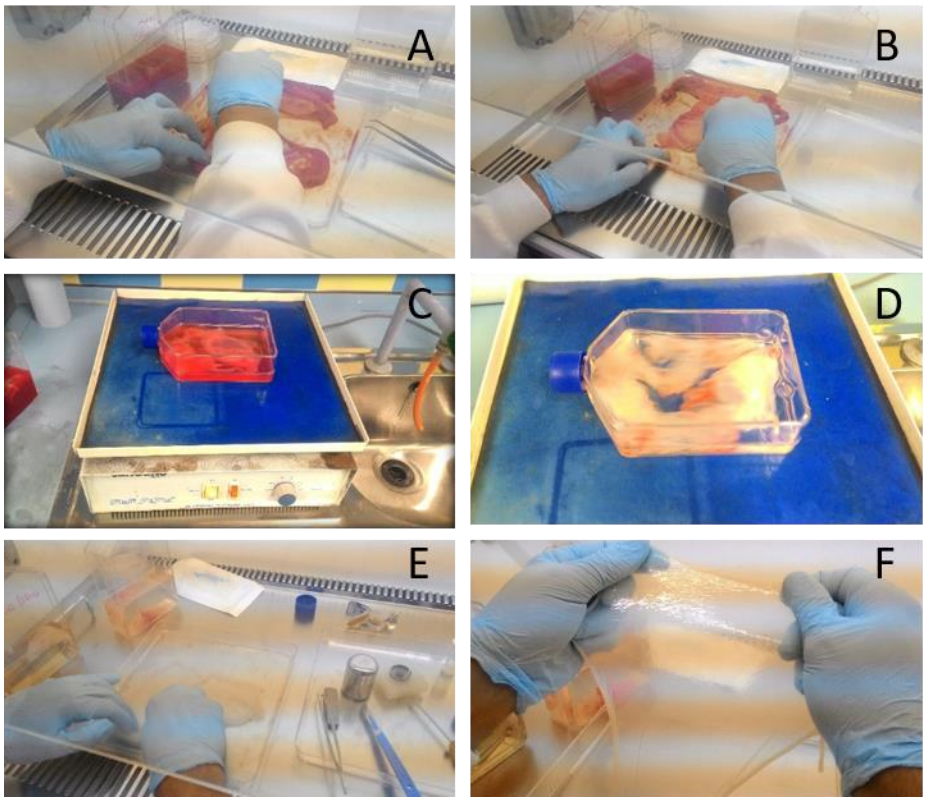

Figure 11: Processing of amniotic membrane: (A & B) Removal of Chorion layer (C& D) Washing to remove blood stains for a clean membrane (E & F) Removal of the Spongy layer from the amniotic membrane.

Amniotic membrane was denuded using thermolysin treatment to remove the epithelial layer of amniotic membrane. Treatment with thermolysin was shown to

remove the epithelial cells from the amniotic membrane making AM free of donor cells. This was demonstrated by H & E staining. H & E staining of AM before and after denuding showed striking differences. AM before denuding showed the outer layer of epithelial cells intact on the membrane (Figure. 12A) while after denuding the cells were removed and the staining showed the membrane devoid of cells (Figure. 12B).

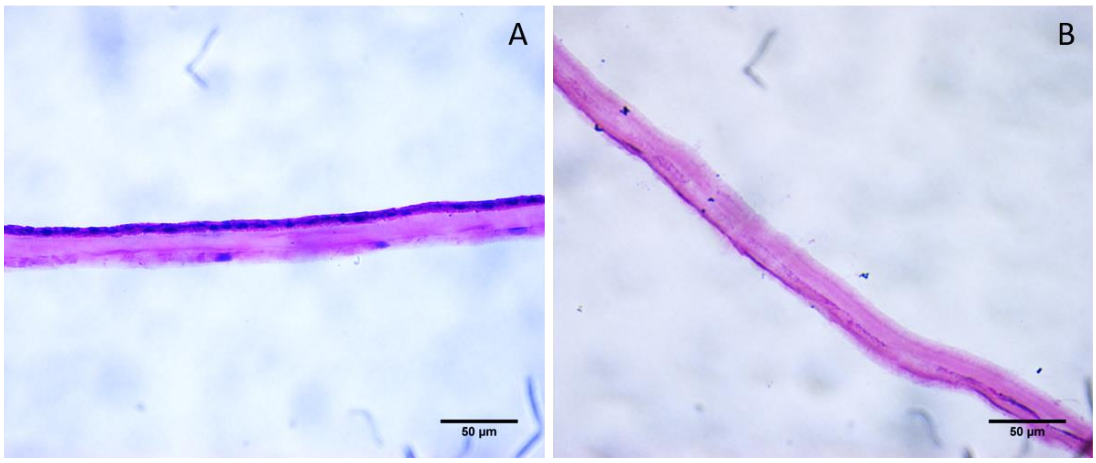

Figure 12: Denuding of the Amniotic membrane; Demonstration with H & E staining (A) Outer epithelial lining visible when stained by H & E before denuding (B) epithelial lining removed after denuding process.

4.6. Extraction and Estimation of AM Protein

The protein was extracted from the membrane using Urea thiourea buffer system and the buffer was later exchanged to PBS at pH 5 using viva spin concentrator columns. The protein concentration was estimated using the 2D quant kit and was found to have 35.5ug of total protein and was set to 1µg/µl for experiments.

4.7. Confirmation of Conjugation of AM protein to NGMA

4.7.1. FT-IR – Epoxy Ring Opening

Initial evidence towards conjugation of proteins was elucidated by comparing the FT–IR spectra of NGMA before and after conjugation. A prominent peak present in the epoxy ring region of NGMA at around 1028.7cm^{-1} was absent in the AMpro-NGMA conjugated system (Figure 13). This difference of absence of the peak after conjugation with AM indicates utilization of epoxide ring opening and thereby conjugation. As a direct evidence, this is an indication of the opening of the epoxy ring.

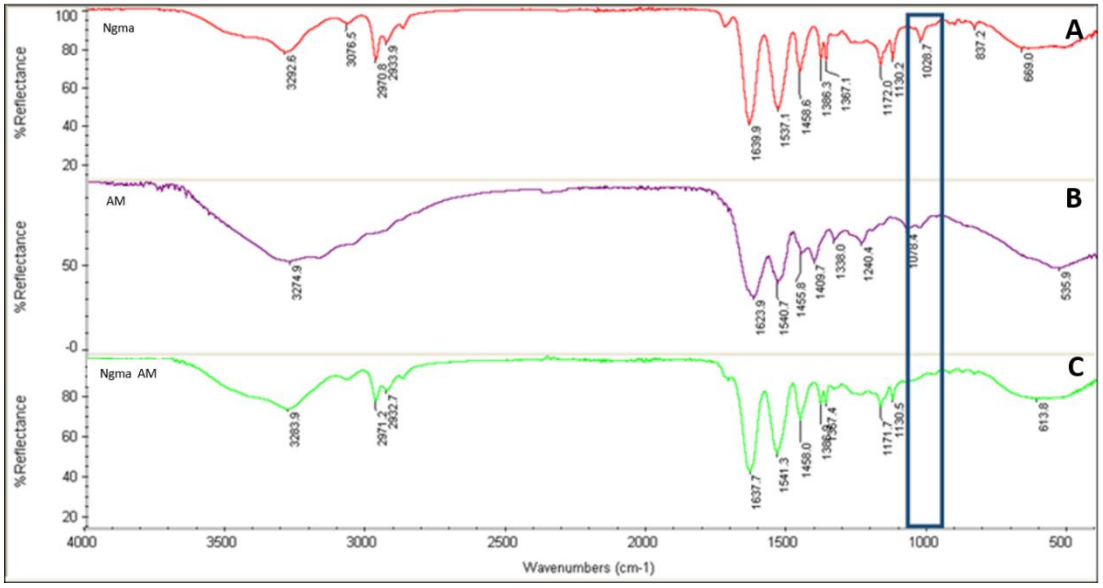

Figure 13: FT-IR evaluation of conjugated Protein (A) FT-IR of NGMA (B) FT-IR spectrum of AM protein (C) FT-IR spectrum of AM conjugated NGMA showing the absence of a peak at 1028cm^{-1} in comparison to NGMA alone.

4.7.2. Confirmation of Bio-functionalization

Bio-functionalization of NGMA with AM proteins was confirmed using SDS PAGE and western blot. NGMA is a copolymer of poly NIPAAm and glycidyl

methacrylate (GMA). Conjugation with AM protein occurs through the epoxy ring opening mechanism of GMA. So conjugation happens only on NGMA and not on its main chain polymer, PNIPAAm.

AMpro-NGMA, AM control, NGMA and PNIPAAm was run on different lanes on SDS PAGE. It was shown that, only on AMpro-NGMA, the proteins (AM) did not run down the lane as it was conjugated with the polymer (Figure. 14A). This is due to the higher molecular weight achieved by conjugation of protein with the polymer. In PNIPAAm lane, since the polymer was not able to conjugate the proteins, they run down as in case of the control. This also serves as a control to state that proteins are not entangled or trapped within the polymer but were conjugated. This proved that the AM protein got conjugated to GMA group of NGMA. This was further re-confirmed by western blot analysis of AM protein Decorin, Mimican and Lumican (Figure. 14B). These are abundant proteins present in the amniotic membrane. The results showed that Decorin and Mimican got conjugated to the NGMA since the band formed in AMpro-NGMA was faint in comparison with the control AM. This suggests that the protein is held by the polymer on the well and is not free to run down the gel. Lumican showed similar thick bands in both control and conjugated system. This also suggests that low molecular weight proteins prefer to conjugate in comparison to large molecular weight proteins such as lumican. Lumican is a large molecular weight protein, did not effectively get conjugated to NGMA.

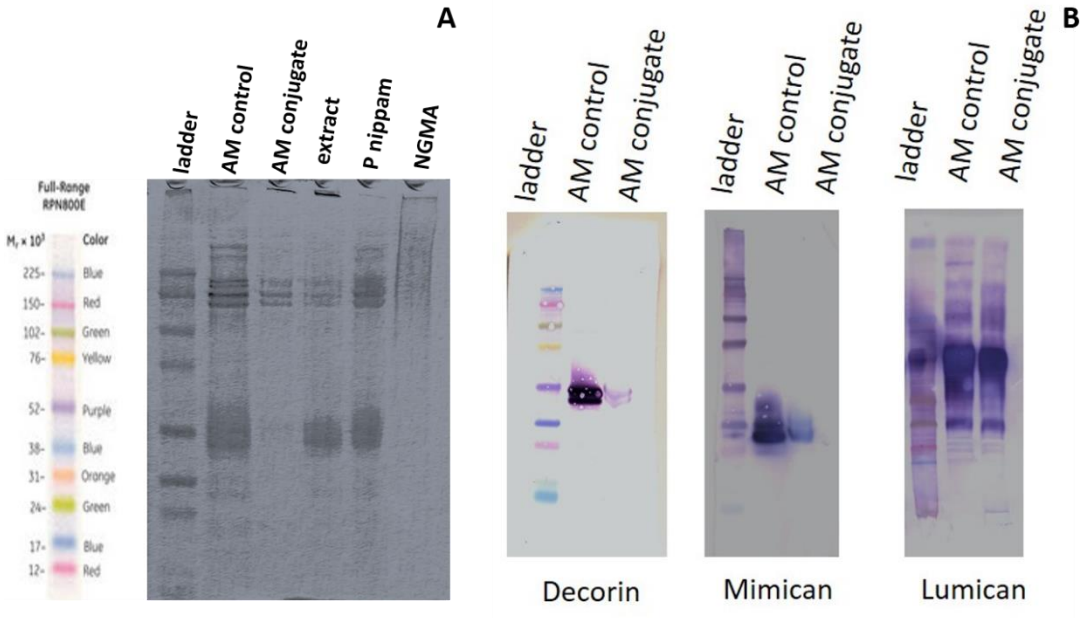

Figure 14: Confirmation of Bio-functionalization: (A) SDS PAGE Analysis showing trapping of conjugated protein in the wells of PAGE. (B) Western blot showing a decrease in band intensity of conjugated protein due to trapping of conjugated protein.

CHAPTER - V

5. RESULTS: *IN VITRO* STUDIES

5.1. Adipose Mesenchymal Stem Cells

5.1.1. Isolation, culture and characterization of ASCs

ASCs were isolated from rabbit subcutaneous fat pad by collagenase digestion method and cultured *in vitro* based on their property of plastic adherence.

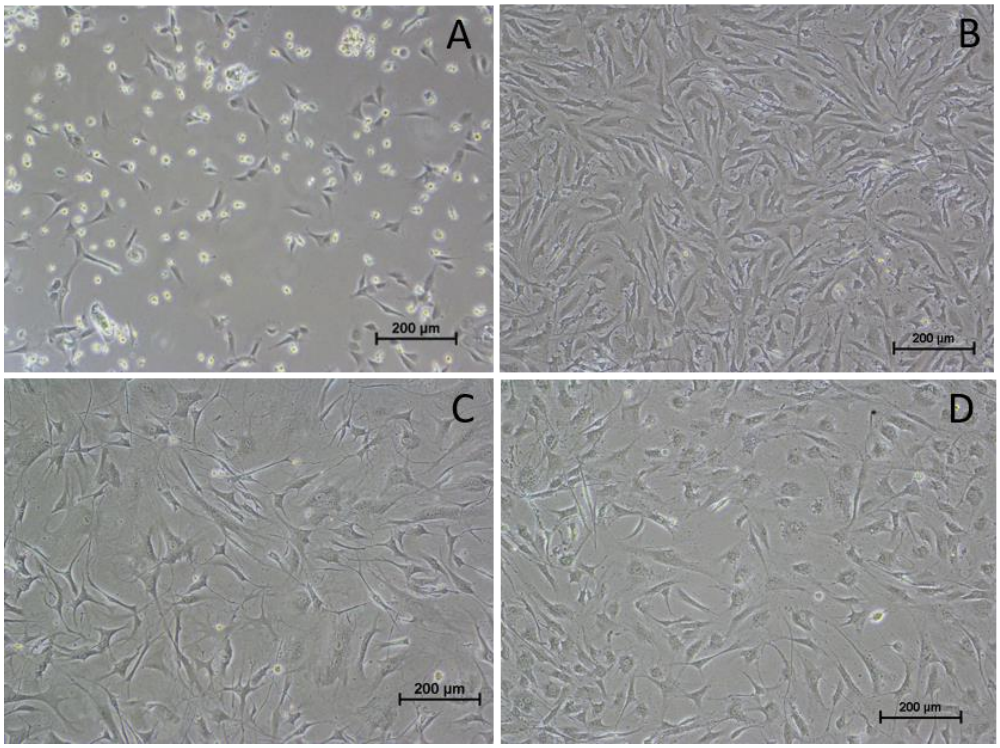

Figure 15: Isolation and morphological evaluation of mesenchymal stem cells (ASCs) (A) passage 0, day 2 after isolation (B) A monolayer of ASCs passage 3 depicting fibroblastic morphology (C) ASCs exhibiting morphological changes at passage 8 and (D) passage 10

When the isolated cells were directly plated on to plastic cell culture plates, in two days they started adhering and formed small colonies (Figure. 15A) and in 5 – 6 days they formed a confluent monolayer of ASCs. Most of the non-adherent cells were removed during the first media change after 11-16 hours. The media was changed every 2 days to remove non-adherent cells and other debris of isolation. The adherent cells showed spindle-shaped morphology (Figure. 15B), proliferated and were passaged at the confluence. ASCs at 80% confluency were trypsinized and passaged. Each passage took around 3 to 4 days for attaining confluence. Healthy cells were observed until 6 to 8 passages and thereafter on prolonged sub culture of MSCs, their typical spindle shaped morphology was seen deteriorating. Stretching out / rounding up of the cell was microscopically observed as seen in the micrograph provided. (Figure. 15C & 15D).

5.1.2. Flow Cytometry analysis for characterization of ASCs

ASCs were characterized for their stemness using flow cytometry (BD, FACS ARIA). The cells showed more than 85% positivity for CD 105 (Figure. 16C), CD 90 (Figure. 16D), and CD 44 (Figure. 16E) when incubated with mesenchymal stem cell markers and were negative for CD 34 (Figure 16F). Figure. 16A, represents the side scattered dot plot and Figure.16B, represented the unstained control. These CD markers are standard mesenchymal stem cell characterization markers according to the International Society for Cellular Therapy (ISCT).

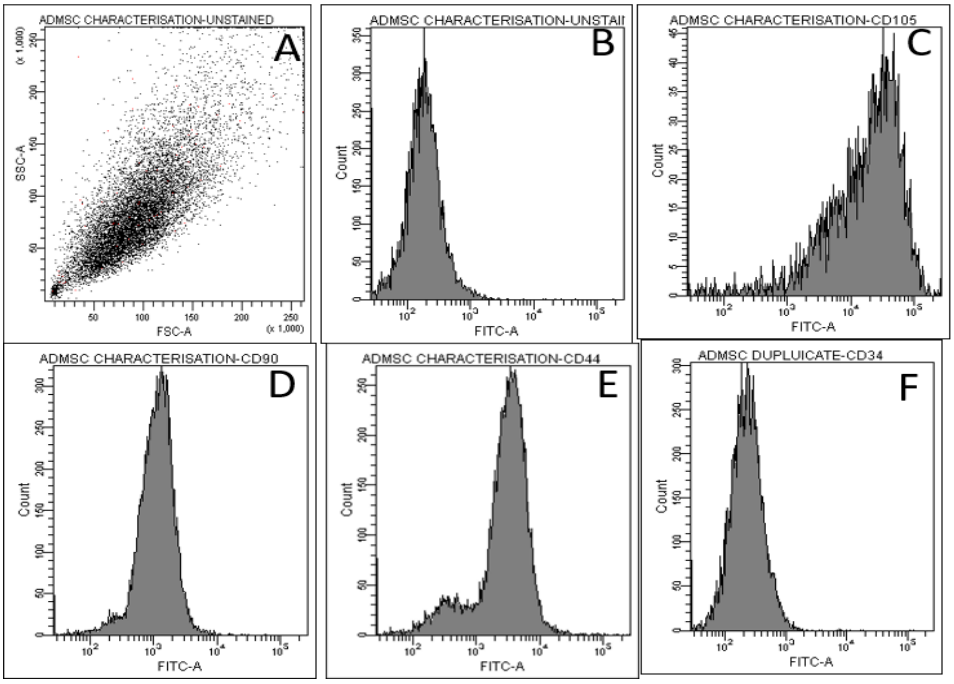

Figure 16: Flow cytometry analysis of rabbit ASCs (A) Dot Plot - distribution of ASCs; Histogram of (B) Control (C) CD 105 – 92.7% (D) CD 90 – 86.5% (E) CD 44 – 91% (F) CD 34 - 16.5 % positivity

5.1.3. Multi-lineage differentiation of ASCs

Adipose mesenchymal stem cell population was also evaluated for multi-lineage differentiation potential to adipo- and osteo- lineages. ASCs induced to adipogenic lineage showed lipid accumulation within the cytoplasm of the cell. Oil red O stain got dissolved in the fat globules and gave bright red colour (Figure. 17A) when imaged in comparison with the control (Figure. 17B). ASCs when induced to osteo- lineage for 28 days, showed calcium and phosphorus deposition evident from alizarin red (Figure. 17C) and silver nitrate staining (Von kossa) (Figure. 17E) indicating osteogenesis. Alizarin red staining (Figure. 17D) and silver nitrate staining (Figure. 17F) for the non-induced controls did not show evident deposition of divalent calcium and phosphorous ions.

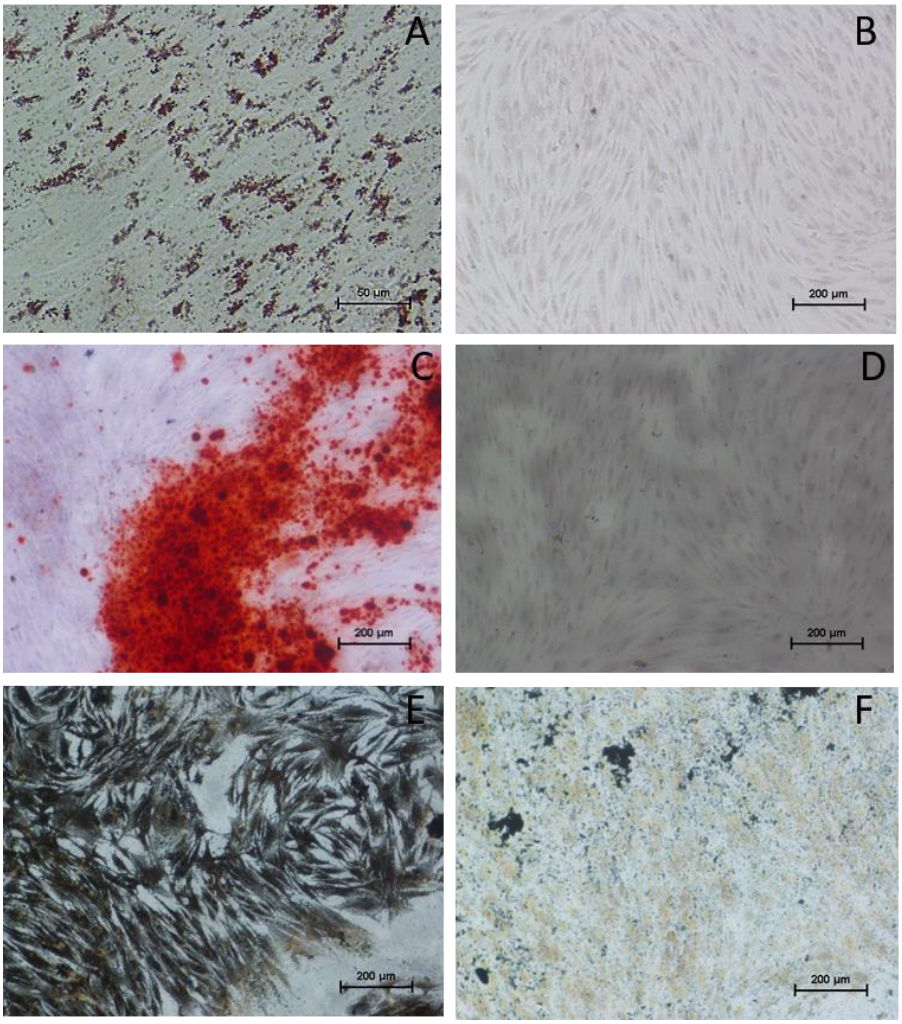

Figure 17: Multi-lineage differentiation of rabbit ASCs: (A) induction to adipogenic lineage 21 days shows lipid accumulation in red colour when stained by Oil Red O (B) non-induced control stained by Oil red O (C) Induction to osteogenic lineage for 28 days when stained by Alizarin Red showed calcium deposition in red colour (D) non induced control stained by Alizarin Red (E) Induction to Osteogenic lineage 28 days when stained by Von kossa showing phosphorous deposition as black colour. (F) non-induced control stained by Von kossa.

5.2. Specific cytotoxic evaluation of NGMA using ASCs

NGMA was evaluated for specific cytotoxicity against ASCs. Even though studies with L929 have shown that NGMA is non-cytotoxic, specific cytotoxicity was evaluated with ASCs to see if NGMA alters any of the ASC properties. In the test on extract studies, the cell monolayer incubated with the NGMA extract was examined microscopically for cell morphology. No specific signs of vacuolization, detachment and membrane disintegration was observed (Figure. 18A). ASCs exhibited characteristic fibroblastic morphology.

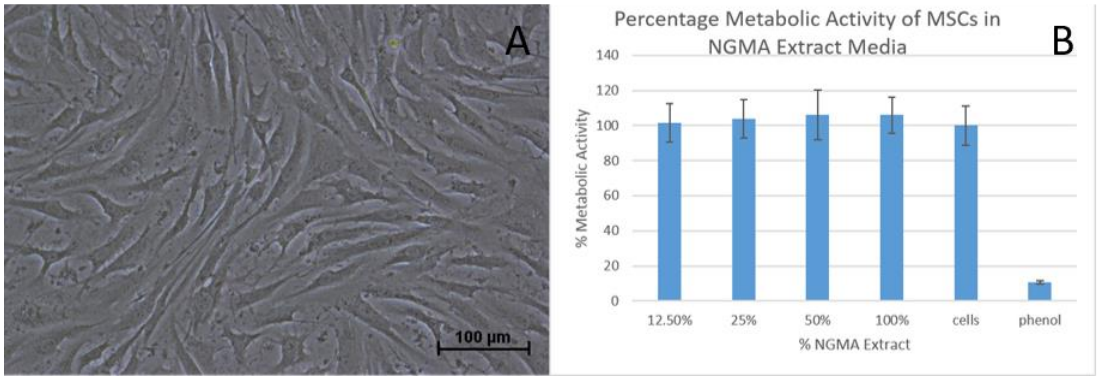

Figure 18: *In vitro* cytotoxicity of NGMA using ASCs: (A) Mesenchymal stem cells maintained their morphological features 24h after incubation with NGMA extract. (B) Effect of NGMA extract concentrations on metabolic activity of ASCs by MTT assay.

MTT assay replicated the same observation. The ASCs incubated with extract were compared with ASCs in normal growth medium (control medium) and cells cultured with phenol as positive control. The extract dilutions showed comparable OD reading with control medium at 570 nm, which corresponded to

similar metabolic activity (Figure. 17B) at various dilutions. The NGMA extract did not affect the proliferation or metabolic activity of ASCs

5.3. Evaluation of ASC characteristics on NGMA

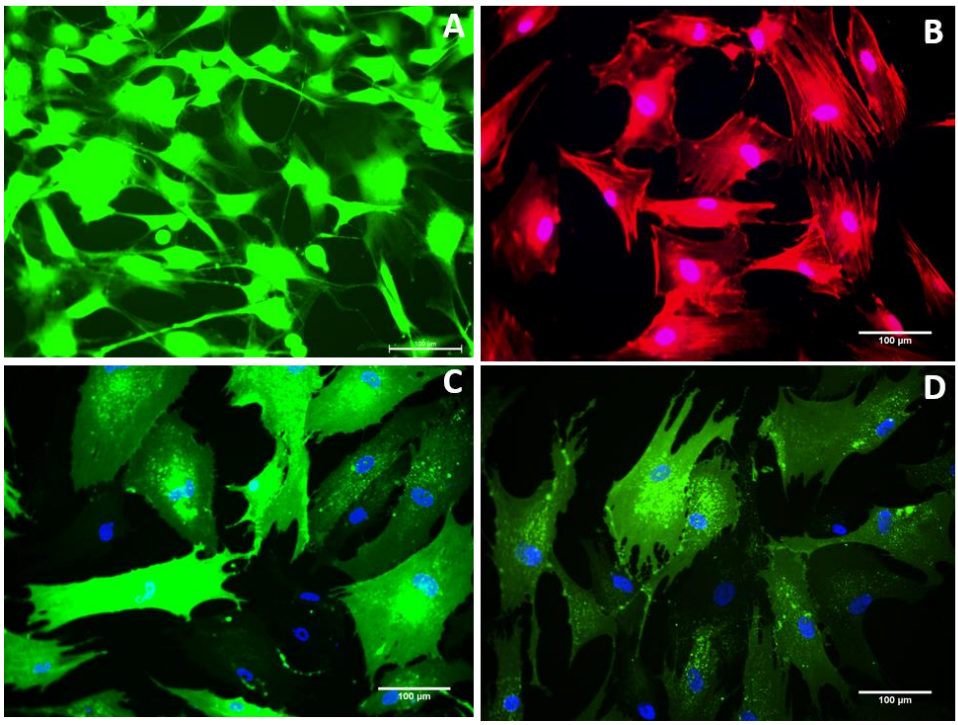

Figure 19: Evaluation of ASCs on NGMA: (A) Calcein AM stained viable ASCs showing spindle-shaped cells when cultured on NGMA. (B) Actin cytoskeletal staining of ASCs cultured on NGMA showing well-developed actin fibres. (C) Fluorescent micrographs for immunostaining of ASCs on NGMA for CD 90 and (D) CD 105.

The viability staining using calcein AM of cells grown on NGMA showed green fluorescent, viable ASCs with spindle-shaped morphology (Figure. 19A). Actin cytoskeletal staining also showed well developed cytoskeletal filaments (Figure. 19B). Actin cytoskeletal staining along with Calcein AM showed a well-spread

population of cells on the NGMA dish. Moreover stem cell properties of ASCs on NGMA was confirmed using CD 90 (Figure. 19C) and CD 105 staining (Figure.19D).These mesenchymal stem cell markers confirmed that the NGMA-ASC interaction has not altered the stemness of ASCs which is very important in terms of a regenerative therapy.

5.4. Isolation and characterization of limbal explant culture.

Limbal explants when cultured *in vitro*, showed migration or movement of cells from the explant to the culture dish. These cells included a diverse population of fibroblastic and polygonal (Figure. 20A & 20B) shaped cells. Limbal explant cells stained differentially for CK 3/12 (Figure. 20C) indicating cells at various phases of differentiation as the culture was initiated from the explant. MEM medium used to culture these cells were collected and stored for differentiating ASCs.

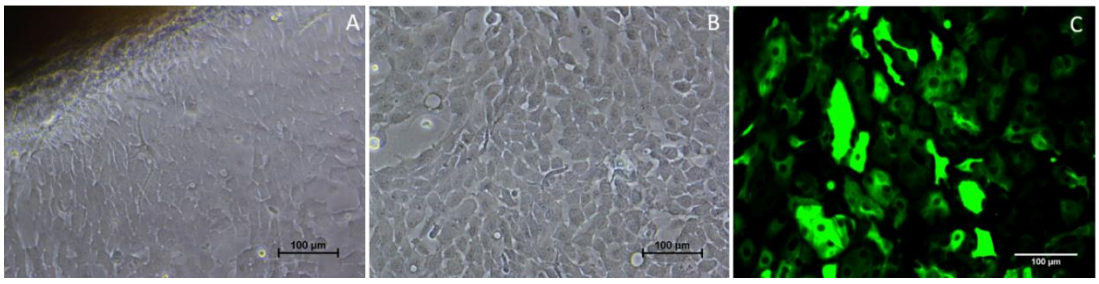

Figure 20: Limbal Explant Culture: (A) Migration of cells from the limbal explant (B) Phase contrast image of a monolayer of limbal explant migrated cells (C) immunostaining of limbal explant culture with corneal epithelial marker CK 3/12.

5.5. Differentiation of ASCs to corneal epithelial lineage

The procedure was to confirm if ASCs have the potential to differentiate to corneal epithelial lineage. ASCs were differentiated to corneal epithelial lineage by incubating with limbal conditioned medium for 14 days.

5.5.1. Standardization of differentiation medium.

Differentiation was attempted with limbal stem cell condition media and Dulbecco's defined keratinocyte medium (DSFM) with growth supplements.

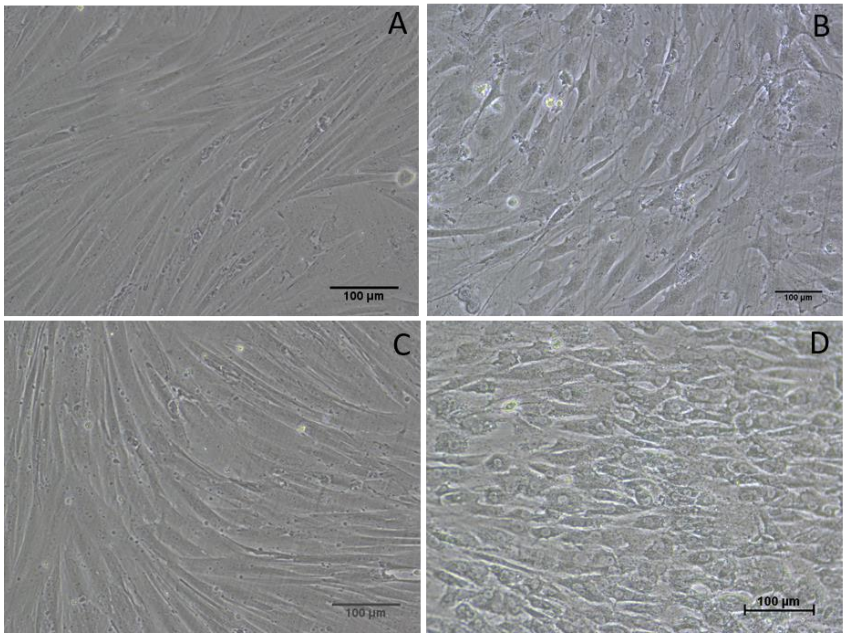

Figure 21: Standardization of ASC differentiation – studies done at day 14 (A) Control media –non induced cells (B) differentiation using limbal conditioned media (C) Differentiation using DSFM (D) differentiation using limbal conditioned media on NGMA

ASCs differentiated in limbal condition medium showed slight morphological variations after 14 days in differentiation (Figure. 21B). ASCs with limbal condition medium induced differentiation, attained a more broaden morphology in comparison

to the non-induced control ASC (Figure. 21A). While ASCs do not show evident morphological changes after 14 days in DSFM (Figure. 21C). ASCs differentiated in NGMA using limbal condition medium also showed a slight morphological change towards epithelial phenotype (Figure. 21D). On NGMA, cells seemed to be more aligned and packed with evident epithelial-like cells in differentiated culture. Limbal explant morphology is evident from the earlier image (Figure. 20B).

5.5.2. Standardization of medium for corneal epithelial differentiation: by Real-time PCR

The initial objective of real-time PCR was to determine the suitable differentiation media for corneal epithelial differentiation. ASC differentiation to corneal epithelial lineage was compared between limbal condition medium and DKSFM.

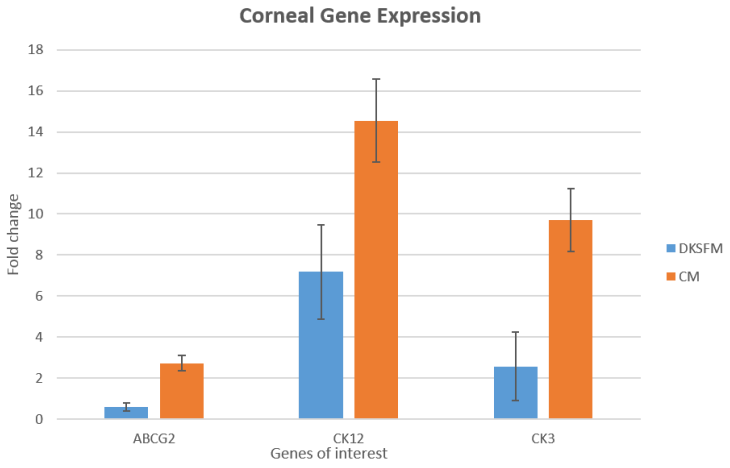

Figure 22: Standardization of Differentiation: DKSFM *vs* Condition medium (CM)

While comparing the expression of CK3/CK12 mRNA, a corneal epithelial differentiation marker, condition medium showed more than fivefold up-regulation in comparison to DSFM.

ABCG2 a limbal/Mesenchymal stem cell marker also showed two fold up-regulation. The data (n=3) is represented as mean ± SD. (Figure. 22). The values derived for DSFM and CM mediated ASC diferentiation was normalized with uninduced control ASCs. Statistical significance was evaluated based on p-value < 0.05.

5.5.3. Evaluation of corneal epithelial differentiation: by Immunocytochemistry

ASCs were stained positive for CK 3/12 both on limbal condition media (Figure. 23B) and DKSFM (Figure. 23C). Control ASCs cultured in growth medium did not show up CK 3/12 positive cells (Figure. 23A).

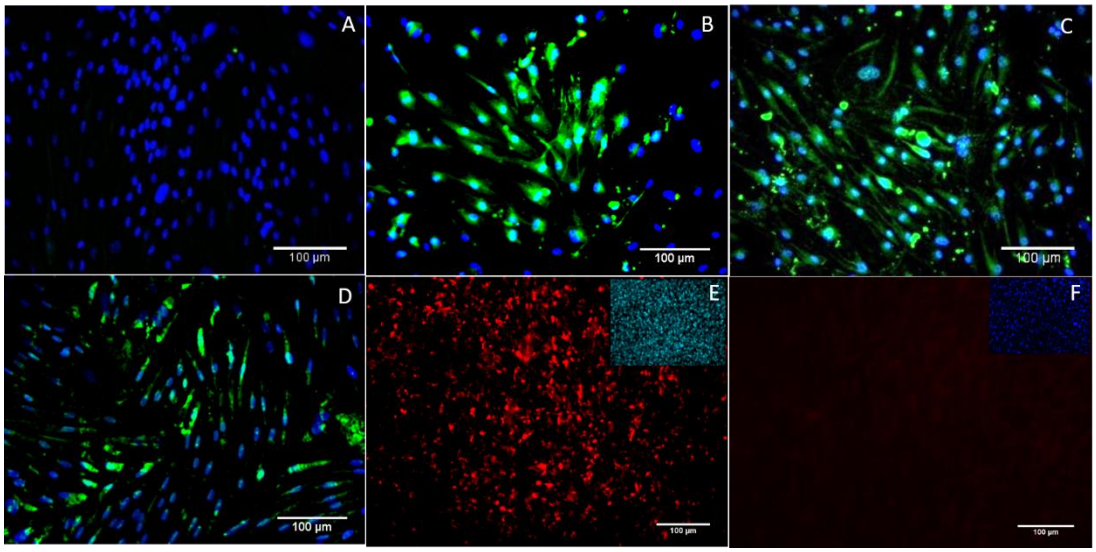

Figure 23: ASC differentiation to corneal epithelial lineage (Immunocytochemistry), 14-day studies: (A) Non induced ASCs stained with corneal epithelial marker CK 3/12. (B) Trans differentiation of ASCs using limbal condition media stained with CK 3/12 (C) Trans differentiation of ASCs using DSFM stained with CK 3/12 (D) Trans differentiation of ASCs using limbal condition media on NGMA stained with CK 3/12 (E) Trans differentiation of ASCs using limbal condition media on NGMA stained with connexion 43. (F) non induced ASCs stained with connexion 43.

CK 3/12 is a specific marker for corneal epithelium, showing corneal epithelial differentiation of ASCs. Evident bright staining was obtained in limbal condition medium in comparison to DKSFM (Figure. 23B and 23C).

For further analysis of differentiation and sheet formation, limbal condition medium was selected.

ASCs differentiated on NGMA using limbal condition medium also stained positive for CK 3/12 and showed an aligned population of cells with respect to cells in TCPS (Figure 23D). Differentiated cells were also positive for cell junction marker Connexin 43 on NGMA (Figure. 23E) in comparison to the control (Figure 23F), which is again an indicator of epithelial differentiation.

5.5.4. Evaluation of corneal epithelial differentiation by Gene expression analysis - Real-time PCR

The objective of the real-time qPCR analysis was to assess the influence of limbal conditioned medium on the differentiation of ASCs at the molecular level. Analyzing the gene expression at day 14, the molecular phenotype determination of corneal epithelium-specific genes, CK 3 and CK 12 showed 2 to 3 fold increase in comparison with the non-induced control ASCs. p63 and PAX6 showed around 1.5 fold upregulation while ABCG2 showed around 2 fold upregulation in comparison with the 14-day control ASCs. Comparing the 7 day induced cells with the 14 day induced cells, there is a statistically significant increase in expression of CK3, ABCG2 and PAX6, while CK 12 and p63 were not significant. The values derived for CM mediated ASC differentiation was normalized with uninduced control ASCs. The relative comparison of gene expression with non-induced cell population

graphically displayed an increased fold change in the genes of interest. The data (n=3) is represented as mean ± SD (Figure. 24). Statistical significance was considered based on p-value < 0.05.

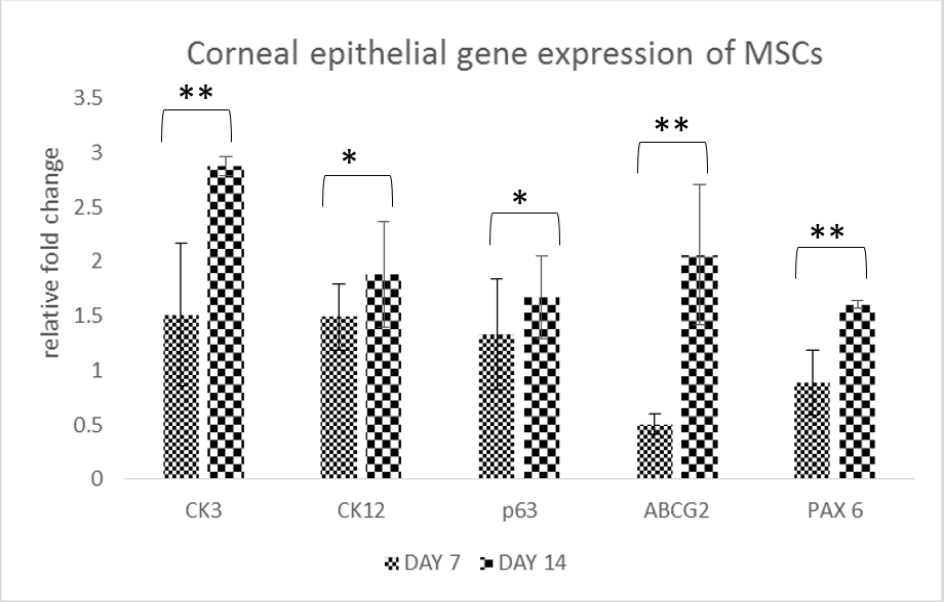

Figure 24: Gene expression pattern of induced ASCs: Normalized to ASCs after 14 days in control medium. ** is significant, * is not significant.

5.5.5. Evaluation of corneal epithelial differentiation by Flow cytometry

Flow cytometry analysis of differentiated cell population showed cells at various phases of differentiation after 14 days of induction. Flow cytometry analysis of the 14 day non-induced cells (control) showed less than 5 % CK 3/12 positive cells (Figure. 25A-C) while 28.65 ± 3.18 % (p-value ≥0.01) of cells were stained positive for CK 3/12 at day 14 (Figure. 25D-F) when ASCs were induced with limbal conditioned medium. Apart from the terminal differentiation marker CK 3/12, 61.6% of cells were stained positive for GAP junction protein connexin 43 (Cx 43) (Figure. 25H) and less than 10% of cells were stained positive for CD 90 (Figure. 25I), a

mesenchymal stem cell marker after differentiation to corneal epithelial cells. Figure 25G shows the histogram of the secondary stained for 14 days induced cell population which served as the control.

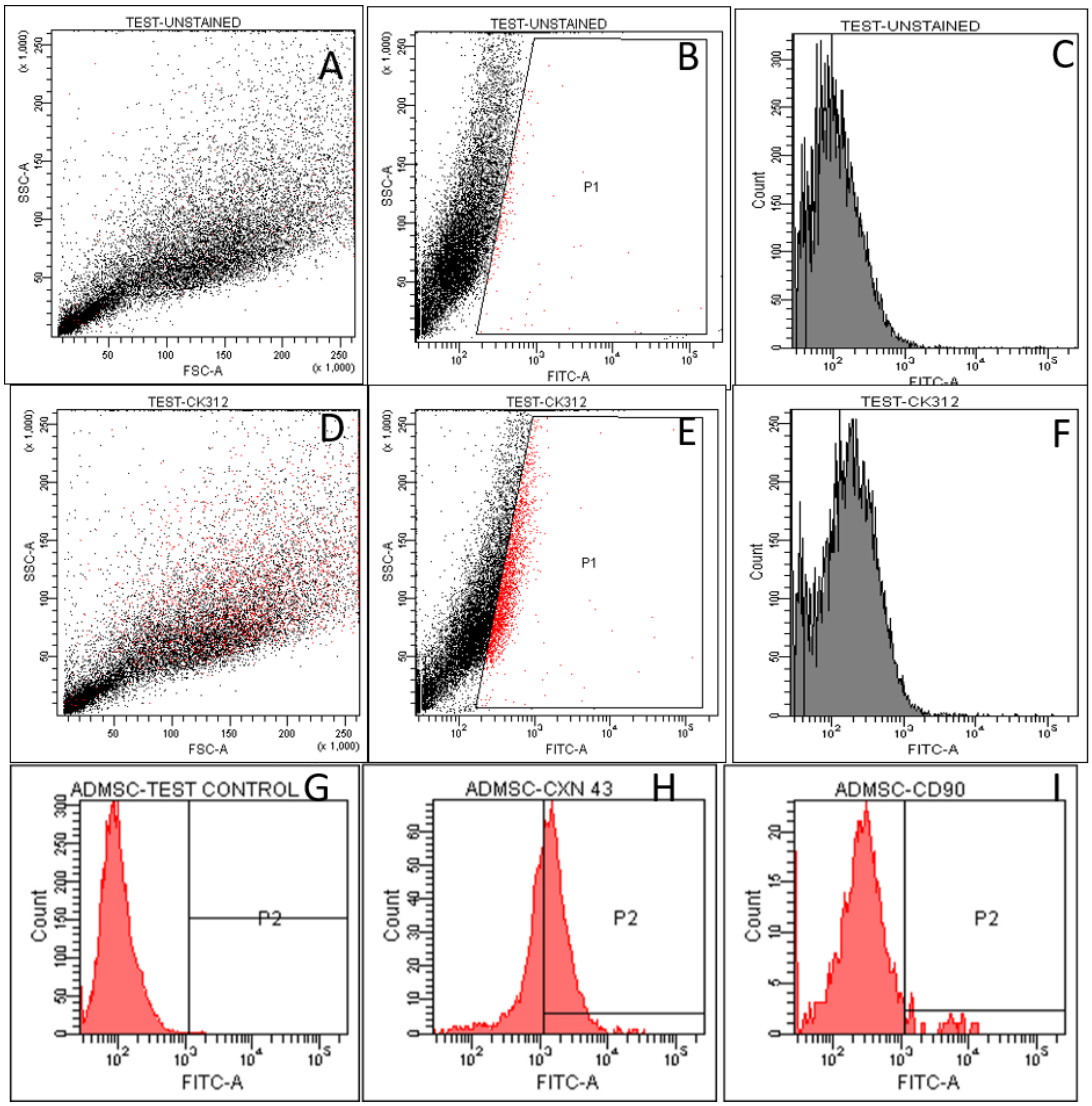

Figure 25: Flow cytometry analysis for corneal epithelial differentiation of ASCs (A-C) ASCs after 14 days in control medium - CK 3/12 staining: (A) dot plot (B) Gated population (C) Histogram - 2.4% (D-F) ASCs after 14 days in limbal conditioned medium - CK 3/12 staining: (D) dot plot (E) Gated population (F) Histogram – 28.6 %. (G) Secondary stained control for Connexin 43 and CD 90 (H)

Connexin 43 stained ASCs after 14 days in limbal conditioned medium – 61.6 % (I) CD 90 stained ASCs after 14 days in limbal conditioned medium – 8.6 %.

5.6. Culture, retrieval and transfer of ASC sheets from NGMA

Mesenchymal stem cells sheets were constructed by culturing adipose stem cells to confluence on NGMA coated cell culture dishes at 37^{o}C. When the temperature is brought down to 20^{o}C or below, NGMA undergoes phase transition making the cell sheet to detach from the polymer surface. The phase contrast images before cell sheet retrieval showed a dense monolayer of cells on the NGMA surface (Figure.26A).

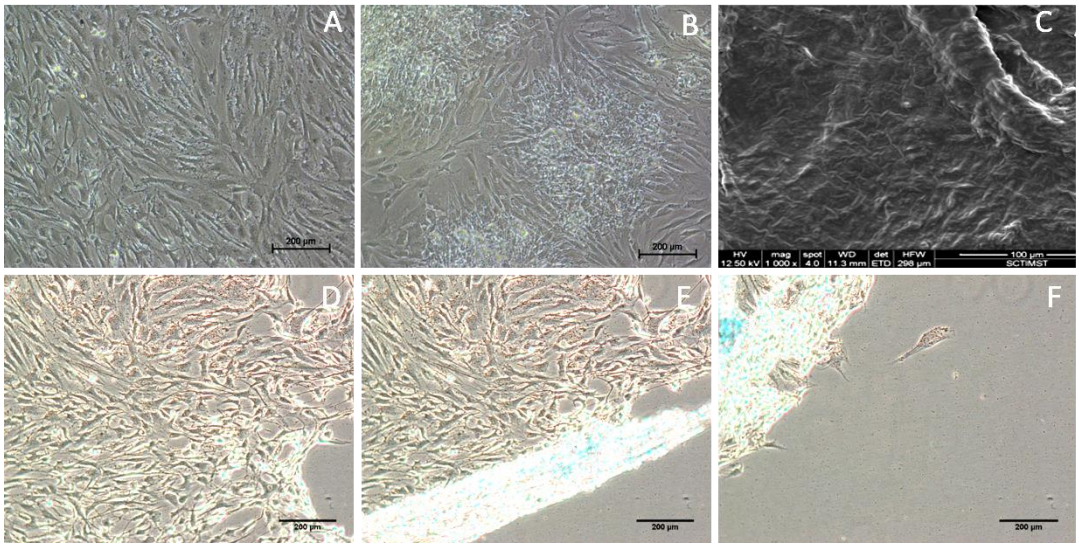

Figure 26: Phase contrast images of Mesenchymal Cell Sheet detachment and replating: (A) Monolayer of cells on NGMA before sheet detachment. (B) ASC sheet after replating to a new dish appeared like cell clusters. (C) Scanning electron micrograph of mesenchymal cell sheet. (D, E, and F) Time-lapse image of Mesenchymal Cell sheet detachment from NGMA.

The time lapse image of cell sheet detachment using phase contrast microscopy showed a network of interconnected cell structures detaching from the polymer surface as a sheet (Figure. 26D-F). After transferring to the new dish using PVDF as the transfer tool, they remained stable as sheet or clusters (Figure. 26B). The scanning electron micrographs revealed the thick dense pattern of the cells transformed into a sheet (Figure. 26C).

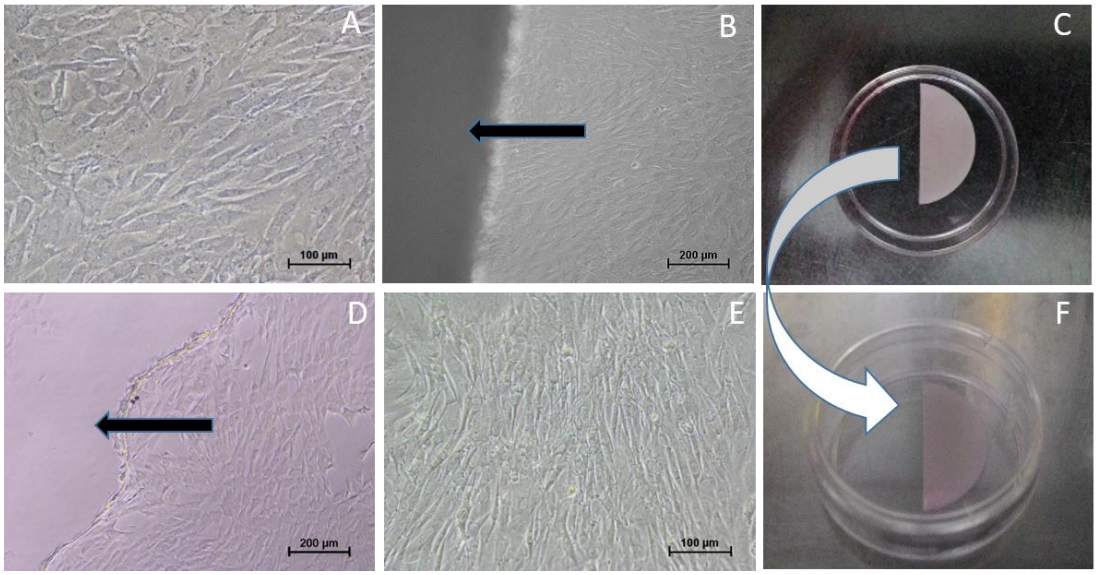

Figure 27: Demonstration of Cell sheet transfer using PVDF (A) confluent monolayer of cells on NGMA (B) PVDF membrane placed on NGMA (indicated by arrow mark) while incubating at a temp below 20^{o}C. (C) A gross image of PVDF membrane on NGMA dish for better demonstration (D) Image of the NGMA dish after PVDF membrane was removed. Arrow mark indicates the region where PVDF membrane was placed on the cell monolayer. (E) Cell sheet 24h after transfer on to a new dish. (F) Cell sheet adhered on to the PVDF was transferred on to a new dish along with PVDF membrane- a demonstration. PVDF membrane was removed after the cell sheet attached to the new dish.

Transfer of the cell sheet to a new surface is achieved with help of a transfer system – PVDF membrane (Figure. 27). Transfer using PVDF membrane was demonstrated earlier in detail in section 4.3. Cells adhere on to the PVDF membrane (Figure. 27B) when incubated at a temperature below 20^{o}C and were then transferred to a new dish (Figure 27E).

The cell sheet formed was imaged digitally (Figure. 28A) and was evaluated for its transparency (Figure. 28B). The alphabets were clear and legible when read through the cell sheet. Thus, the sheet formed and transferred was proven to be transparent since these sheets were to be clinically evaluated in rabbit models.

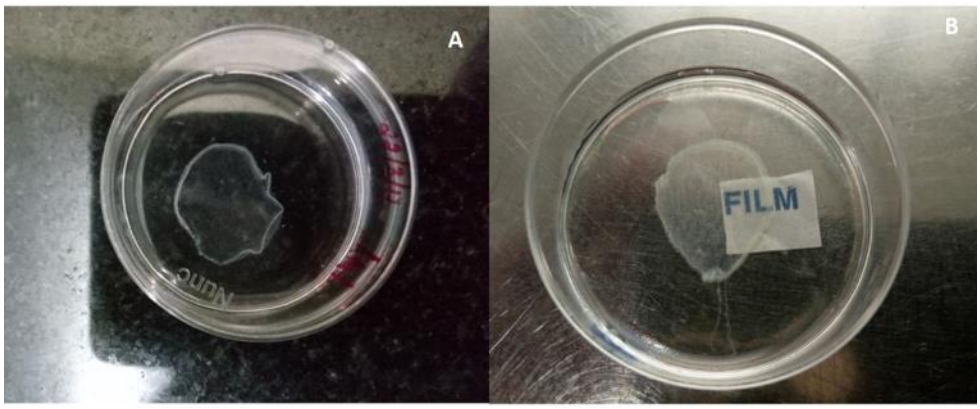

Figure 28: Cell sheet evaluation for transparency: (A) Gross image of cell sheet formed (B) Legible alphabets demonstrating transparency of cell sheet.

The Cell sheet formation on NGMA was evaluated for actin cytoskeletal morphology and viability at various stages of cell sheet transfer. The cell sheet before the transfer was assessed for actin cytoskeletal morphology (Figure. 29A) and viability using calcein AM staining which showed a dense network of viable cells (Figure. 29D). Actin cytoskeletal staining of a detached floating cell sheet showed a network of rolled up floating cells (Figure. 29B). The detached floating cell sheet

also demonstrated a cluster of viable cells when stained with calcein AM (Figure. 29E). Rolling up of cell sheet indicated the need for a transfer tool, as manipulating a floating sheet will be difficult while transferring without a support. The cell sheet was transferred to a new dish using PVDF membrane as a transfer tool and was imaged after 24h which showed an aligned group of cell cluster in actin staining while a viable network of calcein AM stained cells (Figure. 29C) showed the integrity of the cell sheet after replating (Figure. 29F). Transferred cell sheet maintained characteristic spindle-shaped morphology clustered to form a network of cells transformed to a sheet with closely packed almost aligned cells.

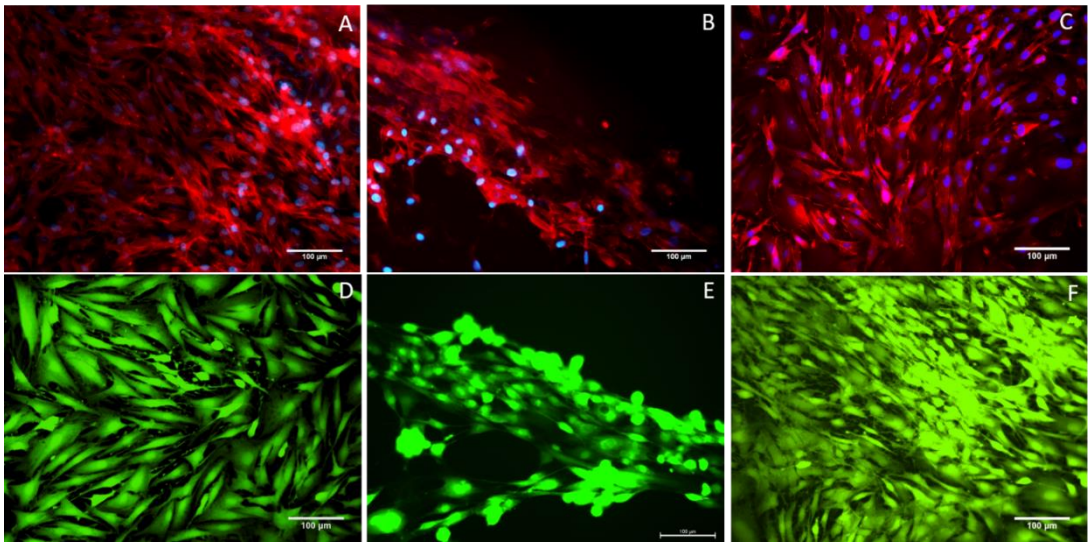

Figure 29: Evaluation of Cytoskeletal morphology and Viability before and after ASC cell sheet transfer. (A) Actin cytoskeletal staining of ASCs on NGMA before cell sheet retrieval. (B) Actin cytoskeletal staining of the detached cell sheet (C) Actin cytoskeletal staining of ASC cell sheet after transfer to a new dish. (D) Calcein AM staining of cells on NGMA before cell sheet retrieval. (E) Viability assessment of a detached cell sheet (F) Calcein AM staining of cell sheet after transfer to a new dish.

5.7. Cell sheet Formation on Biofunctionalized NGMA

AM bio-functionalized NGMA was developed and was evaluated for cell sheet retrieval using corneal stromal stem cells.

5.7.1. Culture and characterization of CSSC

CSSCs were isolated using collagen digestion method and based on their property of adherence to protein-coated surfaces. CSSCs when cultured on patented combination medium called Stem Cell Medium (SCM) (Patented product of Academic Ophthalmology, University of Nottingham, UK). Cells, when cultured on SCM media, are claimed to have maintained their stemness over passages, but will adhere only on to protein-coated surfaces. CSSCs in SCM fail to attach on to cell culture dishes (Figure. 30A) and are always cultured on 1% gelatin-coated surfaces. When the isolated cells were directly plated on to gelatin-coated plastic cell culture plates, the adherent cells formed a spindle-shaped morphology, proliferated and were passaged at confluence (Figure. 30B).

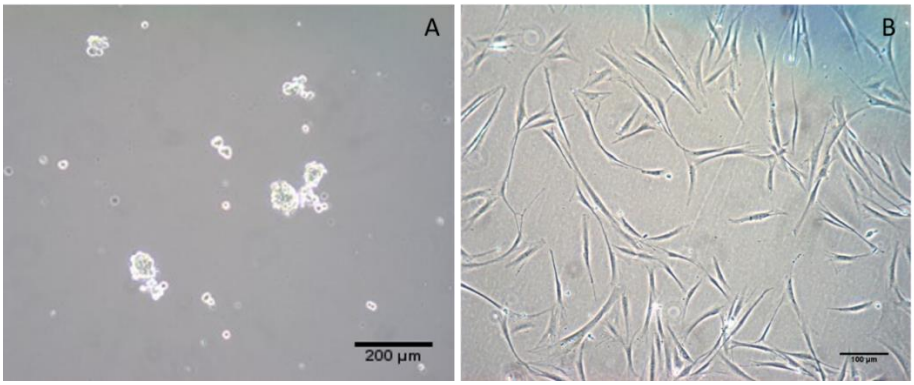

Figure 30: Corneal Stromal stem cells, Passage 2: (A) on non-coated cell culture dishes – cells round up (B) on gelatin-coated cell culture treated culture dishes – cells spread

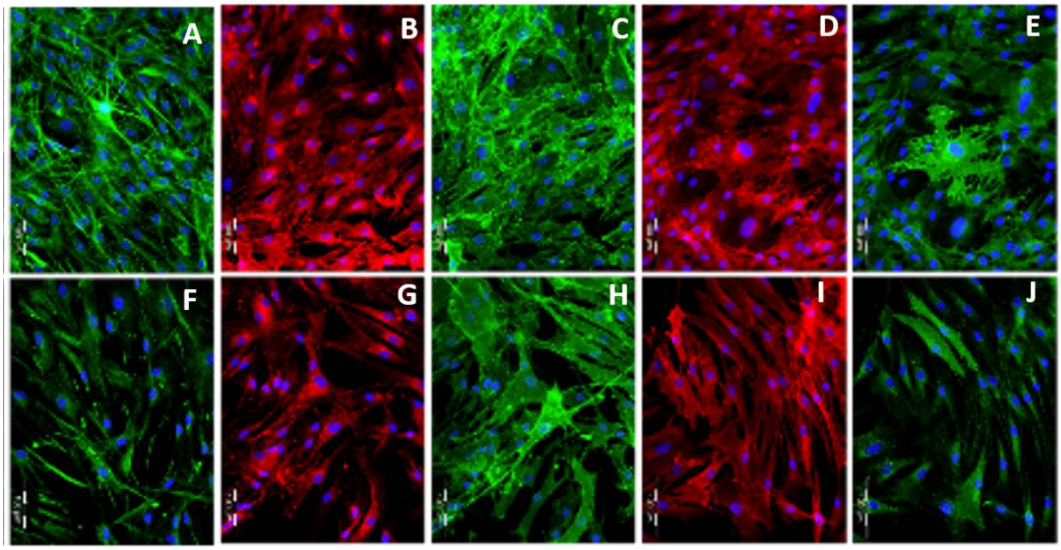

Figure 31: Characterization of CSSCs: (A-E) CSSCs on Gelatin coated surfaces (A) ABCG2 (B) CD 73 (C) CD90 (D) CD105 (E) CD34. (F-J) CSSCs on Amniotic membrane protein-coated surfaces (F) ABCG2 (G) CD 73 (H) CD90 (I) CD105 (J) CD34.

CSSCs are supposed to be cells expressing MSC markers and when analyzed were found to be positive for ABCG2 on gelatin-coated surface (Figure. 31A) and the expression was comparable with AM coated surfaces (Figure 31F). CD 73 on Gelatin (Figure. 31B) and AM (Figure. 31G); CD 90 on Gelatin (Figure. 31C) and AM (Figure. 31H); CD 105 on Gelatin (Figure. 31D) and AM (Figure. 31I); CD 34 on Gelatin (Figure. 31E) and AM (Figure. 31J) were also found to be positive for CSSCs. CSSCs were characterized on both gelatin and AM coated surfaces and was found to express the CD markers at the same intensity.

5.7.2. Cell spreading and initial adhesion of CSSCs on AMpro

Cells spreading of CSSCs were evaluated to determine the optimum concentration of AMpro required for conjugation with NGMA.

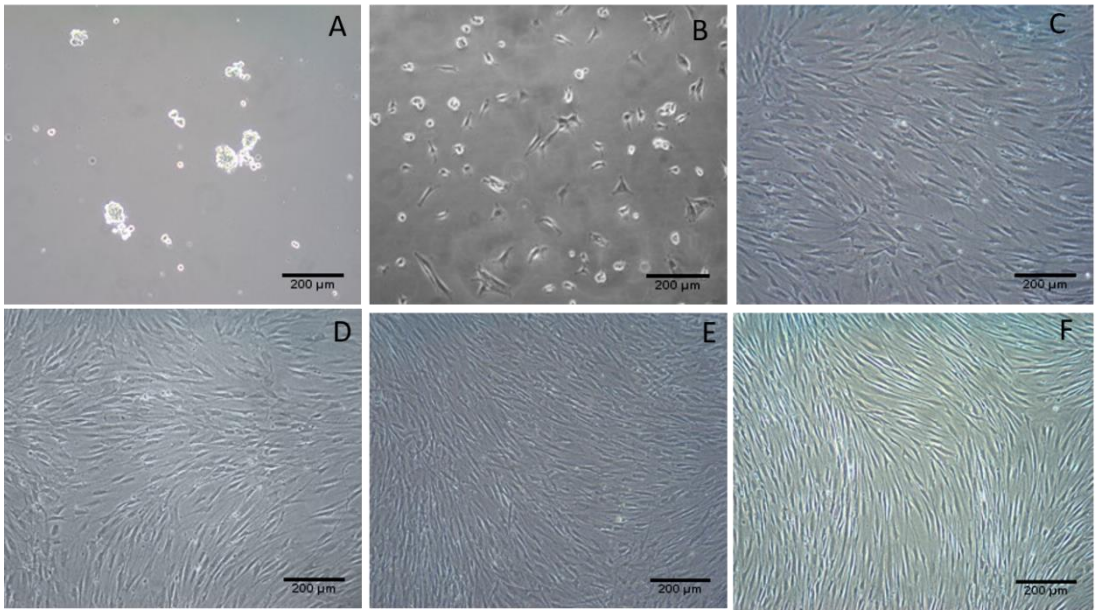

Figure 32: Spreading of CSSC on the variable concentration of AMpro: (A) cell culture dish without AMpro (B) 3µg AMpro (C) 6µg AMpro (D) 10µg AMpro (E) 20µg AMpro (F) 40µg AMpro.

Even after uniform cell seeding, the cell spreading was found depended on the amniotic membrane protein concentration. Cell spreading was not observed in cell culture dishes without AMpro (Figure. 32A). On 3µg AMpro cell spreading was much less (Figure. 32B) compared to other higher concentration ranging from 6µg to 40µg. From 6 to 40µg (Figure. 32C to 32F) cells seem relatively adhere and spread. Quantitative estimation of initial adhesion after 24h showed almost similar results as on phase contrast imaging. Cell spreading of CSSCs on AMpro was compared to gelatin-coated surfaces which served as the control. CSSCs showed almost same adhesion potential to both gelatin and AM coated surfaces from 6µg concentration onwards (Figure. 33) when evaluated using presto blue staining. The data is expressed as relative fluorescence units (RFU) of presto blue stain ten up by the life cells adhered to AM pro coated dishes with variable concentration. For further

experiments, 10µg AMpro (Figure. 32D) was used, since 6µg AMpro (Figure. 32C) even though minor, showed a significant difference in protein adhesion when comparing AM to gelatin. Higher concentrations including 20µg AMpro (Figure. 32E) and 40µg AMpro (Figure. 32F), when attempted for cell sheet retrieval seemed to be affecting the viability of the cells. The data follows in next section

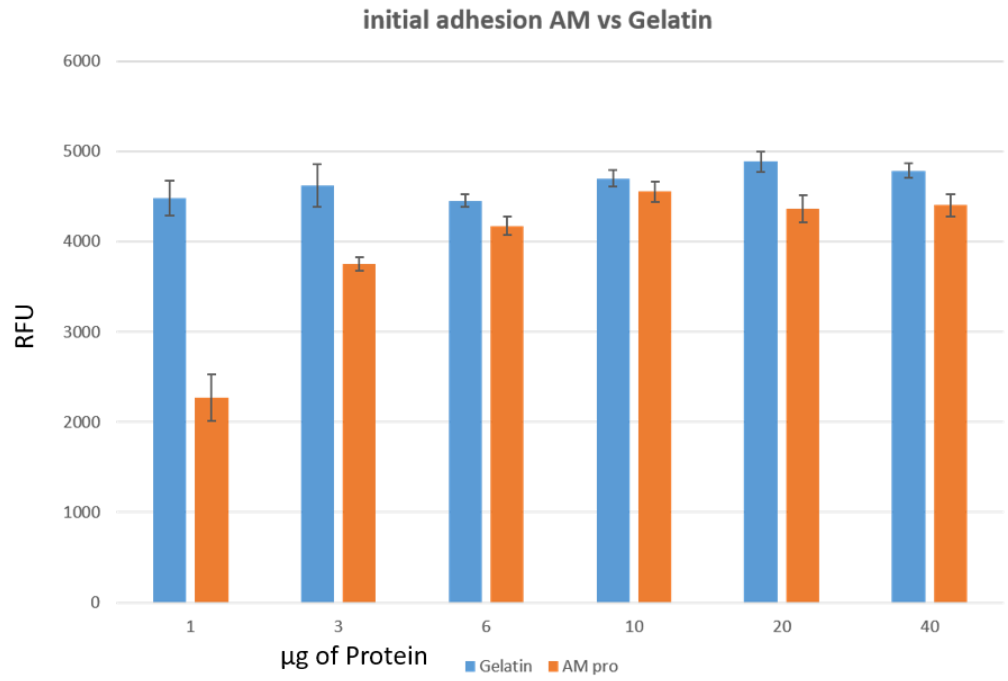

Figure 33: Initial adhesion of CSSCs: On variable concentrations of AMpro Vs Gelatin

5.7.3. Confirmation of Bio-functionalization based on Cell adhesion to patterned surfaces

AM conjugated NGMA was patterned to non-adherent dishes and were evaluated for cell adhesion using CSSCs on SCM media. A graphical representation of the pattern is given in Figure. 34A. The AMpro-NGMA patterned surface showed

the presence of proteins (AM) when stained with SimplyBlue^{TM} safe stain (Thermo scientific) which stains proteins (Figure. 34B -1). NGMA patterned dishes showed no staining due to the absence of AM proteins (Figure. 34B-2). Figure. 34C and 34D give a zoomed image of SimplyBlue^{TM} staining of NGMA and AMpro–NGMA patterns respectively. AMpro–NGMA shows blue colour due to the presence of AM proteins within the NGMA polymer indicating entangled protein or conjugation.

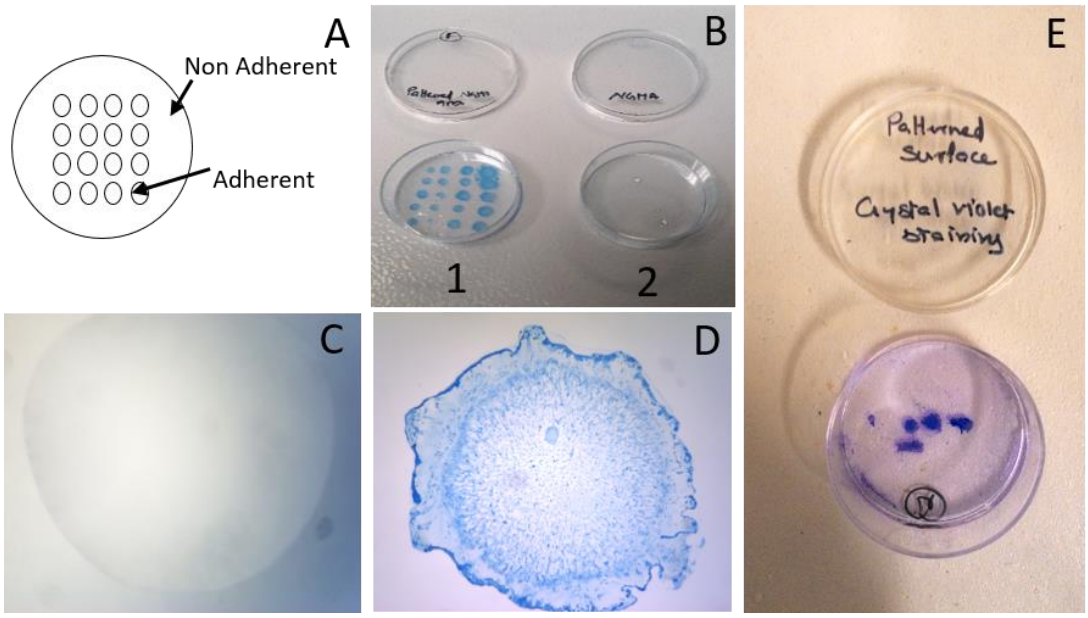

Figure 34: Proof for AM conjugation to NGMA: (A) Pictorial representation of patterns made for the study **(B)** (1) AMpro-NGMA patterned surface stained by SimplyBlue^{TM} safe stain **(2)** NGMA patterned surface stained by SimplyBlue^{TM} safe stain **(C)** NGMA patterned surface stained by SimplyBlue^{TM} safe stain (D) AMpro-NGMA patterned surface stained by SimplyBlue^{TM} safe stain (E) CSSCs adhered on to the patterned areas evident from crystal violet staining.

When CSSCs were cultured on these patterned surfaces cell growth was restricted to AMpro-NGMA patterned regions only confirming the presence of protein AM within the polymer allowing CSSCs to adhere. This was demonstrated using crystal violet staining, which stained the cell patterns on AMpro-NGMA (Figure. 34E) and CSSCs fail to adhere on NGMA alone, which is evident from phase contrast image of CSSCs on NGMA (Figure. 35A) and this served as a negative control for pattern adhesion studies.

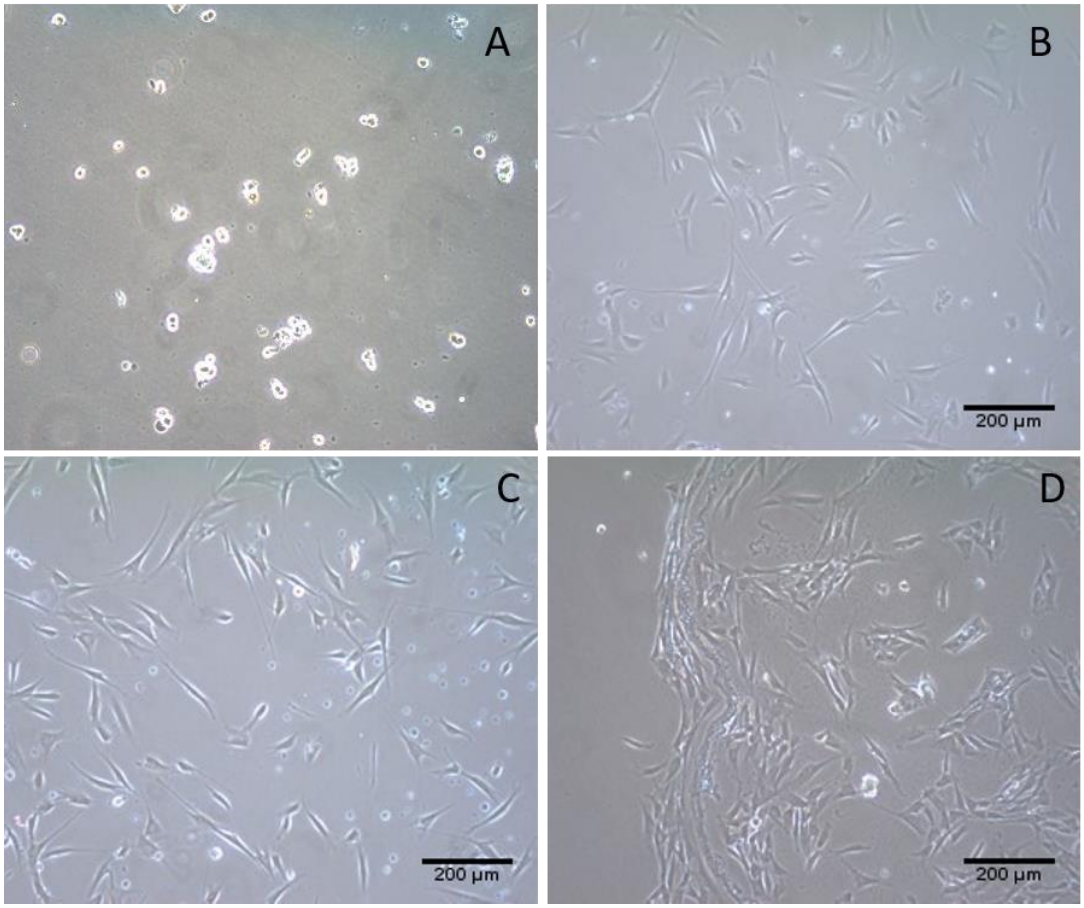

Figure 35: CSSC attachment to various surfaces: (A) CSSC on NGMA (B) CSSC on Gelatin coated surface (C) CSSCs on AM coated surface (D) CSSCs on AMpro-NGMA patterns (cells restricted to patterned surface).

Figure. 35B shows that CSSCs on gelatin-coated surface spread well and served as a positive control. Figure. 35C indicated CSSCs on AM coated surfaces also served as a positive control. These are comparable to the cell spreading of CSSCs on the AMpro-NGMA patterns (Figure. 35D), further confirming the bio-functionalization of NGMA with amniotic membrane proteins.

5.7.4. CSSC sheet transfer from AMpro-NGMA using PVDF membrane

40µg (Figure. 36A) and 20µg (Figure. 36C) AMpro-NGMA formed a confluent monolayer in a period of 3 to 4 days and these monolayers failed to get transferred or detach as a sheet (Figure 36B and 36D) while using PVDF membrane as a transfer tool.

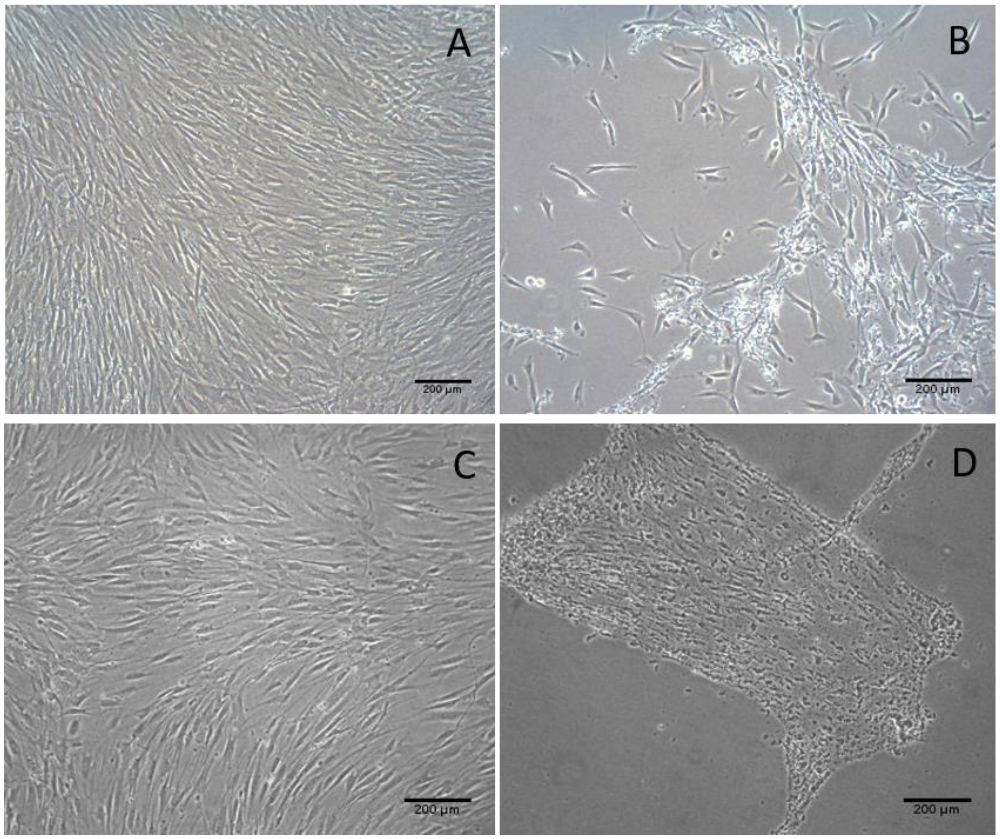

Figure 36: Cell sheet retrieval attempts (A) confluent monolayer on 40µg AMpro-NGMA (B) transferred cells on to AM coated culture dish from 40µg AMpro-NGMA (C) confluent monolayer on 20µg AMpro-NGMA (B) transferred cells on to AM coated culture dish from 20µg AMpro-NGMA.

CSSCs on 40µg conjugated AMpro-NGMA (Figure. 36A) and 20µg conjugated AMpro-NGMA (Figure. 36C) were not successfully detached or transferred to a new dish. Very few cells got transferred on from 40µg AMpro-NGMA dish (Figure. 36B) and a partially viable sheet got transferred from 20µg AMpro-NGMA dish (Figure. 36D), which was not viable after a period of 24h.

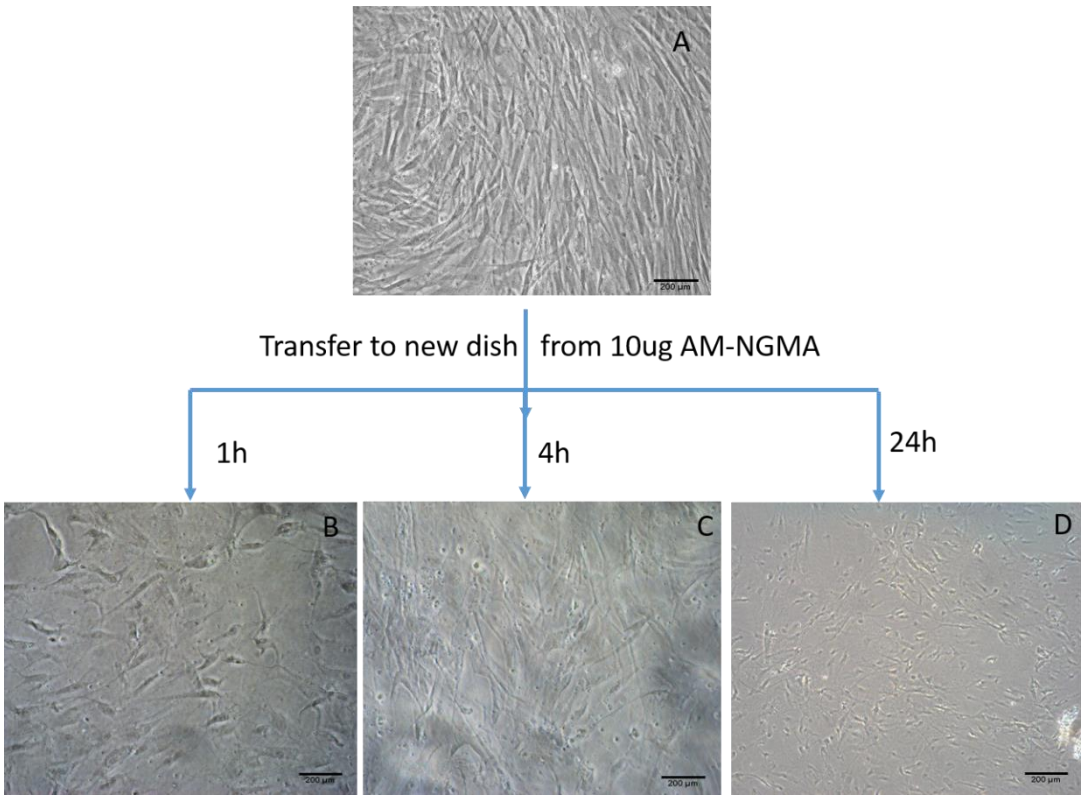

Figure 37: CSSC sheet from 10µg AMpro-NGMA: (A) confluent monolayer on 10µg AMpro-NGMA. (B-D) sheet transferred to AM coated culture dishes using PVDF membrane (B) after 1h (C) 4h (C) 24h.

CSSCs on 10µg AMpro-NGMA also formed a confluent monolayer (Figure. 37A) and were transferred to a new dish using PVDF membrane successfully. Transferred cell sheet attached on to the new AM coated dish (Figure. 37B&C), but by 72h the cells completely detached from the culture surface undergoing cell death. (Figure 37D).

5.7.5. CSSC sheet transfer using Gelatin gel.

PVDF membrane was not successful as a transfer tool, as the transferred cells were not found viable. The modified gelatin based transfer was then introduced to transfer cells from one dish to another in case of conjugated AMpro-NGMA and is demonstrated in section 3.10.5. Using gelatin transfer system CSSCs from 10µg AMpro–NGMA was successfully transferred to new substrates.

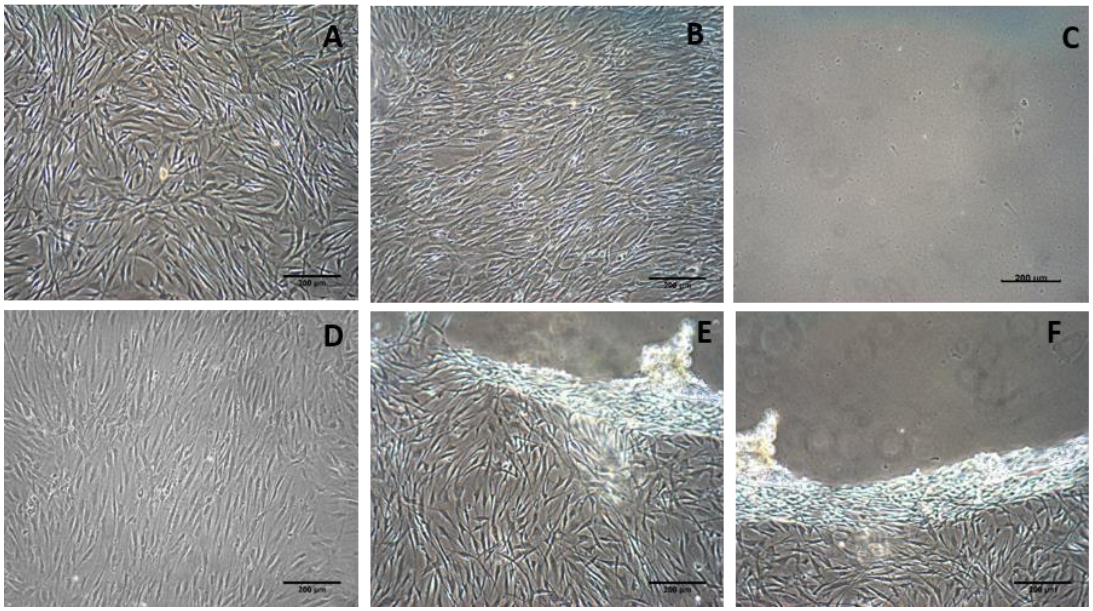

Figure 38: CSSC sheet transfer using gelatin-based protocol: (A) Confluent monolayer of CSSCs on 10µg AMpro–NGMA. (B) Transferred CSSC sheet on a

new cell culture dish (C) AMpro–NGMA dish after cell sheet transfer (D-F) Cell monolayer observed through gelatin gel at various phases of cell sheet detachment.

A complete transfer of a confluent monolayer of CSSCs (Figure. 38A) was achieved using the gelatin-based transfer. The transferred sheet formed a well-adhered monolayer of CSSC sheet on the new substrate (Figure. 38B). The AMpro-NGMA dish after transfer was devoid of cells confirming a complete successful transfer (Figure. 38C). An attempt was made to image cells through the gelatin gel while transferring the cell sheet which showed cells at various phases of detachment. Successful transfer was achieved and demonstrated using 10% gelatin gel.

5.7.6. Viability of Cells during transfer

AMpro-NGMA showed similar adhesion and proliferation potential when assayed using PrestoBlue in comparison with AM coated dishes. On the third day cells were transferred from 10ug AMpro–NGMA to another AM coated culture dish where they attached and proliferated. The transferred cell sheet showed almost similar intensity for presto blue staining indicating viability when compared with AMpro coated dishes (Figure. 39). This was evaluated using the relative fluorescence uptake of presto Blue stain by viable cells indicated by relative fluorescence units. This indicates the minimum loss of cells during transfer and survival post transfer. This also indicates that the conjugated system works with similar efficiency as protein alone (AMpro) in considering cellular properties like spreading, proliferation and viability.

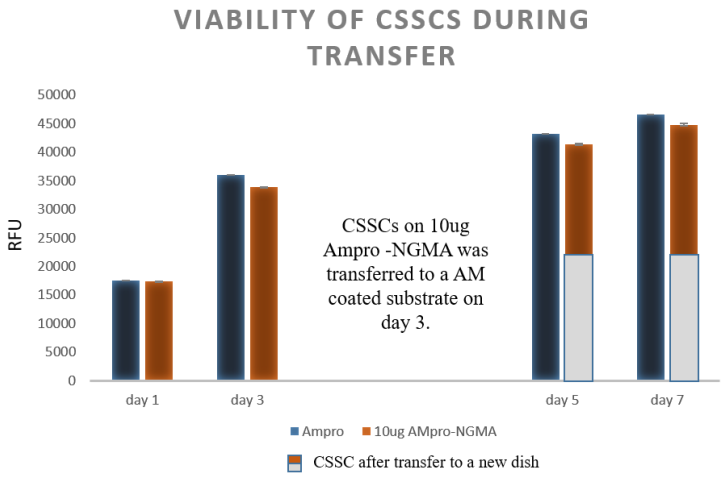

Figure 39: Viability of CSSCs on 10µg AMpro–NGMA *vs* AMpro during transfer.

CHAPTER - VI

6. *IN VIVO* STUDIES: ASC SHEETS IN RABBIT CORNEAL INJURY MODEL

Trans differentiated ASC sheets were evaluated for its efficacy in rabbit corneal injury models. Prior to cell sheet transfer in rabbit models, transfer potential of cell sheets was evaluated in an ex vivo excised rabbit eye to assess the feasibility of cell sheet transfer.

6.1. Demonstration of feasibility of cell sheet transfer to ex vivo excised rabbit eye

ASC cell sheets were transferred to an ex vivo excised rabbit eye on which an injury was created by n-heptanol (alkali-induced corneal surface damage).

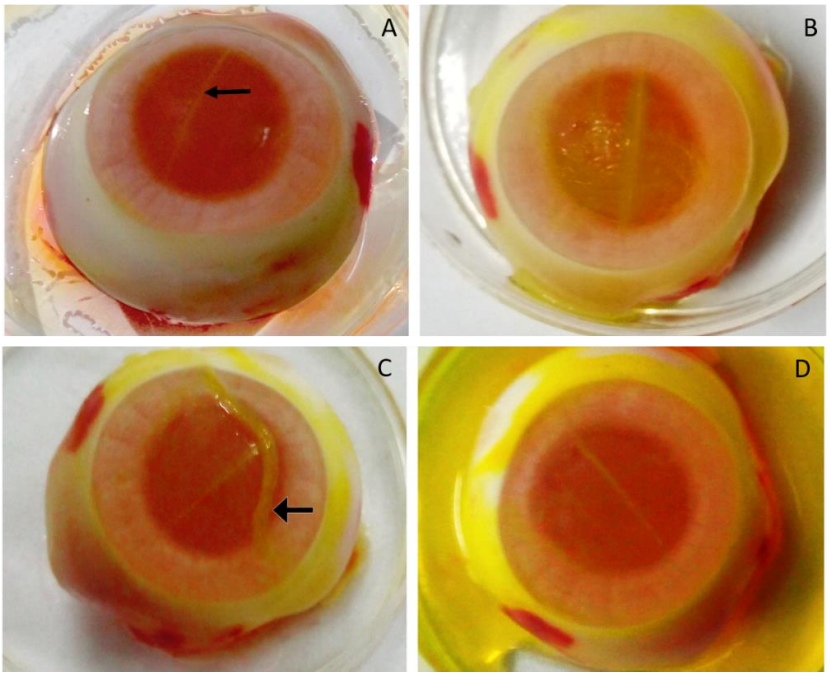

Figure 40: Cell sheet transfer in corneal surface damage model; ex vivo demonstration: (A) control eye: with a small bade cut (indicated by arrow mark to demonstrate fluorescein staining. (B) fluorescein staining after n-heptanol treatment along with mechanical debridement (C) cell sheet transfer on to the corneal injury model (D) After cell sheet transfer to the injury model.

Ex vivo demonstration was aimed at standardizing the transfer protocol for in vivo studies and evaluate sodium fluorescein dye staining. The control eye was imaged after a minor scalpel blade cut. This when stained with fluorescein, the cut region alone took up the fluorescein while the dye was washed out from rest of the uninjured region (Figure. 40A). Induced chemical burn along with mechanical debridement was also evaluated using sodium fluorescein dye intake (Figure. 40B). Cell sheet was detached from the NGMA dish with a change in temperature and was transferred on to the eye surface without support or transfer tool (Figure. 40C). The sheet even though folded a bit, could be spread over the eye surface using a blunt end angled forceps without damage to the sheet. The transferred sheet was found to be intact and transparent (Figure.40D) over the corneal surface thereby successfully demonstrating the feasibility of cell sheet transfer.

6.2. Corneal injury Model development

Cornea damage was induced by chemical and mechanical damage. The limbal region was scarified and the 360^{-}degree scarification of the limbus was carried out using a microsurgical knife (Figure. 41A). Limbal damage was then confirmed using sodium fluorescein staining. When visualized using a UV lamp the green fluorescence emitted formed a ring around the cornea in the limbal region depicting

damage to limbal ring (Figure. 41B). This was followed by chemically induced damage to corneal epithelium using n-heptanol. n- heptanol treatment of corneal epithelium was followed by mechanical debridement of the corneal surface ensuring complete removal of existing corneal epithelium (Figure. 41C). Sodium fluorescein test after chemical damage and mechanical debridement of corneal epithelium stained the entire corneal surface indicating complete removal of corneal epithelium (Figure. 41D).

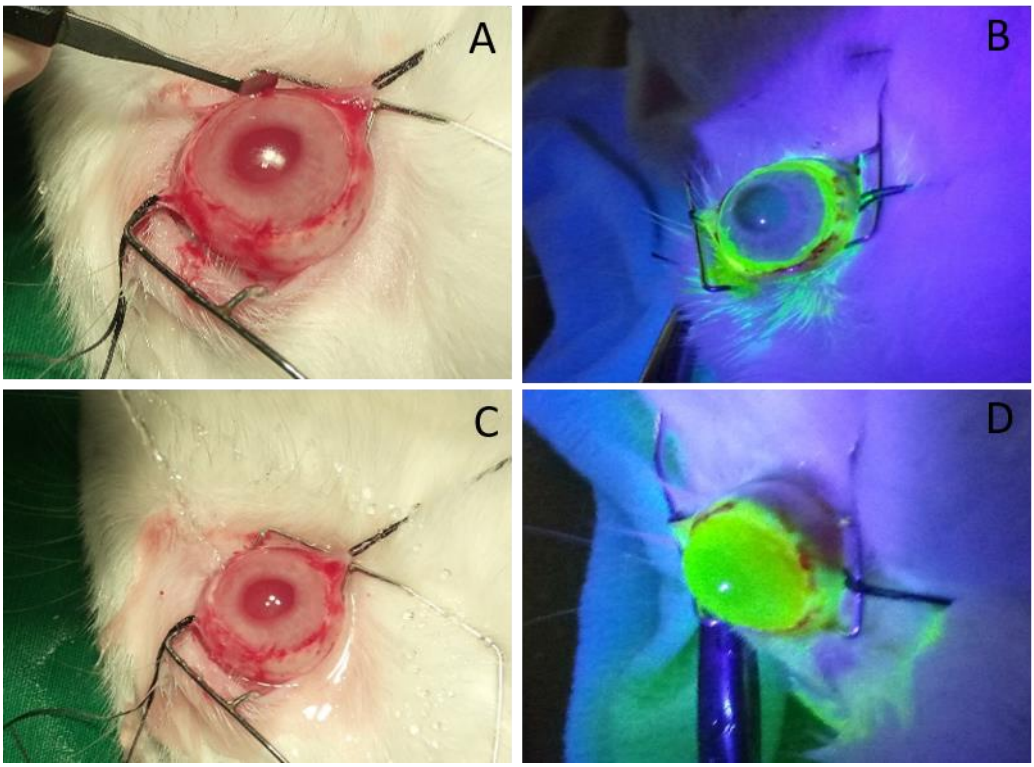

Figure 41: Corneal injury model creation (A) Procedure for limbal scarification (B) Sodium fluorescein staining after limbal scarification (C) Corneal surface debridement and n heptanol treatment (D) Sodium fluorescein staining after corneal epithelial debridement.

6.3. Confirmation of model development

Rabbit corneal injury models were observed for a period of one month before transplantation of cells sheets. Over a few days after model developments evident signs of neovascularization were observed in rabbit models (Figure. 42A). Over a period of 30 days, corneal opacity and surface irregularity were evident with enhanced vascularization over the corneal surface (Figure. 42B). One month after the damage, conjunctival overgrowth on the corneal surface was evident by the presence of goblet cells, a hallmark histological marker for corneal surface damage (Figure. 42C). This was followed by epithelial damage evaluation to corneal surface by sodium fluorescein staining which showed evident surface staining of fluorescein dye indicating ocular surface damage (Figure 42D).

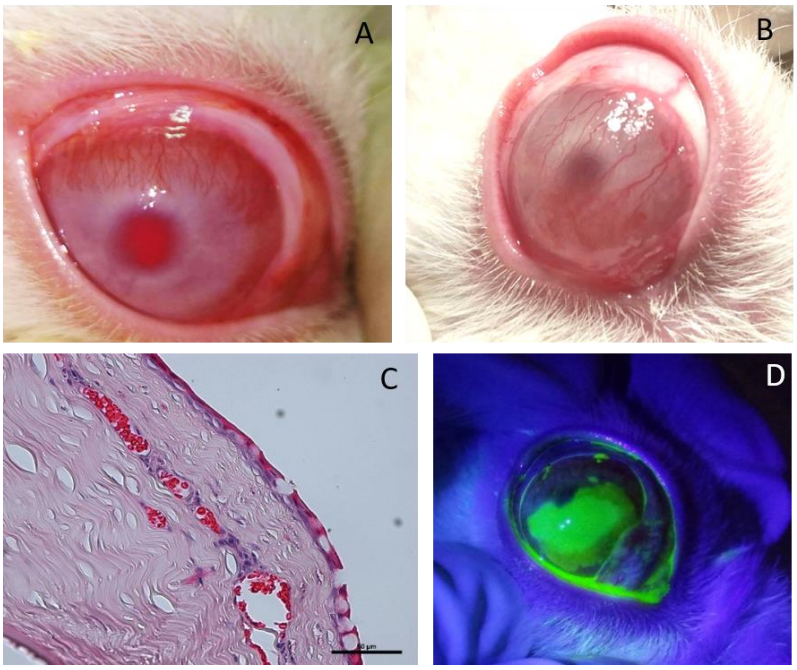

Figure 42: Confirmation of corneal injury development: (A) Neovascularization at day 10 (B) corneal surface at day 30 (C) presence of goblet cells in H & E staining (D) Epithelial damage stained by Sodium fluorescein

6.4. Scoring of Animal models for transplantation studies

Rabbit models after one month of model creation were evaluated for injury development based on a scoring pattern. The eye was divided in to four quadrants and was evaluated for effects like vascularization, opacity, surface irregularity and epithelial damage. Those models with damage extended to 3 quadrants of the eye in any three of the parameters were considered as proven models and were selected for transplantation of cell sheet. Table 6, gives the scoring pattern of rabbit models that qualified transplantation of cell sheet. Representative scoring of 5 animals out of 8 are given in the table.

Rabbit No / Scoring	360	402	414	527	465
Corneal Opacity	3	4	3	4	4
Surface irregularity	3	4	3	4	4
Epithelial damage	3	3	4	3	3
Neovascularization	3	3	3	3	2

Table 6: Scoring pattern for selection of rabbit models for transplantation

6.5. *In vivo* efficacy demonstration of trans differentiated cell sheets in rabbit models

After injury development, rabbit models were selected for the study based on their scoring pattern. In cell sheet transplanted models, corneal surface clarity had improved after 15 days of transplantation (Figure. 43B) in comparison to day 0 of transplantation after injury development (Figure. 43A). Vascularization

persisted till 15 to 20 days and then showed a reduction in vascularization by 30 days (Figure. 43C). After 30 days the cornea seemed to be clear with less vascularization and even corneal surface in 3 of the 4 models transplanted with cell sheet, representative images are shown in (Figure. 43C, Figure 44C, and Figure 45C). In one model persisting vascularization was seen with slightly opaque cornea (Figure 43D).

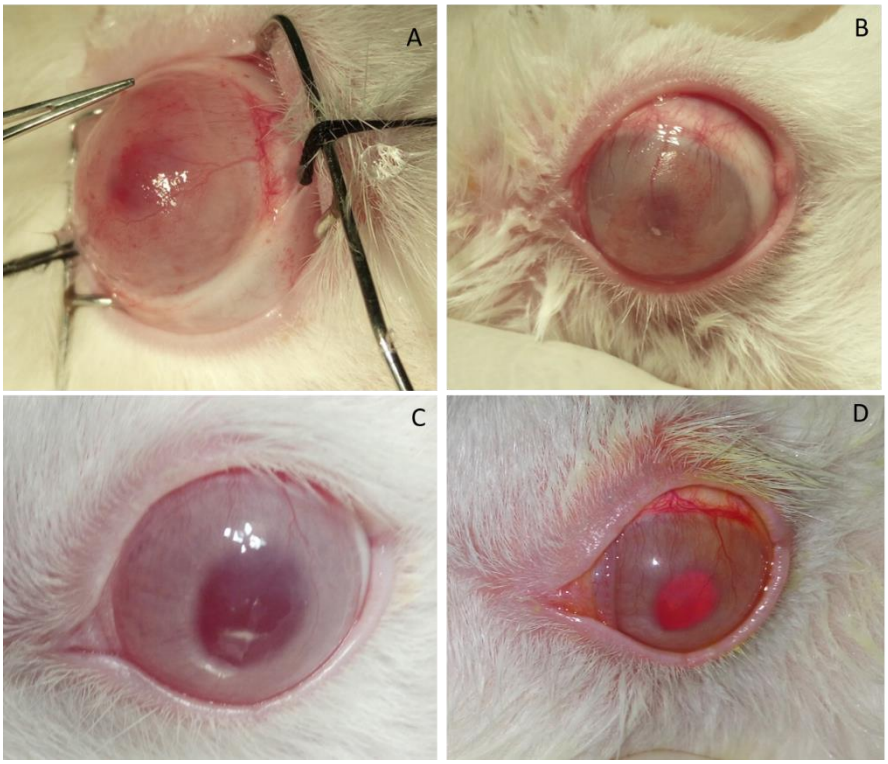

Figure 43: In vivo efficacy studies of transplanted cell sheet: (A) day 0 of transplantation (B) day 15 after transplantation (C) day 30 after transplantation (D) day 30 after transplantation with vascularization.

In all four models, conjunctival growth over cornea was completely absent and epithelial damage could not be demonstrated in sodium fluorescein uptake staining one month after cell sheet transplantation. A representative image of epithelial

damage on day 0 of transplantation is demonstrated with heavy sodium fluorescein uptake (Figure. 44B) along with the digital image (Figure. 44A). The same rabbit was imaged 30 days after cell sheet transplantation with minimum epithelial damage indicated by sodium fluorescein staining (Figure. 44D). The digital image of the corneal surface showed a clear cornea with minimum vascularization (Figure. 44C). This indicated that the transplanted cells had helped the animal to recover from the corneal injury damage to great extent considering facts like vascularization, conjunctival outgrowth, corneal surface clarity and epithelial damage.

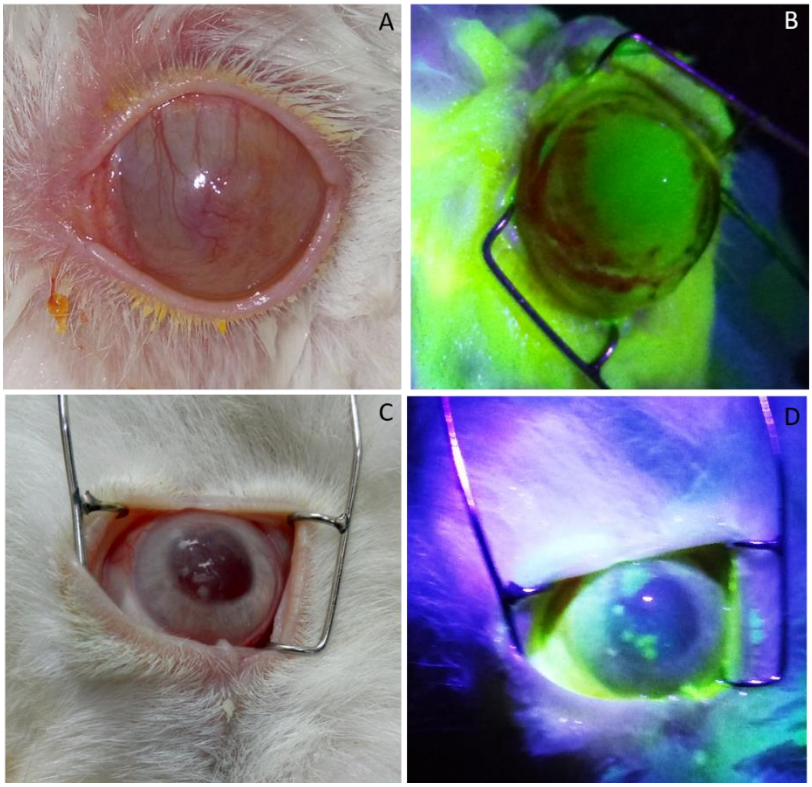

Figure 44: In vivo efficacy studies of transplanted cell sheet – (A) digital image before transplantation (B) sodium fluorescein staining before transplantation (C) digital image 30 days after transplantation of cell sheet (D) sodium fluorescein staining after transplantation

Cornea seems to be clear compared to the sham model even though quantitative data could not be extracted on the opacity of the cornea. Sham models showed persistent neovascularization and surface irregularity after the study period. Neovascularization was evident with visible scar formation in one model after the study period (Figure 45B). Figure 45A is a control eye with no surgical interventions. Comparing with the Sham model there is a drastic improvement in the cell sheet transplanted models with a reduction in vascularization and corneal surface clarity (Figure 45C).

6.6. Histological evaluation of corneal surface

The histological evaluation revealed conjunctivalisation of the peripheral cornea in the sham models which staining positive for goblet cells in H& E (Figure 45E –indicated by arrow mark) and PAS staining (Figure 45H – indicated by arrow mark). Presence of goblet cells is a hallmark indication of conjunctivalization which in turn indicates corneal surface damage. Whereas the cornea of cell sheet transplanted animals showed the presence of well-organized multilayered cells integrating to the stromal layer in H& E and (Figure 45F) and PAS staining (Figure 45I). Presence goblet cells did not show up on histological evaluation of cell sheet transplanted models indicating the absence of conjunctival layer or cells on the cornea indicating path a recovery in transplanted models. Control eye was also stained for H&E (Figure. 45D) and PAS staining (Figure 45G) to demonstrate the normal histology of corneal layers. In normal eye the corneal epithelium is continuous and extends from the limbus (Figure 45J). In the sham model, the epithelium was damaged or discontinuous, the limbus was devoid of any type of cells

and appears to be damaged (Figure 45K). In the cell sheet transplanted model, a surface epithelium like layer was reformed and was continuous across the corneal surface (Figure 45L). The limbus appeared to be damaged and devoid of cells.

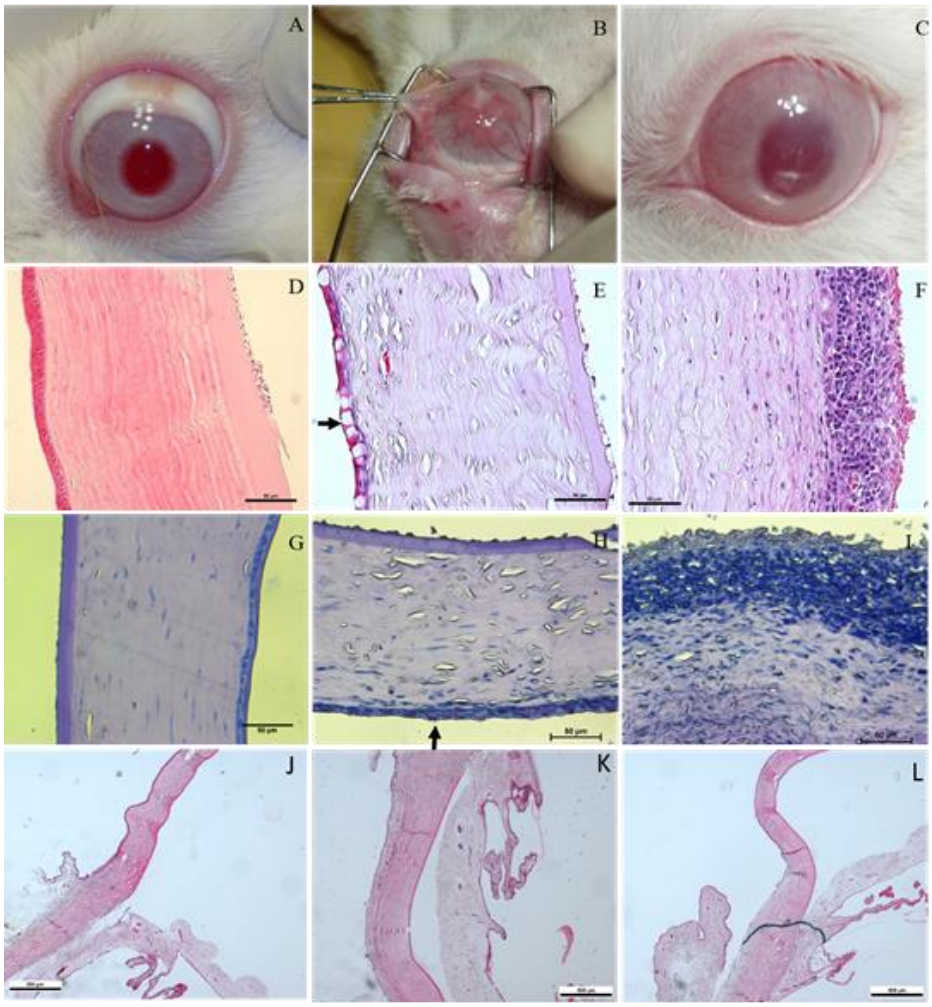

Figure 45: (A-C) Digital image - of transplantation study (A) control eye (B) Sham model (C). Histology staining (D-F) H& E staining of (D) control eye (E) sham model (F) Cell sheet transplanted model (G-I) PAS staining of (G) control eye (H) Sham model (I) Cell sheet transplanted model. (J-L) Histology of Corneo-limbal region: (j) Control eye (K) Sham model (L) Cell sheet transplanted model.

In cell sheet transplanted models a multilayered sheet over the stroma on the corneal surface was very evident. Cells towards the out layers of the cell sheet are showing signs of apoptosis. But rest of the cell layers have an intact nucleus and broaden cytoplasm. These cell sheet survived for a period of one month on the rabbit eyes and has helped these models to recover from corneal injury.

6.7. Corneal epithelial wound recovery based on Scoring

The rabbit models were evaluated for various parameters including corneal haze, fluorescein staining, epithelial damage and neo vascularization to determine the wound recovery in transplanted models. The rabbits used were compared for corneal surface features before and after transplantation and were graded and scored according to the pattern given in Table 7. Rabbits with score less than 3 was considered as successful corneal injury models and those transplanted rabbits with score above 7 was considered successful transplantation and those above 5 was considered partially successful. According to the soring pattern adopted from Sitalashmi et al., 2009, 3 of the transplanted models gave successful reconstruction visually and histologically while one model was a partial success with persisting neo vascularization and associated opacity.

Scoring pattern before and after transplantation	Rabbit NO 1		Rabbit NO 2		Rabbit NO 3		Rabbit NO 4	
	Before	After	Before	After	Before	After	Before	After
Corneal Haze	0	2	0	1	0	2	0	1
Fluorescein staining	0	1	0	1	0	1	0	1
Epithelial damage (data from sham models)	0	3	0	2	0	3	0	2
Neovascularization	1	3	1	3	2	3	1	2
Total score in 10	**1**	**9**	**1**	**7**	**2**	**9**	**1**	**6**

Corneal Haze :
No haze: clear cornea, iris details seen clearly - 2
Mild haze: visible but iris details visible - 1
Severe haze: iris details obscured – 0

Fluorescein Staining
Negative - 1
Positive - 0

Epithelial damage
Nearly normal epithelial layer – 3
Nearly normal epithelial layer with goblet cells - 2
Discontinuous epithelium at few places with goblet cells - 1
Damaged or completely discontinuous epithelium with goblet cells – 0

Neovascularization
No vascularization in any area - 4
B. Neovascularization in <3 clock hours - 3
C. Neovascularization in >3 to <6 clock hours - 2
D. Neovascularization in >6 to <9 clock hours - 1
E. Neovascularization in >9 clock hours - 0

Table 7: Scoring of Animal models before and after transplantation with grading parameters and grade scores. Scoring Scale: Rabbit eye was visually divided in to four quadrants for examination and evaluation. The numbers of quadrants affected were graded from 1 to 4 (1 representing minimum total area affected, 4 representing maximum total area affected).

CHAPTER - VII

7. DISCUSSION

Corneal problems are the fourth leading cause of blindness in the world and are increasing at an alarmingly high rate all around the globe. Corneal epithelium the outer most layer of the cornea is renewed continuously by stem cells residing within the cornea in the limbal region. Once the limbal region gets damaged, it affects the renewal of corneal epithelium and thereby vision (Daniels and Secker, 2009). The cornea gradually becomes opaque and if left untreated it can cause blindness. The extent of damage to limbus determines the treatment criteria and in case of complete limbal damage, a transplantation therapy is essential. One of the best options is an autologous limbal transplantation from the contralateral eye or an allogeneic transplantation of limbus from a healthy donor, preferably a close relative (Bakhtiari and Djalilian, 2010).

Both of these approaches have their own limitations. A surgical intervention on the contralateral eye is usually not preferred by patients as it can cause limbal stem cell deficiency in the normal eye, while allogeneic and cadaveric transplantation is followed mostly by immune rejection and immune suppression therapies. Long-term survival of the graft is also an alarming issue in case of corneal transplantation (Liang et al., 2009). Apart from all these in bilateral limbal stem cell deficiency conditions, a patient lacks his own stem cells making allogeneic

transplantation a necessity. Unfortunately, non-availability of donor tissue is another major limitation hindering allogeneic therapy.

The complications of graft rejection in allograft transplantation can be overruled by identifying alternate autologous stem cell sources to replace limbal stem cells (Eberwein and Reinhard, 2017). Identifying an alternate cell source from a non-ocular region will also address the issue of surgical intervention in contralateral eye and crisis due to donor shortage. These isolated stem cells should have the advantage of *in vitro* expansion to the required numbers before transplantation. But the *ex vivo* expanded cells, which had an exponential supply of nutrients and growth factors *in vitro* when transplanted to a damaged site, may fail to adapt with the wound-induced microenvironment prevailing at the site of damage (Wong and Gurtner, 2012) (Rameshwar, 2009). Finally, these transplanted donor cells fail to perform the intended function and gradually undergo apoptosis. An attempt was made to overcome this issue by providing autologous cells as a sheet instead of cells in suspension, as the survival rate of cells transplanted as suspensions seems limited. Cells as sheets instead of cell infusions were demonstrated to be more influential for tissue engineering strategies (Narita et al., 2013).

In the light of these observations, it was suggested and proved that autologous stem cells can be a functional alternative to corneal limbal stem cells as they exhibit corneal epithelial differentiation potential. These werethen developed in to bioengineered cell sheets by culturing them on a thermoresponsive culture substrate. This works has two parallel experimental strategies attempting towards corneal surface reconstruction.

1. Adipose-derived MSC (ASCs) were differentiated to corneal epithelial lineage to project them as a functional alternative to limbal stem cells and to streamline these cells to a therapeutic strategy for corneal surface reconstruction using cell sheet technology and prove its efficacy in vivo in rabbit models
2. To develop a bio-functionalized transplantable amniotic membrane alternative for use in enhanced corneal regenerative studies.

Along with identifying an ideal alternate cell source, the focus was also on to streamlining these cells with a technology that can mould this cell population to a transplantable form for clinical application. This study has utilized cell sheet technology using an in-house developed thermos responsive polymer. Cell sheet has gained importance in regenerative medicine by enabling transplanted cells to be engrafted for a long time (Matsuura et al., 2014), with greater donor cell presence (Narita et al., 2013). Identifying an alternative autologous cell source along with developing a stable platform for corneal epithelial transplantation procedures will make the surgical experience a lot easier from a surgeon's point of view.

Cell sheet engineering using thermoresponsive culture dishes allows harvesting of intact *in vitro* cell sheets and is reported to be used in various tissue engineering applications, including cornea (Tang et al., 2012b). NGMA is an in-house developed thermoresponsive polymer copolymer made from PNIPAAm and Glycidyl methacrylate and was reported previously by Joesph *et al.*, (Joseph et al., 2010). PNIPAAm is a well-demonstrated thermos responsive polymer for regenerative medicine applications (Yamato and Okano, 2004).

The FTIR spectrum of the NGMA showed the specific peaks of an amide group (-NHCO) in PNIPAAm and the epoxy rings in GMA demonstrating the formation of the copolymer. The peaks were displayed in the FTIR spectrum was similar to those reported by Joesph *et al.,* (Joseph et al., 2010). This copolymer of PNIPAAm was shown to have thermo responsive property and displayed a phase transition at 32ºC due to the hydration/ dehydration property of the polymer as reported in Gandhi et al., (Gandhi et al., 2015). Joseph et al. reported that. "Above the LCST, the isopropyl groups in PNIPAAm predominates and exhibits hydrophobic nature, while below LCST the hydrophilic amide groups form hydrogen bonds with water turning NGMA hydrophilic in nature"(Joseph et al., 2010). At a temperature above 32ºC the polymer precipitates and forms a white turbid colour in contrast to its colourless nature at a temperature below its LCST. The contact angle measurements are critical for cell culture substrates as the surface wettability can influence cell adhesion on the substrate (Kim et al., 2007). The surface property evidenced from contact angle measurement suggests that NGMA coated surfaces are suitable for cell adhesion and proliferation as any surface with contact angle around 70ºC is reported to be suitable for cell adhesion and proliferation (da Silva et al., 2007). Water contact angle values at different points of a single dish also showed very close values depicting an evenly coated surface. Moreover the epoxy ring opening mechanism of GMA will help to incorporate biomolecules to the existing NGMA copolymer for cell-specific biofunctionalization.

Suitability of using NGMA for cell culture studies revealed interesting observations. The cytotoxicity evaluation using L929 cells, conducted based on ISO 10993-5 standards confirmed the non-cytotoxicity of NGMA coated dishes. The

polymer extract was identified as nontoxic and does not contain any leachates that are harmful to cells or its metabolic activity. Varghese *et al.,* has earlier reported the same method to establish non-cytotoxic behaviour of a thermos responsive polymer NIPAAM- MMA using L929 cells and reported the non-cytotoxic behaviour of NIPAAm based copolymers (Varghese et al., 2010). The efficiency of NGMA as a thermos responsive surface was evaluated using L929 cells. When a monolayer of L929 cells was subjected to change in temperatures cells detached from the polymer surface without using proteolytic enzymes or mechanical force. This observation is consistent with results of cell sheet engineering using PNIPAAm (Tang et al., 2012).

Detaching the cell sheet from NGMA polymer depends on the thickness of the polymer coating on the cell culture dish. The thickness of the polymer coating will affect cell adhesion and detachment from the polymer (Patel and Zhang, 2013). Another work on the thickness of PNIPPAm films has suggested using spin coating technique to reduce the thickness of the coating film so as to improve cell adhesion and detachment (Dzhoyashvili et al., 2016). This work utilized hand coating NGMA polymer to set a thin coating on the cell culture dishes. The polymer solution was spread over the culture dish and time of contact was restricted to less than 10 seconds later dried. The restricted minimal contact time of the polymer solution with cell culture dish was expected to control the thickness of the coating and thereby helped to achieve cell adhesion and detachment. Increased thickness will affect the wettability characteristics of the surface which in turn can affect the thermos responsive behaviour of the polymer (Elloumi-Hannachi et al., 2010).

Incorporating GMA group to PNIPAAm backbone to modify the thermoresponsive polymer was a novel approach to enhance the bio-functionality of the polymer. Similar modifications of PNIPAAm was earlier attempted using methyl methacrylate copolymerization (Varghese et al., 2010) to fine tune LSCT. The GMA group within the copolymer has an unreacted, epoxy group within, which allows incorporating any functional moiety enabling guided modification of polymer matrix by an epoxy ring opening mechanism as reported by Joseph et al., (Nithya Joseph et al., 2010). Epoxy ring opening in an acidic environment will allow a reactive nucleophile to bind to the opened ring stabilizing the reaction and product. The presence of "-NH_2" group makes any protein reactive to the opened ring of the GMA group. The theory behind conjugation is the epoxy ring opening mechanism of GMA at sight acidic pH. This opened ring is highly reactive and can bind with any nucleophiles available in its proximity. Various other methods have been attempted by different groups to bio functionalize PNIPAAm. Copolymerization of PNIPAAm with acrylic acid was one such attempt to include a reactive carboxyl group in the main chain (Stile and Healy, 2002). This modification had a drawback as it often affected the phase transition behaviour of PNIPAAm (Chen and Hoffman, 1995). To overcome this problem 2-carboxyisopropylacrilamide (CIPAAm) was synthesized which contained a functional carboxylate group as a side chain structure to PNIPAAm (Aoyagi et al., 2000), but was found to have accelerated cell detachment as compared to PNIPAAm (Ebara et al., 2003). Epoxide ring opening mechanism of GMA in this work helped to develop a bio-functionalized amniotic membrane alternative thermos responsive platform to generate transplantable cell sheets for use in corneal regenerative therapies, as an amniotic membrane alternative.

Bio functionalizing NGMA with amniotic membrane-derived proteins will help NGMA coated surface to mimic the substrate properties of the amniotic membrane. This will in turn help to develop an innovative platform for expansion and carrier free transplantation of human corneal stromal derived stem cells. The bio-functionalization of the NGMA is expected to improve the stem cell growth and corneal wound healing potential of CSSCs.

Crude amniotic membrane protein extract was used to simulate the amniotic membrane substrate properties. The Amniotic membrane processing is a standard procedure and was adapted from other published literature (Hopkinson et al., 2005), (Hopkinson et al., 2008). Denuding of the amniotic membrane to remove the epithelial layer was done using thermolysin treatment. Various enzymes have been used for denuding amniotic membrane including ethylenediaminetetraacetic acid (EDTA) (Koizumi et al., 2000), sodium dodecyl sulphate (SDS) containing EDTA (Taghiabadi et al., 2017),alkali treatment (Saghizadeh et al., 2013), type IV collagenase (Zhang et al., 2016). Hopkinson *et al.* compared the effect of EDTA, dispase and thermolysin on denuding amniotic membrane and concluded that thermolysin provided effective denuding in minimum time (Hopkinson et al., 2008) and this standardized protocol using thermolysin was adopted for the current study.

Amniotic membrane proteins were extracted with Urea – thiourea buffer. Conjugation of AMpro in urea-thiourea buffer to NGMA was ineffective because urea is a better nucleophile compared to AM proteins and is present in the buffer in excess. Urea being a strong nucleophile than AM proteins, so in a competitive binding scenario urea will outrun AM proteins and will bind to NGMA. So the

extracted proteins were buffer exchanged to PBS which is a very simple buffer and the pH was set to a slightly acidic range pH 5.

Initial evidence for conjugation was derived from FT-IR analysis of the AMpro conjugated NGMA (AMpro-NGMA). The conjugated polymer displayed a spectral variation in the peak around the GMA region in comparison with the spectrum of NGMA. The FT–IR spectra before and after conjugation showed difference in the region of the epoxide peaks demonstrating epoxide ring opening and there by initiating the process of conjugation. Conjugation was achieved by incubating AMpro with 4% NGMA in isopropanol in an acidic environment. There was an initial effervescence with turbidity formation which subsided and turned in to a colourless solution with minimal shaking.

A direct evidence for conjugation of AMpro to NGMA came from SDS PAGE electrophoresis. As mentioned earlier, the conjugation happens only on GMA copolymer of NGMA and not on its main chain polymer PNIPAAm. When AMpro-NGMA, AM control, NGMA and PNIPAAm was run on different lanes on SDS PAGE. It was shown that only on the AMpro–NGMA lane, the proteins (AM) didn't run down the lane as it was conjugated with the polymer. On PNIPAAm since the polymer was not able to conjugate the proteins, they run down the lane similar to as in case of the control (AM proteins alone). This proved that the protein AM got conjugated to GMA group of NGMA and was not just entangled or trapped within the polymer chains. Formation of the protein–polymer conjugate was thus confirmed by the absence of discrete free protein bands in the SDS–PAGE gels of AMpro-NGMA when compared with native AM as a control. This protocol was earlier adopted by Haung *et al.,* for identifying the formation of protein – polymer nano

conjugates (Huang et al., 2013). This was reconfirmed by western blot analysis of AM protein Decorin, Mimican and Lumican, the abundant proteins present in the amniotic membrane. The results showed that Decorin and Mimican got conjugated to the NGMA as the band formed in AMpro-NGMA was faint in comparison with the control (AM proteins), suggesting that the protein was held by the polymer and was not free to run down the gel. Lumican showed similar thick bands in both control and conjugated system. This also suggested that low molecular weight proteins preferred to conjugate in comparison to large molecular weight proteins. Lumican is a large molecular weight protein did not effectively get conjugated to NGMA. Similar studies with modified thermo responsive polymers attempted to immobilize Arg-Gly-Asp-Ser (RGDS) peptides to thermo responsive polymer grafted TCPS dishes (Ebara et al., 2004). Modification of the same system with co-immobilization of RGDS and Pro-His-Ser-Arg-Asn (PHSRN) helped to control cell adhesion and detachment more precisely than in RGDS immobilized polymer (Ebara et al., 2008) The current work attempted to conjugate AM protein covalently to the copolymer.

Apart from setting up a thermos responsive platform, identifying a suitable cell source as an alternate to limbal stem cells was another main aim of this work. Many other cell sources including various non-ocular cell sources have been investigated as a part of the constant search for novel cell types that could potentially revert corneal injuries. Cell types currently attempted for corneal surface reconstruction include bone marrow-derived mesenchymal stem cells, epidermal stem cells, hair follicle-derived stem cells, immature dental pulp stem, and umbilical cord stem cells (Sehic et al., 2015). Oral mucosal epithelial cells are the best non limbal autologous cell source practised (Utheim et al., 2016), but is associated with

in vivo keratinization and peripheral corneal neo vascularization (Haagdorens et al., 2016).

Current work has utilized adipose derived mesenchymal stem cells and corneal stromal stem cells to attempt corneal surface reconstruction. MSC are a proven autologous cell source for use in tissue engineering applications isolated from various anatomical locations including bone marrow and adipose tissue (Wei et al., 2013). Adipose MSC's (ASCs) hold the advantage of ease of isolation and abundance of stem cell population within the tissue. ASCs isolated from the subcutaneous fat pad of rabbits were used in this study. The cells were isolated by type I collagenase digestion of the tissue, a well-reported protocol in the literature (Venugopal et al., 2012). The cells isolated were screened for mesenchymal stem cell markers and was found positive for CD 105, CD 90, CD44. The cells were negative for CD34 expression and were plastic adherent forming spindle-shaped morphology exhibiting multi lineage differentiation potential upon providing appropriate stimuli. As per The Mesenchymal and Tissue Stem Cell Committee of the International Society for Cellular Therapy (ISCT) criteria, if the cell express and exhibit the above markers and properties, it can fall in to the group of mesenchymal stem cells (Dominici et al., 2006). Cells isolated from the rabbit subcutaneous fat pad meets the minimal requirements to be called as MSCs. International Fat Applied Technology Society has reached a consensus to adopt the term "adipose-derived stem cells" (ASCs) to stem cells isolated from adipose tissue (Gimble et al., 2007) and so in this work the stem cells are abbreviated as ASCs.

Use of corneal stromal stem cells (CSSCs) in corneal surface regeneration is less reported compared to limbal stem cells, but increasing evidence

suggest that CSSCs would be an ideal alternate to limbal stem cells in designing tissue-engineering strategies (Du et al., 2009), (Gonzalez-Andrades et al., 2011), (Hatou et al., 2013). Notably, Polisetty *et al.,* and *Choong et al.,* have reported the presence of cells with MSC characteristics isolated from the limbal stromal regions (Polisetty et al., 2008) (Choong et al., 2007).These cells are derived from the neural crust, a tissue of mesenchymal origin (Kulkarni et al., 2010). CSSCs even though express most of the mesenchymal stem cell markers including CD13, CD29, CD44, CD56, CD73, CD90, and CD105 (Branch et al., 2012) (Kureshi et al., 2015) (Polisetty et al., 2008) they are equally positive for hematopoietic markers like CD11b, CD34, and CD133 (Funderburgh et al., 2005) (Sidney et al., 2015). Corneal stromal cells were isolated from donor limbus which was not qualified for transplantation studies and were characterized positive for ABCG2, CD73, CD90, CD105 and CD 34 as reported (Sidney et al., 2015). These cells from corneal limbal stroma is said to be stem like and possess a degree of multi linage differentiation potential (Branch et al., 2012). The presence of CD34+ positive population of cells in CSSCs make these cells of particular interest. Increasing evidence suggests that CD34 marker is associated with mesenchymal/epithelial progenitor in other tissues (Dan et al., 2006), (Li et al., 2011). Later Hashmani *et al.,* confirmed these cells as mesenchymal derived limbal stromal progenitors validating the presence of MSCs according to the International Society for Cellular Therapy's (ISCT's) defined criteria (Hashmani et al., 2013). These isolated cells were cultured in a patented medium with 20% FBS, basic fibroblast growth factor and leukaemia inhibitory factor called stem cell medium as reported by Sidney et al., 2015. This particular medium was shown to maintain the stemness of CSSCs for a longer period of time in culture

(Sidney et al., 2015). Also when cultured in SCM media CSSCs failed to attach and grow in culture dishes but will grow only on protein coated surfaces. So CSSCs were grown on 2% gelatin-coated surfaces in SCM media for better performance and maintenance of MSC properties and was reported in the literature to support the growth of CSSCs (Hashmani et al., 2013; Sidney et al., 2015).

Since the thermoresponsive platform and the cell types under study have been selected, now the idea is to evaluate the effectiveness of using these cells types on NGMA for further studies. ASCs grown on NGMA coated dishes did not show any signs of growth arrest or necrosis, maintained their viability, cytoskeletal morphology and stemness. Expression of stem cell-specific markers by ASCs cultured on NGMA coated surfaces confirmed the retention of stemness by ASCs on NGMA surface.

Even though the exact role of ASC's in repair mechanism is still debated, it is reported that undifferentiated ASCs can also play an equally important role in modifying the damaged microenvironment (Nuschke, 2014) suggesting that the beneficial effects may be from the paracrine signaling potential of MSCs and their role in wound healing (Caplan and Dennis, 2006). The differentiation potential of MSCs largely relies on their plasticity and microenvironmental cues surrounding them (Sun et al., 2012). .Differentiation of MSCs to extra-mesenchymal lineages with the ability to repair or replace injured tissues especially in locations where resident stem cells are unavailable will be a major advantage (Hocking and Gibran, 2010) (Li and Zhao, 2014). In this work, ASCs were differentiated into corneal epithelial lineage using limbal condition media and also a commercially defined media. Previous reports states that limbal conditioned medium can induce cellular

differentiation and the conditioned target cells will develop certain specific characters induced by the cell mediators present in the conditioned media (Jiang et al., 2010). They also demonstrated that rat MSCs expressed cytokeratin 12, a corneal epithelium specific marker when induced with corneal stromal condition medium (Jiang et al., 2010). Gu et al, had shown that rabbit MSCs can express CK3 and play a crucial role in corneal wound healing (Gu et al., 2009). In this study, after evaluating the expression pattern of cytokeratin 3/12 in molecular and protein level in both the differentiation mediums used, limbal condition medium demonstrated more potential to transdifferentiate ASCs to corneal epithelial lineage. So limbal condition medium was used for the rest of the experiments. Flow cytometry analysis of differentiated cell population showed a significant increase in the CK 3/12 positive cell population when compared to the uninduced control. Around 30% of ASCs showed terminal differentiation towards cornea epithelial lineage, while 61.6% of cells were stained positive for connexin 43 (Cx 43) which is a strong indication towards corneal epithelial differentiation. Cx 43 is expressed in the corneal epithelial layer and in the supra basal cells of limbus (Chen et al., 2006) (Zhang et al., 2016). This indicates that majority of the cells were in the path of corneal epithelial differentiation. Differentiated mesenchymal stem cell population evaluated by FACS showed around 10% positivity for CD 90, which was above 90% before differentiation. This also indicated that the differentiation media had a profound effect on ASCs resulting in epithelial differentiation. After evaluating differentiation using immuno cytochemistry, differentiation was analyzed at the molecular level. The Gene expression studies conducted in three different biological replicates showed up-regulation of CK3 and CK12 which are corneal epithelial markers. As

reported by Gu et al., CK 3 showed a higher expression as compared to CK 12 (Gu et al., 2009). Mathews et al., reported up regulation of CK 3 but not CK 12 when differentiated using stromal condition medium (Mathews et al., 2017). ABCG2 is considered as a general stem cell marker usually expressed in most stem cells (Ebrahimi et al., 2009) and is also found in limbal epithelial stem cells (de Paiva et al., 2005) . At day 7 there was not much change as compared to the control population but there was a significant increase at day 14. Delta Np63 is considered an epithelial stem cell marker that identifies limbal stem cells in cornea and doesn't show a significant change from 7 days to 14 days (Pellegrini et al., 2001). Both ABCG2 and p63 markers have a maximum expression in the limbal region when compared to the central corneal region and their presence helped to characterize a cell population as putative epithelial stem cells (Morita et al., 2015). Activation of Paired box homeotic gene 6 (Pax 6) is required for proliferation, differentiation and normal development of corneal epithelium (Li et al., 2008). PAX 6 was also found to be up-regulated significantly from day 7 to day 14 in the differentiated ASC population, demonstration PAX6 activation.

The differentiated cells on NGMA were then retrieved as a cell sheet by virtue of the thermoresponsive property of the polymer NGMA. Mesenchymal stem cells are known for their cell-matrix interactions, but reports suggest that when cells are cultured to confluence or to over confluence i.e., when the cell density per unit area increases, the cells show more tendency to form cell-cell contacts (Gebbink et al., 1995), (Zhang et al., 2002) overcoming cell-matrix interactions. Below phase transition temperature, NGMA changes its properties, decreasing cell-substrate interactions. Cells now form sheet-like structures, as the cell-cell interaction

predominates overriding cell-matrix (NGMA) interactions and is well demonstrated by time-lapse imaging of cell sheet detachment. The presence of Gap junction protein connexin 43 further demonstrated the formation of the effective cell-cell contact. The cell sheet completely detaches out from the polymer surface forming an independent unit. Retrieval and transfer of cell sheet *in vitro* were achieved by using PVDF membranes and was well demonstrated. Soft gels like gelatin have also been used as a carrier to transfer the detached cell sheets to a new surface (Kikuchi et al., 2014). The sheets when transferred to a fresh culture dish attached to the surface and were viable maintaining the morphology. This can be considered as a quick adaptation of cell sheet to a new environment and directs the potential to integrate, stabilize and survive upon transplantation. Cell sheets can also secrete, harbour and deliver growth factors, cytokines promoting tissue repair and help the sheets to adhere on to the transplanted region (Matsuura et al., 2014), (Tang et al., 2012).

After detachment, transfer of intact cell sheet to another surface is an art of perfection, gained by hands-on experience over time. Normally the cell sheets were transferred using some sort of supporting tools like poly (ethylene terephthalate) sheet (Joseph et al., 2010), Gelatin gel (Kikuchi et al., 2014). This work has utilized PVDF (Polyvinylidene di fluoride) membrane as a tool for *in vitro* cell sheet transfer. Transferred sheets on the new surface maintained their viability and integrity as a cell sheet, withstanding the manipulation stress during transfer. In short, trans differentiated ASC cell sheets were developed from NGMA polymer coated platforms and were evaluated *in vivo* for its efficacy in corneal surface reconstruction.

In case of CSSCs, they failed to grow on NGMA dishes while attachment and spreading were found only on AMpro-NGMA or on other protein coated surfaces like gelatin. This opened up other avenues to provide supporting proofs for conjugation. Further proofs towards biofunctionalization were unveiled while validating the AMpro-NGMA polymer for cell culture studies using human corneal stromal stem cells. Non-adherent dishes when patterned with AMpro–NGMA took up SimpleBlue^{TM} safe stain indicating the presence of protein in comparison with stained NGMA patterns. This experiment does not give an indication whether the protein is entangled or conjugated. This was further validated using CSSCs, as they will adhere only to protein coated surfaces. This property of CSSCs were also exploited to confirm bio functionalization. CSSCs when cultured on the non-adherent dish restricted themselves to AMpro–NGMA patterns evidenced by crystal violet staining of cells.

Once conjugation was confirmed the next hurdle was to optimise the protein concentration to be used for conjugation that enables effective cell growth and cell sheet retrieval. Initial attempt was to determine the minimum protein concentration required for cell adhesion, which will enable effective sheet retrieval with maximum cell viability. Between 10ug - 40 ug protein concentrations, the adhesion of CSSCs on both gelatin coated surfaces and AMpro conjugated surfaces were same and so all these concentration ranges were attempted for cell sheet retrieval. Cell sheet detachment from AMpro–NGMA was difficult in comparison to NGMA alone due to the presence of amniotic membrane proteins. The cells were attached to the protein that was conjugated to the polymer. So to detach the cells as a sheet from AMpro-NGMA was a difficult task. With PVDF membrane as a transfer

tool, the detachment and transfer failed at all different concentrations. The transfer from one dish to another was incomplete and most of the times the cells were not viable after transfer owing to the strain on cells during transfer. In 10ug protein conjugated NGMA, the cell sheet was transferred using PVDF, but underwent apoptosis in 72h time. However 10ug concentration was the optimal minimum concentration identified by considering the adhesion of CSSCs on AMpro in comparison with gelatin,

Gelatin transfer system adopted was effective in transferring cell sheet compared to PVDF membrane based transfer. PVDF transfer is based on simple adherence, but in case of conjugated system a small amount of force is expected to help lifting the cell sheet from protein conjugated surface. The gelatin solution at 37°C was poured on to the cell sheet and was transferred to a temperature near to 10°C. Here the gelatin forms a gel with the cell sheet within the gelatin gel. It is assumed that the gelatin solution flows underneath the detaching cell cluster and after solidifying it hooks the cell sheet from the base of the polymer rather than the pealing mechanism happening in PVDF based transfer. Gelatin is a cell adhesive matrix protein and cell sheets harvested from temperature-responsive surfaces retain many adhesive proteins. Here the cell sheet detachment is also based on the protein adhesiveness between both the surfaces (Kikuchi et al., 2014). The transferred cell sheet was viable, adhered and survived on to the new transferred substrate without much loss of cells during transfer protocol.

The Amniotic protein components present in the polymer is anticipated to contribute in enhancing the wound healing potential of corneal stromal stem cells (Omran et al., 2016). AM conjugation and CSSC cell sheet retrieval was successfully

attempted which will open up innumerable avenues towards guided cell sheet engineering by conjugating required proteins and other components helping in guided selection and differentiation of cells.

Using NGMA as a basic platform, two cell sheet based technologies were demonstrated towards addressing corneal surface disorders. Trans differentiated ASC cell sheet from rabbit models and CSSC sheets developed from modified NGMA. The work on ASC cell sheets were taken to the next step with animal model studies, to evaluate the efficacy of trans differentiated ASC sheets in rabbit injury models.

To standardize the surgical procedure and to determine if the cell sheet will hold the mechanical manipulation happening during the time of transfer cell sheet transfer was attempted on an *ex vivo* excised rabbit eye model. *In vivo* evaluation of these cell sheets were done using rabbit models of induced corneal injury. Test eyes showed signs of total LSCD in one month time period after debridement of limbus and alkali damage. The corneal surface over time became irregular with increased corneal opacity. The fluorescein staining showed evident epithelial damage, in total indicating LSCD condition. Similar observations on LSCD development was reported by Sitalashmi et al., (Sitalakshmi et al., 2009). Later on histological analysis, goblet cells were seen in corneal injury models, a hallmark of LSCD development and is reported in conjunctival overgrowth on cornea (Yang et al., 2008) a major symptom of LSCD. Corneal injury models were selected and evaluated based on corneal opacity, surface irregularity, neo vascularization and epithelial damage, and is a standard procedure followed to evaluate corneal injury (Sitalakshmi et al., 2009). The selected models after

transplantation of cell sheet was monitored for a period of one month before explantation and histological evaluation. The clinical outcome was evaluated by comparing preoperative and postoperative photographs. The success of cell sheet transplantation was evaluated based on, if the cornea has regained its smoothness, avascular nature and clarity. The procedure was graded as partial success if the cornea showed partial vascularization with a smooth and avascular surface in two or more quadrants. This methods were adopted from a published report from Sitalakshmi et al., (Sitalakshmi et al., 2009). Jiang et al., has demonstrated the grades of cornea damage based on vascularization, opacity and sodium fluorescein staining (Jiang et al., 2010).

The transplanted cell sheet was found to adapt to the corneal injury area and adhered to the stromal surface. The cell sheets were not sutured to the corneal surface and was fixed in place with a bandage contact lens, providing a suture less therapy for corneal surface reconstruction and reducing tedious surgical interventions on cornea. This was previously reported in rabbit models using oral mucosal cell sheets (Nishida et al., 2004). Over a period of one month, transplanted cell sheets integrated well to the corneal stroma, survived the wound environment for a period of 30 days, and became more transparent and achieved smoother and clear appearance resembling normal corneal epithelium. The transplanted models showed significant reduction in neo vascularization in comparison with the sham control. Reduction in vascularization is one symptom of recovering corneal surface integrity and was observed in 3 of the transplanted models. In one of the models partial reduction in vascularization was observed, but has recurring vascularization in the peripheral corneal region. Sub conjunctival injection of MSCs has demonstrated accelerated

corneal epithelial recovery by inhibiting neovascularization in a corneal alkali burn rat model (Yao et al., 2012).

Histology of cell sheet treated animals showed multi-layer of viable cells which were well oriented, organized and adhering on to the underlying stromal layer. In H&E staining cells demonstrated both coble stone morphology and aligined fibroblastic morphology indicating the presence of differentiated cells *in vivo* witin the transplanted cell sheet. The transplanted cell sheet was transformed into thick pack of live cells with few dead cells towards the periphery. H&E and PAS staining showed almost similar observations. In the sham models, H&E and PAS staining demonstrated goblet cells, indicating conjunctivaization. PAS is a routine stain used to demonstrate mucins within the goblet cells and is reported by various groups (Yang et al., 2008). Sham models showed heavy vascularization and opaque cornea which are hallmarks of corneal surface damage (Thoft et al., 1979). Within a period of one month, the cell sheet had integrated well on to the injured cornea with a well aligned and layered morphology. Cells to the periphery of the cell sheet was showing signs of apoptosis due to the external interference of contact lens and availabity of less nutrients. Over time this sheet is expected to remodel itself and form a corneal epithelial layer. The scoring of cell sheet transplanted models showed success in three models with partial success in one model without any failures.

Earlier works with cell sheets has also reported successful corneal surface reconstruction. Oral mucosal cells are one of the non-ocular cell source widely attempted for corneal surface reconstruction. Oral mucosa cell sheets have been successfully demonstrated in LSCD rabbit models and these cells showed characteristics of corneal epithelium rather than oral mucosal epithelial properties

indicating suitability of these cells for corneal surface reconstruction (Hayashida et al., 2005). Utility of oral mucosal sheets were demonstrated in human patients with a mean follow up of 12 months (Nishida et al., 2004). Cell sheet technology has already been in experimental pipeline for various diseases in the clinical setting. This include cornea, esophagus, heart, periodontal ligament, and cartilage (Matsuura et al., 2014). Transplanted cell sheets, along with replacing the injured tissue, will also compensate for its impaired function. They also harbour and deliver growth factors cytokines in a spatiotemporal manner over long duration time periods which can lead to promotion of tissue repair (Tang et al., 2012).

Apart from the other reported works, here an attempt was made to, establish adipose MSC as an alternative autologous source which can functionally replace limbal stem cells to address the donor tissue scarcity. Being an autologous cell source, ASCs can completely eliminate the complexities of graft rejection. It can also be attributed to the immune modulatory, anti-inflammatory and anti angiogenic properties of ASCs. It averts the risks of allogeneic immunorejection and immunosuppression. These cells were then engineered to form a cell sheet which can enhance the therapeutic effect of transplantation and its efficacy was successfully demonstrated *in viv*o in rabbit models of corneal injury.

It is known that limbal stem cells reside in the basal layer of palisades of Vogt within corneo scleral junction called limbus. During injury or on corneal epithelial regeneration, these stem cells divide or self-renew forming one daughter cell and a transit amplified cell. These transit amplified cells migrate centripetally, become post mitotic cells, finally forming terminally differentiated to corneal epithelial cells. Therefore, the identified Adipose MSCs used in this study having demonstrated the

capacity to differentiate in to corneal epithelial lineage on induction with limbal explant conditioned medium could be a potential cell population for corneal surface regeneration which is normally performed by limbal stem cells. However, an ideal alternative to limbal stem cells has to meet the functional requirements which include (1) Replacement or reconstruction of the corneal epithelial surface and (2) replenishment of the stem cell pool within limbus to ensure long term renewal of corneal epithelium.

In the current study, with regard to replacing/ reconstructing the corneal epithelial surface, the results of the one month rabbit transplant model, indicate that histologically, corneal epithelium like structure was formed in the damaged corneal surface upon cell sheet transplantation. Even though the properties of the reformed epithelial like layer was not explored, it was proven *in vitro* that the transplanted cell sheet exhibited corneal epithelial differentiation potential (indications form IHC and Flow cytometry of CK 3/12 data). However, from the histology it was evident that the cell sheet has well adhered onto the stromal surface and the continuity of the corneal layers were reformed. Moreover, in concern of replenishing the stem cell pool, it has to be noted that the cell sheet generated in vitro harbours both stem cells and cells differentiated to corneal epithelial lineage (FACS data from invitro evaluation of cell sheet for differentiation). It has been reported that transplanted MSCs through their paracrine & cytokine activity show potential in recruiting MSCs (from deep beneath the limbal stroma and circulating MSCs from the bone marrow) as well as in replenishing the host tissue stem cell pool & its associated niche by promoting and recruiting resident stem cells along with transplanted stem cells" (Galindo et al.,2017).

In short, reconstruction of corneal epithelium was a combined effect of the trans differentiated cell population and the properties of MSCs as stem cells, both being present in the cell sheet construct.

CHAPTER - VIII

8. SUMMARY AND CONCLUSION

This study puts forward a carrier free cell sheet transplantation methodology which has not been attempted with ASCs using thermos responsive polymer NGMA. Cell sheet technology using thermo responsive culture surface can provide in vitro carrier free corneal epithelial constructs qualified for transplantation.

- An in house developed thermos responsive polymer NGMA was synthesised characterized for its physico chemical properties, cytocompatibility and thermoresponsive behaviour.
- The base polymer NGMA was modified for bio functionalization with crude Amniotic membrane proteins and was evaluated for AMpro conjugation to the polymer
- Adipose derived Mesenchymal stem cells (ASC) were isolated from rabbit subcutaneous fats pads, characterized for its MSC properties, and evaluated for cell sheet formation on NGMA
- ASCs were differentiated to corneal epithelial lineage to evaluate its efficacy as an alternative to limbal stem cells for corneal epithelial regeneration.
- Trans differentiated ASC sheets were evaluated for their feasibility for cell sheet transfer in *ex vivo* excised rabbit eye models

- Corneal stromal stem cells were isolated from human limbus and was characterized for its MSC properties.
- Cell sheets of human derived corneal stromal stem cells were developed and demonstrated using AM protein bio functionalized NGMA (AMpro-NGMA)
- *In vivo* efficacy of trans differentiated ASC cell sheet were demonstrated in rabbit corneal injury model and evaluated using imaging and histological studies.

In vitro evaluated mesenchymal cell sheet with corneal epithelial differentiation potential was evaluated for its efficacy *in vivo* using a rabbit corneal injury model for a period of one month. Here, corneal epithelial differentiation of adipose tissue derived MSCs was achieved and was stream lined with a technology for ease of use in corneal surface reconstruction. Identifying adipose MSC as an alternate autologous source will address the donor tissue scarcity. Adipose tissue can also serve as an autologous cell source and completely eliminate the complexities of graft rejection.

NGMA was also modified for bio functionalization with amniotic membrane proteins. Simultaneously human corneal stromal cell sheets were developed on AM protein conjugated NGMA. This work attempted to see if growing CSSCs in presence of amniotic membrane proteins on a thermo responsive polymer adds advantage to these cells modifying cell behaviour. Cell sheets of CSSC is demonstrated for the first time on a novel tunable thermo responsive polymer. Corneal stromal cells being a recently identified cell population with mesenchymal properties and epithelial differentiation potential, would be an ideal candidate for

wound surface therapies when developed to a cell sheet, making it in to a ready to use transplantable format. The presence of amniotic membrane proteins is expected to induce even healing and minimize scarring.

Both the cell sheet techniques were developed on the platform NGMA, which is an effective substrate for cell sheet engineering and can also be bio-functionalized by epoxy ring opening mechanism. The use of mesenchymal stem cells for cell sheet technology opens up avenues in the field of tissue engineering and regenerative medicine. Cells as a sheet will enhance the number of cells per damaged area and there by the effect of cell sheet will be much more than cell suspensions or other cell transplantation methods. MSC being an easily available autologous stem cell source, with a proven multi lineage differentiation and extra mesenchymal lineage differentiation beyond plasticity, along with cell sheet technology will prove a more stable system for transplantation studies. This study reports that epithelial like reconstruction of the corneal surface after injury, may be due to the presence of both differentiated and stem cell population within the cell sheet. The combined effect of differentiation along with the paracrine and cytokine signaling potential may have contributed towards successful reconstruction. Since the ECM and the cell surface receptors remain intact while transplantation this will help in survival of the construct in the damaged host micro environment. Achieving corneal epithelial regeneration using MSCs from various sources combined with use of NGMA for cell sheet engineering helps in addressing corneal problems like limbal stem cell deficiency conditions, other corneal surface disorders including cornal burns and chemical induced damages. This will also address the donor shortage for corneal transplantation as in clinical practice, this can be an autologous therapy where MSCs

can be obtained from tissues at various anatomical locations. Mesenchymal stem cells derived Corneal epithelial cell sheets is a novel attempt towards corneal surface reconstruction.

The future perspective of the work include pre-clinical long terms studies of ASC cell sheets in rabbit corneal injury models. Also *in vitro* analysis for corneal epithelial differentiation of ASCs are restricted to a subset of markers, a full panel of differentiation markers including epithelia stem cell marker p63 and corneal epithelial differentiation marker PAX 6 for complete conformation on corneal epithelial differentiation of MSCs. Even though this has been demonstrated using gene expression data, immunohistochemistry was not carried out was not carried out. *In vivo* demonstration was restricted to one month to evaluate the immediate response of the cell sheet in corneal injury models. However long terms results would be beneficiary when looking forwards towards a corneal surface therapy. Cell sheets derived from human adipose tissue would stay closer in terms of practical applications towards addressing corneal injuries in a clinical setting. But the current work would remain a strong proof of concept to take this work to the next stage. Bio functionalizing the NGMA polymer with specific peptides or RGD peptides would give more control over conjugation and will have potential benefits rather than using crude proteins. Guided tissue engineering using thermos responsive polymers may open up new avenues in this field of corneal reconstruction.

Bibliography

1. Agrawal Vinay B, Tsai Ray JF (2003) Corneal epithelial wound healing. *Indian J Ophthalmol* 51: 5–15.
2. Ahmad Sajjad, Stewart Rebecca, Yung Sun, Kolli Sai, Armstrong Lyle, Stojkovic Miodrag, Figueiredo Francisco, Lako Majlinda (2007) Differentiation of human embryonic stem cells into corneal epithelial-like cells by in vitro replication of the corneal epithelial stem cell niche. *Stem Cells* 25: 1145–1155. doi:10.1634/stemcells.2006-0516.
3. Al Arfaj Khalid (2015) Boston keratoprosthesis – Clinical outcomes with wider geographic use and expanding indications – A systematic review. *Saudi Journal of Ophthalmology* 29: 212–221. doi:10.1016/j.sjopt.2015.02.001.
4. Al Arfaj Khalid, Hantera Mohamed (2012) Short-Term Visual Outcomes of Boston Keratoprosthesis Type I in Saudi Arabia. *Middle East African Journal of Ophthalmology* 19: 88–92. doi:10.4103/0974-9233.92121.
5. Alhadlaq Adel, Mao Jeremy J (2004) Mesenchymal stem cells: isolation and therapeutics. *Stem Cells Dev.* 13: 436–448. doi:10.1089/scd.2004.13.436.
6. Anderson DF (2001) Amniotic membrane transplantation for partial limbal stem cell deficiency. *British Journal of Ophthalmology* 85: 567–575. doi:10.1136/bjo.85.5.567.
7. Aoki Takashi, Kawashima Masahiko, Katono Hiroki, Sanui Kohei, Ogata Naoya, Okano Teruo, Sakurai Yasuhisa (1994) Temperature-Responsive Interpenetrating Polymer Networks Constructed with Poly(acrylic acid) and

Poly(N,N-dimethylacrylamide). *Macromolecules* 27: 947–952. doi:10.1021/ma00082a010.

8. Aoyagi T, Ebara M, Sakai K, Sakurai Y, Okano T (2000) Novel bifunctional polymer with reactivity and temperature sensitivity. *J Biomater Sci Polym Ed* 11: 101–110.
9. de Araujo Aline Lütz (2015) Corneal stem cells and tissue engineering: Current advances and future perspectives. *World Journal of Stem Cells* 7: 806. doi:10.4252/wjsc.v7.i5.806.
10. Augustin Mona, Mahar Muhammad Ali Asim, Lakkisto Päivi, Tikkanen Ilkka, Vento Antti, Pätilä Tommi, Harjula Ari (2013) VEGF overexpression improves mesenchymal stem cell sheet transplantation therapy for acute myocardial infarction: VEGF overexpression in stem cell sheet therapy. *Journal of Tissue Engineering and Regenerative Medicine* 7: 742–750. doi:10.1002/term.1471.
11. Bakhtiari Pejman, Djalilian Ali (2010) Update on Limbal Stem Cell Transplantation. *Middle East African Journal of Ophthalmology* 17: 9–14. doi:10.4103/0974-9233.61211.
12. Bessou-Touya S, Picardo M, Maresca V, Surlève-Bazeille JE, Pain C, Taïeb A (1998) Chimeric human epidermal reconstructs to study the role of melanocytes and keratinocytes in pigmentation and photoprotection. *J. Invest. Dermatol.* 111: 1103–1108. doi:10.1046/j.1523-1747.1998.00405.x.
13. Blazejewska Ewa Anna, Schlötzer-Schrehardt Ursula, Zenkel Matthias, Bachmann Björn, Chankiewitz Erik, Jacobi Christina, Kruse Friedrich E (2009) Corneal limbal microenvironment can induce transdifferentiation of hair

follicle stem cells into corneal epithelial-like cells. *Stem Cells* 27: 642–652. doi:10.1634/stemcells.2008-0721.

14. Boulton Mike, Albon Julie (2004) Stem cells in the eye. *Int. J. Biochem. Cell Biol.* 36: 643–657. doi:10.1016/j.biocel.2003.10.013.

15. Bourne Rupert RA, Flaxman Seth R, Braithwaite Tasanee, Cicinelli Maria V, Das Aditi, Jonas Jost B, Keeffe Jill, Kempen John H, Leasher Janet, Limburg Hans, Naidoo Kovin, Pesudovs Konrad, Resnikoff Serge, Silvester Alex, Stevens Gretchen A, Tahhan Nina, Wong Tien Y, Taylor Hugh R, Bourne Rupert, Ackland Peter, Zheng Yingfeng, et al. Magnitude, Temporal Trends, and Projections of the Global Prevalence of Blindness and Distance and Near Vision Impairment: A Systematic Review and Meta-Analysis. *The Lancet Global Health* 5: e888–e897. doi:10.1016/S2214-109X(17)30293-0.

16. Branch Matthew James, Hashmani Khurram, Dhillon Permesh, Jones D Rhodri E, Dua Harminder Singh, Hopkinson Andrew (2012) Mesenchymal stem cells in the human corneal limbal stroma. *Invest. Ophthalmol. Vis. Sci.* 53: 5109–5116. doi:10.1167/iovs.11-8673.

17. Buck RC (1979) Cell migration in repair of mouse corneal epithelium. *Invest. Ophthalmol. Vis. Sci.* 18: 767–784.

18. Buck RC (1985) Measurement of centripetal migration of normal corneal epithelial cells in the mouse. *Invest. Ophthalmol. Vis. Sci.* 26: 1296–1299.

19. Caplan Arnold I, Dennis James E (2006) Mesenchymal stem cells as trophic mediators. *J. Cell. Biochem.* 98: 1076–1084. doi:10.1002/jcb.20886.

20. Chen G, Hoffman AS (1995) Graft copolymers that exhibit temperature-induced phase transitions over a wide range of pH. *Nature* 373: 49–52. doi:10.1038/373049a0.

21. Chen Guangnan, Qi Yiying, Niu Lie, Di Tuoyu, Zhong Jinwei, Fang Tingting, Yan Weiqi (2015) Application of the cell sheet technique in tissue engineering. *Biomedical Reports* 3: 749–757. doi:10.3892/br.2015.522.

22. Chen JJ, Tseng SC (1991) Abnormal corneal epithelial wound healing in partial-thickness removal of limbal epithelium. *Invest. Ophthalmol. Vis. Sci.* 32: 2219–2233.

23. Chen Zhuo, Evans W Howard, Pflugfelder Stephen C, Li De-Quan (2006) Gap junction protein connexin 43 serves as a negative marker for a stem cell-containing population of human limbal epithelial cells. *Stem Cells* 24: 1265–1273. doi:10.1634/stemcells.2005-0363.

24. Choong PF, Mok PL, Cheong SK, Then KY (2007) Mesenchymal stromal cell-like characteristics of corneal keratocytes. *Cytotherapy* 9: 252–258. doi:10.1080/14653240701218508.

25. Coster DJ, Aggarwal RK, Williams KA (1995) Surgical management of ocular surface disorders using conjunctival and stem cell allografts. *The British Journal of Ophthalmology* 79: 977–982.

26. Cotsarelis G, Cheng SZ, Dong G, Sun TT, Lavker RM (1989) Existence of slow-cycling limbal epithelial basal cells that can be preferentially stimulated to proliferate: implications on epithelial stem cells. *Cell* 57: 201–209.

27. Dan YY, Riehle KJ, Lazaro C, Teoh N, Haque J, Campbell JS, Fausto N (2006) Isolation of multipotent progenitor cells from human fetal liver capable

of differentiating into liver and mesenchymal lineages. *Proceedings of the National Academy of Sciences* 103: 9912–9917. doi:10.1073/pnas.0603824103.

28. Daniels JT, Secker GA (2009) Limbal epithelial stem cells of the cornea. *StemBook*. doi:10.3824/stembook.1.48.1. http://www.stembook.org/node/588.

29. Davanger M, Evensen A (1971) Role of the pericorneal papillary structure in renewal of corneal epithelium. *Nature* 229: 560–561.

30. Davis J (1910) Skin transplantation with a review of 550 cases at the Johns Hopkins Hospital. *Johns Hopkins Hospital Report* 15: 307–310.

31. DelMonte Derek W, Kim Terry (2011) Anatomy and physiology of the cornea. *J Cataract Refract Surg* 37: 588–598. doi:10.1016/j.jcrs.2010.12.037.

32. Deng SophieX, Sejpal Kunjal, Bakhtiari Pejman (2013) Presentation, diagnosis and management of limbal stem cell deficiency. *Middle East African Journal of Ophthalmology* 20: 5. doi:10.4103/0974-9233.106381.

33. Dominici M, Le Blanc K, Mueller I, Slaper-Cortenbach I, Marini Fc, Krause Ds, Deans Rj, Keating A, Prockop Dj, Horwitz Em (2006) Minimal criteria for defining multipotent mesenchymal stromal cells. The International Society for Cellular Therapy position statement. *Cytotherapy* 8: 315–317. doi:10.1080/14653240600855905.

34. Du Yiqin, Carlson Eric C, Funderburgh Martha L, Birk David E, Pearlman Eric, Guo Naxin, Kao Winston WY, Funderburgh James L (2009) Stem cell therapy restores transparency to defective murine corneas. *Stem Cells* 27: 1635–1642. doi:10.1002/stem.91.

35. Du Yiqin, Chen Jing, Funderburgh James L, Zhu Xiuan, Li Lingsong (2003) Functional reconstruction of rabbit corneal epithelium by human limbal cells cultured on amniotic membrane. *Molecular vision* 9: 635–643.

36. Dua H (1998) The conjunctiva in corneal epithelial wound healing. *The British Journal of Ophthalmology* 82: 1407–1411.

37. Dua HS (2001) A new classification of ocular surface burns. *British Journal of Ophthalmology* 85: 1379–1383. doi:10.1136/bjo.85.11.1379.

38. Dua HS, Forrester JV (1990) The corneoscleral limbus in human corneal epithelial wound healing. *Am. J. Ophthalmol.* 110: 646–656.

39. Dua HS, Gomes JA, Singh A (1994) Corneal epithelial wound healing. *The British Journal of Ophthalmology* 78: 401–408.

40. Dua HS, Saini JS, Azuara-Blanco A, Gupta P (2000) Limbal stem cell deficiency: concept, aetiology, clinical presentation, diagnosis and management. *Indian J Ophthalmol* 48: 83–92.

41. Dua HS, Shanmuganathan VA, Powell-Richards AO, Tighe PJ, Joseph A (2005) Limbal epithelial crypts: a novel anatomical structure and a putative limbal stem cell niche. *Br J Ophthalmol* 89: 529–532. doi:10.1136/bjo.2004.049742.

42. Dua Harminder S, Miri Ammar, Alomar Thaer, Yeung Aaron M, Said Dalia G (2009) The role of limbal stem cells in corneal epithelial maintenance: testing the dogma. *Ophthalmology* 116: 856–863. doi:10.1016/j.ophtha.2008.12.017.

43. Dzhoyashvili Nina A, Thompson Kerry, Gorelov Alexander V, Rochev Yuri A (2016) Film Thickness Determines Cell Growth and Cell Sheet Detachment

from Spin-Coated Poly(*N* -Isopropylacrylamide) Substrates. *ACS Applied Materials & Interfaces* 8: 27564–27572. doi:10.1021/acsami.6b09711.

44. Ebara Mitsuhiro, Yamato Masayuki, Aoyagi Takao, Kikuchi Akihiko, Sakai Kiyotaka, Okano Teruo (2004) Immobilization of cell-adhesive peptides to temperature-responsive surfaces facilitates both serum-free cell adhesion and noninvasive cell harvest. *Tissue Eng.* 10: 1125–1135. doi:10.1089/ten.2004.10.1125.

45. Ebara Mitsuhiro, Yamato Masayuki, Aoyagi Takao, Kikuchi Akihiko, Sakai Kiyotaka, Okano Teruo (2008) The effect of extensible PEG tethers on shielding between grafted thermo-responsive polymer chains and integrin-RGD binding. *Biomaterials* 29: 3650–3655. doi:10.1016/j.biomaterials.2008.05.030.

46. Ebara Mitsuhiro, Yamato Masayuki, Hirose Motohiro, Aoyagi Takao, Kikuchi Akihiko, Sakai Kiyotaka, Okano Teruo (2003) Copolymerization of 2-carboxyisopropylacrylamide with N-isopropylacrylamide accelerates cell detachment from grafted surfaces by reducing temperature. *Biomacromolecules* 4: 344–349. doi:10.1021/bm025692t.

47. Eberwein P, Reinhard T (2017) Evaluierung neuer Biomaterialien und alternativer Stammzellpopulationen zur Rekonstruktion der Limbusstammzellnische. *Der Ophthalmologe* 114: 318–326. doi:10.1007/s00347-017-0463-5.

48. Ebrahimi Marzieh, Taghi-Abadi Ehsan, Baharvand Hossein (2009a) Limbal Stem Cells in Review. *Journal of Ophthalmic & Vision Research* 4: 40–58.

49. Ebrahimi Marzieh, Taghi-Abadi Ehsan, Baharvand Hossein (2009b) Limbal Stem Cells in Review. *Journal of Ophthalmic & Vision Research* 4: 40–58.

50. Echevarria Timothy Jerome, Di Girolamo Nick (2011) Tissue-regenerating, vision-restoring corneal epithelial stem cells. *Stem Cell Rev* 7: 256–268. doi:10.1007/s12015-010-9199-1.

51. El Najib (2011) Mesenchymal Stem Cells: Immunology and Therapeutic Benefits. In *Stem Cells in Clinic and Research*, ed. Ali Gholamrezanezhad. InTech, August 23. doi:10.5772/21933.

52. Elloumi-Hannachi I, Yamato M, Okano T (2010) Cell sheet engineering: a unique nanotechnology for scaffold-free tissue reconstruction with clinical applications in regenerative medicine: Symposium: Cell sheet technology for regenerative medicine. *Journal of Internal Medicine* 267: 54–70. doi:10.1111/j.1365-2796.2009.02185.x.

53. Espandar Ladan, Carlson Alan N (2013) Lamellar Keratoplasty: A Literature Review. *Journal of Ophthalmology* 2013: 1–8. doi:10.1155/2013/894319.

54. Feil Herman, Bae You Han, Feijen Jan, Kim Sung Wan (1993) Effect of comonomer hydrophilicity and ionization on the lower critical solution temperature of N-isopropylacrylamide copolymers. *Macromolecules* 26: 2496–2500. doi:10.1021/ma00062a016.

55. Flynn Lauren, Woodhouse Kimberly A (2008) Adipose tissue engineering with cells in engineered matrices. *Organogenesis* 4: 228–235.

56. Fujishige Shouei, Kubota K, Ando I (1989) Phase transition of aqueous solutions of poly(N-isopropylacrylamide) and poly(N-

isopropylmethacrylamide). *The Journal of Physical Chemistry* 93: 3311–3313. doi:10.1021/j100345a085.

57. Funderburgh Martha L, Du Yiqin, Mann Mary M, SundarRaj Nirmala, Funderburgh James L (2005) PAX6 expression identifies progenitor cells for corneal keratocytes. *FASEB J.* 19: 1371–1373. doi:10.1096/fj.04-2770fje.

58. Gandhi Arijit, Paul Abhijit, Sen Suma Oommen, Sen Kalyan Kumar (2015) Studies on thermoresponsive polymers: Phase behaviour, drug delivery and biomedical applications. *Asian Journal of Pharmaceutical Sciences* 10: 99–107. doi:10.1016/j.ajps.2014.08.010.

59. Gao F, Chiu SM, Motan DAL, Zhang Z, Chen L, Ji HL, Tse HF, Fu QL, Lian Q (2016) Mesenchymal stem cells and immunomodulation: current status and future prospects. *Cell Death and Disease* 7: e2062. doi:10.1038/cddis.2015.327.

60. Gebbink MF, Zondag GC, Koningstein GM, Feiken E, Wubbolts RW, Moolenaar WH (1995) Cell surface expression of receptor protein tyrosine phosphatase RPTP mu is regulated by cell-cell contact. *J. Cell Biol.* 131: 251–260.

61. Ghezzi Chiara E, Rnjak-Kovacina Jelena, Kaplan David L (2015) Corneal tissue engineering: recent advances and future perspectives. *Tissue Eng Part B Rev* 21: 278–287. doi:10.1089/ten.TEB.2014.0397.

62. Gimble Jeffrey M, Katz Adam J, Bunnell Bruce A (2007) Adipose-derived stem cells for regenerative medicine. *Circ. Res.* 100: 1249–1260. doi:10.1161/01.RES.0000265074.83288.09.

63. Gomes José Alvaro Pereira, Geraldes Monteiro Bábyla, Melo Gustavo Barreto, Smith Ricardo Luiz, Cavenaghi Pereira da Silva Marcelo, Lizier Nelson Foresto, Kerkis Alexandre, Cerruti Humberto, Kerkis Irina (2010) Corneal reconstruction with tissue-engineered cell sheets composed of human immature dental pulp stem cells. *Invest. Ophthalmol. Vis. Sci.* 51: 1408–1414. doi:10.1167/iovs.09-4029.

64. Gomes José Alvaro Pereira, dos Santos Myrna Serapião, Cunha Marcelo Carvalho, Mascaro Vera Lúcia Degaspare, Barros Jeison de Nadai, de Sousa Luciene Barbosa (2003) Amniotic membrane transplantation for partial and total limbal stem cell deficiency secondary to chemical burn. *Ophthalmology* 110: 466–473.

65. Gomillion Cheryl T, Burg Karen JL (2006) Stem cells and adipose tissue engineering. *Biomaterials* 27: 6052–6063. doi:10.1016/j.biomaterials.2006.07.033.

66. Gonzalez-Andrades Miguel, de la Cruz Cardona Juan, Ionescu Ana Maria, Campos Antonio, Del Mar Perez Maria, Alaminos Miguel (2011) Generation of bioengineered corneas with decellularized xenografts and human keratocytes. *Invest. Ophthalmol. Vis. Sci.* 52: 215–222. doi:10.1167/iovs.09-4773.

67. Gruss JS, Jirsch DW (1978) Human amniotic membrane: a versatile wound dressing. *Can Med Assoc J* 118: 1237–1246.

68. Gu Shaofeng, Xing Chengzhong, Han Jingyi, Tso Mark OM, Hong Jing (2009) Differentiation of rabbit bone marrow mesenchymal stem cells into corneal epithelial cells in vivo and ex vivo. *Mol. Vis.* 15: 99–107.

69. Haagdorens Michel, Van Acker Sara Ilse, Van Gerwen Veerle, Ní Dhubhghaill Sorcha, Koppen Carina, Tassignon Marie-José, Zakaria Nadia (2016) Limbal Stem Cell Deficiency: Current Treatment Options and Emerging Therapies. *Stem Cells International* : 1–22. doi:10.1155/2016/9798374.

70. Hashmani Khurram, Branch Matthew James, Sidney Laura Elizabeth, Dhillon Permesh Singh, Verma Megha, McIntosh Owen Douglas, Hopkinson Andrew, Dua Harminder Singh (2013) Characterization of corneal stromal stem cells with the potential for epithelial transdifferentiation. *Stem Cell Res Ther* 4: 75. doi:10.1186/scrt226.

71. Hatou Shin, Yoshida Satoru, Higa Kazunari, Miyashita Hideyuki, Inagaki Emi, Okano Hideyuki, Tsubota Kazuo, Shimmura Shigeto (2013) Functional corneal endothelium derived from corneal stroma stem cells of neural crest origin by retinoic acid and Wnt/β-catenin signaling. *Stem Cells Dev.* 22: 828–839. doi:10.1089/scd.2012.0286.

72. Hayashida Yasutaka, Nishida Kohji, Yamato Masayuki, Watanabe Katsuhiko, Maeda Naoyuki, Watanabe Hitoshi, Kikuchi Akihiko, Okano Teruo, Tano Yasuo (2005) Ocular Surface Reconstruction Using Autologous Rabbit Oral Mucosal Epithelial Sheets Fabricated Ex Vivo on a Temperature-Responsive Culture Surface. *Investigative Opthalmology & Visual Science* 46: 1632. doi:10.1167/iovs.04-0813.

73. Hazra Sarbani, Nandi Sudip, Naskar Deboki, Guha Rajdeep, Chowdhury Sushovan, Pradhan Nirparaj, Kundu Subhas C, Konar Aditya (2016) Non-mulberry Silk Fibroin Biomaterial for Corneal Regeneration. *Scientific Reports* 6. doi:10.1038/srep21840. http://www.nature.com/articles/srep21840.

74. Hima Bindu A, Srilatha B (2011) Potency of Various Types of Stem Cells and their Transplantation. *Journal of Stem Cell Research & Therapy* 01. doi:10.4172/2157-7633.1000115. https://www.omicsonline.org/potency-of-various-types-of-stem-cells-and-their-transplantation-2157-7633.1000115.php?aid=3527.

75. Hocking Anne M, Gibran Nicole S (2010) Mesenchymal stem cells: paracrine signaling and differentiation during cutaneous wound repair. *Exp. Cell Res.* 316: 2213–2219. doi:10.1016/j.yexcr.2010.05.009.

76. Hoffmann F, Schweichel JU (1972) The Microvilli Structure of the Corneal Epithelium of the Rabbit in Relation to Cell Function. *Ophthalmic Research* 4: 175–184. doi:10.1159/000265970.

77. Holden BA, Mertz GW (1984) Critical oxygen levels to avoid corneal edema for daily and extended wear contact lenses. *Invest. Ophthalmol. Vis. Sci.* 25: 1161–1167.

78. Homma Ryusuke, Yoshikawa Hideshi, Takeno Mitsuhiro, Kurokawa Manae S, Masuda Chieko, Takada Erika, Tsubota Kazuo, Ueno Satoki, Suzuki Noboru (2004) Induction of epithelial progenitors in vitro from mouse embryonic stem cells and application for reconstruction of damaged cornea in mice. *Invest. Ophthalmol. Vis. Sci.* 45: 4320–4326. doi:10.1167/iovs.04-0044.

79. Hopkinson Andrew, McIntosh Richard S, Layfield Robert, Keyte John, Dua Harminder S, Tighe Paddy J (2005) Optimised two-dimensional electrophoresis procedures for the protein characterisation of structural tissues. *PROTEOMICS* 5: 1967–1979. doi:10.1002/pmic.200401073.

80. Hopkinson Andrew, Shanmuganathan Vijay A, Gray Trevor, Yeung Aaron M, Lowe James, James David K, Dua Harminder S (2008) Optimization of Amniotic Membrane (AM) Denuding for Tissue Engineering. *Tissue Engineering Part C: Methods* 14: 371–381. doi:10.1089/ten.tec.2008.0315.

81. Huang Xin, Li Mei, Green David C, Williams David S, Patil Avinash J, Mann Stephen (2013) Interfacial assembly of protein–polymer nano-conjugates into stimulus-responsive biomimetic protocells. *Nature Communications* 4. doi:10.1038/ncomms3239. http://www.nature.com/doifinder/10.1038/ncomms3239.

82. Iwata Takanori, Yamato Masayuki, Washio Kaoru, Ando Tomohiro, Okano Teruo, Ishikawa Isao (2015) Cell Sheets for Periodontal Tissue Engineering. *Current Oral Health Reports* 2: 252–256. doi:10.1007/s40496-015-0063-x.

83. Jester JV, Moller-Pedersen T, Huang J, Sax CM, Kays WT, Cavangh HD, Petroll WM, Piatigorsky J (1999) The cellular basis of corneal transparency: evidence for "corneal crystallins." *J. Cell. Sci.* 112 (Pt 5): 613–622.

84. Jiang Ting-Shuai, Cai Li, Ji Wei-Ying, Hui Yan-Nian, Wang Yu-Sheng, Hu Dan, Zhu Jie (2010) Reconstruction of the corneal epithelium with induced marrow mesenchymal stem cells in rats. *Mol. Vis.* 16: 1304–1316.

85. Kang Sung Keun, Shin Il Seob, Ko Myung Soon, Jo Jung Youn, Ra Jeong Chan (2012) Journey of Mesenchymal Stem Cells for Homing: Strategies to Enhance Efficacy and Safety of Stem Cell Therapy. *Stem Cells International* 2012: 1–11. doi:10.1155/2012/342968.

86. Karring Henrik, Thøgersen Ida B, Klintworth Gordon K, Enghild Jan J, Møller-Pedersen Torben (2004) Proteomic analysis of the soluble fraction from

human corneal fibroblasts with reference to ocular transparency. *Mol. Cell Proteomics* 3: 660–674. doi:10.1074/mcp.M400016-MCP200.

87. Kaye DB (1980) Epithelial response in penetrating keratoplasty. *Am. J. Ophthalmol.* 89: 381–387.

88. Kenyon KR, Tseng SC (1989) Limbal autograft transplantation for ocular surface disorders. *Ophthalmology* 96: 709-722; discussion 722-723.

89. Kikuchi Tetsutaro, Shimizu Tatsuya, Wada Masanori, Yamato Masayuki, Okano Teruo (2014) Automatic fabrication of 3-dimensional tissues using cell sheet manipulator technique. *Biomaterials* 35: 2428–2435. doi:10.1016/j.biomaterials.2013.12.014.

90. Kim Hee Jung, Park Jeong-Soo (2017) Usage of Human Mesenchymal Stem Cells in Cell-based Therapy: Advantages and Disadvantages. *Development & Reproduction* 21: 1–10. doi:10.12717/DR.2017.21.1.001.

91. Kim Nayoun, Cho Seok-Goo (2013) Clinical applications of mesenchymal stem cells. *The Korean Journal of Internal Medicine* 28: 387. doi:10.3904/kjim.2013.28.4.387.

92. Kim Soon Hee, Ha Hyun Jung, Ko Youn Kyung, Yoon Sun Jung, Rhee John M, Kim Moon Suk, Lee Hai Bang, Khang Gilson (2007) Correlation of proliferation, morphology and biological responses of fibroblasts on LDPE with different surface wettability. *J Biomater Sci Polym Ed* 18: 609–622. doi:10.1163/156856207780852514.

93. Kinoshita S, Friend J, Thoft RA (1981) Sex chromatin of donor corneal epithelium in rabbits. *Investigative Ophthalmology & Visual Science* 21: 434–441.

94. Kirby Giles TS, Mills Stuart J, Cowin Allison J, Smith Louise E (2015) Stem Cells for Cutaneous Wound Healing. *BioMed Research International* 2015: 1–11. doi:10.1155/2015/285869.

95. Klenkler Bettina, Sheardown Heather (2004) Growth factors in the anterior segment: role in tissue maintenance, wound healing and ocular pathology. *Exp. Eye Res.* 79: 677–688. doi:10.1016/j.exer.2004.07.008.

96. Klyce SD (1972) Electrical profiles in the corneal epithelium. *J. Physiol. (Lond.)* 226: 407–429.

97. Koizumi N, Fullwood NJ, Bairaktaris G, Inatomi T, Kinoshita S, Quantock AJ (2000) Cultivation of corneal epithelial cells on intact and denuded human amniotic membrane. *Invest. Ophthalmol. Vis. Sci.* 41: 2506–2513.

98. Koob Thomas J, Rennert Robert, Zabek Nicole, Massee Michelle, Lim Jeremy J, Temenoff Johnna S, Li William W, Gurtner Geoffrey (2013) Biological properties of dehydrated human amnion/chorion composite graft: implications for chronic wound healing: Biological properties of dehydrated human amnion/chorion grafts. *International Wound Journal* 10: 493–500. doi:10.1111/iwj.12140.

99. Krishna A Shanti, Radhakumary C, Sreenivasan K (2015) Calcium ion modulates protein release from chitosan-hyaluronic acid poly electrolyte gel. *Polymer Engineering & Science* 55: 2089–2097. doi:10.1002/pen.24050.

100. Kruse FE (1994) Stem cells and corneal epithelial regeneration. *Eye (Lond)* 8 (Pt 2): 170–183. doi:10.1038/eye.1994.42.

101. Kulkarni Bina B, Tighe Patrick J, Mohammed Imran, Yeung Aaron M, Powe Desmond G, Hopkinson Andrew, Shanmuganathan Vijay A, Dua Harminder S

(2010) Comparative transcriptional profiling of the limbal epithelial crypt demonstrates its putative stem cell niche characteristics. *BMC Genomics* 11: 526. doi:10.1186/1471-2164-11-526.

102. Kureshi Alvena K, Dziasko Marc, Funderburgh James L, Daniels Julie T (2015) Human corneal stromal stem cells support limbal epithelial cells cultured on RAFT tissue equivalents. *Scientific Reports* 5. doi:10.1038/srep16186. http://www.nature.com/articles/srep16186.
103. Kuwabara T, Perkins DG, Cogan DG (1976) Sliding of the epithelium in experimental corneal wounds. *Invest Ophthalmol* 15: 4–14.
104. Langer R, Vacanti JP (1993) Tissue engineering. *Science* 260: 920–926.
105. Lavker RM, Dong G, Cheng SZ, Kudoh K, Cotsarelis G, Sun TT (1991) Relative proliferative rates of limbal and corneal epithelia. Implications of corneal epithelial migration, circadian rhythm, and suprabasally located DNA-synthesizing keratinocytes. *Invest. Ophthalmol. Vis. Sci.* 32: 1864–1875.
106. Law Sujata, Chaudhuri Samaresh (2013) Mesenchymal stem cell and regenerative medicine: regeneration versus immunomodulatory challenges. *American Journal of Stem Cells* 2: 22–38.
107. Lemp MA, Mathers WD (1989) Corneal epithelial cell movement in humans. *Eye* 3: 438–445. doi:10.1038/eye.1989.65.
108. Li Bin, Zheng Yun-Wen, Sano Yuuki, Taniguchi Hideki (2011) Evidence for mesenchymal-epithelial transition associated with mouse hepatic stem cell differentiation. *PLoS ONE* 6: e17092. doi:10.1371/journal.pone.0017092.

109. Li Fei, Zhao Shao-Zhen (2014) Mesenchymal stem cells: Potential role in corneal wound repair and transplantation. *World J Stem Cells* 6: 296–304. doi:10.4252/wjsc.v6.i3.296.

110. Li W, Chen YT, Hayashida Y, Blanco G, Kheirkah A, He H, Chen SY, Liu CY, Tseng SCG (2008) Down-regulation of Pax6 is associated with abnormal differentiation of corneal epithelial cells in severe ocular surface diseases. *J. Pathol.* 214: 114–122. doi:10.1002/path.2256.

111. Li Wei, Hayashida Yasutaka, Chen Ying-Ting, Tseng Scheffer CG (2007) Niche regulation of corneal epithelial stem cells at the limbus. *Cell Research* 17: 26–36. doi:10.1038/sj.cr.7310137.

112. Liang L, Sheha H, Li J, Tseng SCG (2009) Limbal stem cell transplantation: new progresses and challenges. *Eye* 23: 1946–1953. doi:10.1038/eye.2008.379.

113. Lin Sin-Daw, Wang Kai-Hung, Kao An-Pei (2008) Engineered adipose tissue of predefined shape and dimensions from human adipose-derived mesenchymal stem cells. *Tissue Eng Part A* 14: 571–581. doi:10.1089/tea.2007.0192.

114. Long Teng, Zhu Zhenan, Awad Hani A, Schwarz Edward M, Hilton Matthew J, Dong Yufeng (2014) The effect of mesenchymal stem cell sheets on structural allograft healing of critical sized femoral defects in mice. *Biomaterials* 35: 2752–2759. doi:10.1016/j.biomaterials.2013.12.039.

115. Ma Yanling, Xu Yongsheng, Xiao Zhifeng, Yang Wei, Zhang Chun, Song E, Du Yiqin, Li Lingsong (2006) Reconstruction of chemically burned rat corneal surface by bone marrow-derived human mesenchymal stem cells. *Stem Cells* 24: 315–321. doi:10.1634/stemcells.2005-0046.

116. Majo François, Rochat Ariane, Nicolas Michael, Jaoudé Georges Abou, Barrandon Yann (2008) Oligopotent stem cells are distributed throughout the mammalian ocular surface. *Nature* 456: 250–254. doi:10.1038/nature07406.

117. Makhaeva Elena E, Tenhu Heikki, Khokhlov Alexei R (1998) Conformational Changes of Poly(vinylcaprolactam) Macromolecules and Their Complexes with Ionic Surfactants in Aqueous Solution. *Macromolecules* 31: 6112–6118. doi:10.1021/ma980158s.

118. Malhotra Chintan, Jain Arun K (2014) Human amniotic membrane transplantation: Different modalities of its use in ophthalmology. *World Journal of Transplantation* 4: 111. doi:10.5500/wjt.v4.i2.111.

119. Manning CN, Schwartz AG, Liu W, Xie J, Havlioglu N, Sakiyama-Elbert SE, Silva MJ, Xia Y, Gelberman RH, Thomopoulos S (2013) Controlled delivery of mesenchymal stem cells and growth factors using a nanofiber scaffold for tendon repair. *Acta Biomater* 9: 6905–6914. doi:10.1016/j.actbio.2013.02.008.

120. Marniemi J, Parkki MG (1975) Radiochemical assay of glutathione S-epoxide transferase and its enhancement by phenobarbital in rat liver in vivo. *Biochem. Pharmacol.* 24: 1569–1572.

121. Mathews Saumi, Prasad Tilak, Venugopal Balu, Palakkan Anwar Azad, PR Anil Kumar, TV Kumary (2017) Standardizing transdifferentiation of rabbit bone marrow mesenchymal stem cells to corneal lineage by simulating corneo-limbal cues. *J Stem Cell Res Med*. doi:DOI: 10.15761/JSCRM.1000119.

122. Matsuura Katsuhisa, Utoh Rie, Nagase Kenichi, Okano Teruo (2014) Cell sheet approach for tissue engineering and regenerative medicine. *J Control Release* 190: 228–239. doi:10.1016/j.jconrel.2014.05.024.

123. Meek Keith M, Knupp Carlo (2015) Corneal structure and transparency. *Progress in Retinal and Eye Research* 49: 1–16. doi:10.1016/j.preteyeres.2015.07.001.

124. Miyagawa Shigeru, Domae Keitaro, Yoshikawa Yasushi, Fukushima Satsuki, Nakamura Teruya, Saito Atsuhiro, Sakata Yasushi, Hamada Seiki, Toda Koichi, Pak Kyongsun, Takeuchi Masahiro, Sawa Yoshiki (2017) Phase I Clinical Trial of Autologous Stem Cell–Sheet Transplantation Therapy for Treating Cardiomyopathy. *Journal of the American Heart Association* 6: e003918. doi:10.1161/JAHA.116.003918.

125. Morita Maresuke, Fujita Naoki, Takahashi Ayaka, Nam Eun Ryel, Yui Sho, Chung Cheng Shu, Kawahara Naoya, Lin Hsing Yi, Tsuzuki Keiko, Nakagawa Takayuki, Nishimura Ryohei (2015) Evaluation of ABCG2 and p63 expression in canine cornea and cultivated corneal epithelial cells. *Vet Ophthalmol* 18: 59–68. doi:10.1111/vop.12147.

126. Mukhopadhyay Mahua, Gorivodsky Marat, Shtrom Svetlana, Grinberg Alexander, Niehrs Christoph, Morasso Maria I, Westphal Heiner (2006) Dkk2 plays an essential role in the corneal fate of the ocular surface epithelium. *Development* 133: 2149–2154. doi:10.1242/dev.02381.

127. Narita Takuya, Shintani Yasunori, Ikebe Chiho, Kaneko Masahiro, Campbell Niall G, Coppen Steven R, Uppal Rakesh, Sawa Yoshiki, Yashiro Kenta, Suzuki Ken (2013) The use of scaffold-free cell sheet technique to refine mesenchymal stromal cell-based therapy for heart failure. *Mol. Ther.* 21: 860–867. doi:10.1038/mt.2013.9.

128. Nishida Kohji, Yamato Masayuki, Hayashida Yasutaka, Watanabe Katsuhiko, Yamamoto Kazuaki, Adachi Eijiro, Nagai Shigeru, Kikuchi Akihiko, Maeda Naoyuki, Watanabe Hitoshi, Okano Teruo, Tano Yasuo (2004) Corneal reconstruction with tissue-engineered cell sheets composed of autologous oral mucosal epithelium. *N. Engl. J. Med.* 351: 1187–1196. doi:10.1056/NEJMoa040455.

129. Nishiwaki-Dantas MC, Dantas PE, Reggi JR (2001) Ipsilateral limbal translocation for treatment of partial limbal deficiency secondary to ocular alkali burn. *Br J Ophthalmol* 85: 1031–1033.

130. Nithya Joseph, Kumar PR Anil, Tilak Prasad, Leena Joseph, Sreenivasan K, Kumary TV (2011) Intelligent thermoresponsive substrate from modified overhead projection sheet as a tool for construction and support of cell sheets in vitro. *Tissue Eng Part C Methods* 17: 181–191. doi:10.1089/ten.TEC.2009.0783.

131. Nithya Joseph, Tilak Prasad, Vidya Raj, P.R. Anil Kumar, K. Sreenivasan, T.V. Kumary (2010) A Cytocompatible Poly(N-isopropylacrylamide-co-glycidylmethacrylate) Coated Surface as New Substrate for Corneal Tissue Engineering. *Journal of Bioactive and Compatible Polymers* 25: 58–74. doi:10.1177/0883911509353481.

132. Nuschke Austin (2014) Activity of mesenchymal stem cells in therapies for chronic skin wound healing. *Organogenesis* 10: 29–37. doi:10.4161/org.27405.

133. O'Brien Fergal J (2011) Biomaterials & scaffolds for tissue engineering. *Materials Today* 14: 88–95. doi:10.1016/S1369-7021(11)70058-X.

134. Omoto Masahiro, Miyashita Hideyuki, Shimmura Shigeto, Higa Kazunari, Kawakita Tetsuya, Yoshida Satoru, McGrogan Michael, Shimazaki Jun, Tsubota Kazuo (2009) The use of human mesenchymal stem cell-derived feeder cells for the cultivation of transplantable epithelial sheets. *Invest. Ophthalmol. Vis. Sci.* 50: 2109–2115. doi:10.1167/iovs.08-2262.

135. Omran Eman, Hieneedy Hossam, Halwagy Ahmed, Al-Inany Hesham, Al-Ansary Mirvat, Gad Amr (2016) Amniotic membrane can be a valid source for wound healing. *International Journal of Women's Health* Volume 8: 225–231. doi:10.2147/IJWH.S96636.

136. Ordonez Paula, Di Girolamo Nick (2012) Limbal Epithelial Stem Cells: Role of the Niche Microenvironment. *STEM CELLS* 30: 100–107. doi:10.1002/stem.794.

137. de Paiva Cintia S, Chen Zhuo, Corrales Rosa M, Pflugfelder Stephen C, Li De-Quan (2005) ABCG2 Transporter Identifies a Population of Clonogenic Human Limbal Epithelial Cells. *Stem Cells* 23: 63–73. doi:10.1634/stemcells.2004-0093.

138. Pajoohesh-Ganji Ahdeah, Stepp Mary Ann (2005) In search of markers for the stem cells of the corneal epithelium. *Biol. Cell* 97: 265–276. doi:10.1042/BC20040114.

139. Park Chae Woon, Kim Keun-Soo, Bae Sohyun, Son Hye Kyeong, Myung Pyung-Keun, Hong Hyo Jeong, Kim Hoeon (2009) Cytokine Secretion Profiling of Human Mesenchymal Stem Cells by Antibody Array. *International Journal of Stem Cells* 2: 59–68.

140. Patel Nikul G, Zhang Ge (2013) Responsive systems for cell sheet detachment. *Organogenesis* 9: 93–100. doi:10.4161/org.25149.

141. Pellegrini G, Dellambra E, Golisano O, Martinelli E, Fantozzi I, Bondanza S, Ponzin D, McKeon F, De Luca M (2001) p63 identifies keratinocyte stem cells. *Proc. Natl. Acad. Sci. U.S.A.* 98: 3156–3161. doi:10.1073/pnas.061032098.

142. Pellegrini G, Golisano O, Paterna P, Lambiase A, Bonini S, Rama P, De Luca M (1999) Location and clonal analysis of stem cells and their differentiated progeny in the human ocular surface. *J. Cell Biol.* 145: 769–782.

143. Pellegrini G, Traverso CE, Franzi AT, Zingirian M, Cancedda R, De Luca M (1997) Long-term restoration of damaged corneal surfaces with autologous cultivated corneal epithelium. *Lancet* 349: 990–993. doi:10.1016/S0140-6736(96)11188-0.

144. Poleshko AG, Volotovski ID (2016) [The Role of ABCG2 Protein in Maintenance of Viability and Proliferative Activity of Bone Marrow Mesenchymal Stem Cells Under Hypoxic Conditions]. *Biofizika* 61: 321–327.

145. Polisetty Naresh, Fatima Anees, Madhira Soundarya Lakshmi, Sangwan Virender Singh, Vemuganti Geeta K (2008) Mesenchymal cells from limbal stroma of human eye. *Mol. Vis.* 14: 431–442.

146. Price Francis W, Price Marianne O (2005) Descemet's stripping with endothelial keratoplasty in 50 eyes: a refractive neutral corneal transplant. *J Refract Surg* 21: 339–345.

147. Puangsricharern V, Tseng SC (1995) Cytologic evidence of corneal diseases with limbal stem cell deficiency. *Ophthalmology* 102: 1476–1485.

148. Rahman I, Said DG, Maharajan VS, Dua HS (2009) Amniotic membrane in ophthalmology: indications and limitations. *Eye* 23: 1954–1961. doi:10.1038/eye.2008.410.

149. Rameshwar Pranela (2009) Microenvironment at tissue injury, a key focus for efficient stem cell therapy: A discussion of mesenchymal stem cells. *World J Stem Cells* 1: 3–7. doi:10.4252/wjsc.v1.i1.3.

150. Rathi VarshaM, Sangwan VirenderS, Vyas SharadiniP (2012) Phototherapeutic keratectomy. *Indian Journal of Ophthalmology* 60: 5. doi:10.4103/0301-4738.91335.

151. Reinshagen Helga, Auw-Haedrich Claudia, Sorg Ruediger V, Boehringer Daniel, Eberwein Philipp, Schwartzkopff Johannes, Sundmacher Rainer, Reinhard Thomas (2011) Corneal surface reconstruction using adult mesenchymal stem cells in experimental limbal stem cell deficiency in rabbits. *Acta Ophthalmol* 89: 741–748. doi:10.1111/j.1755-3768.2009.01812.x.

152. Rohaina Che Man, Then Kong Yong, Ng Angela Min Hwei, Wan Abdul Halim Wan Haslina, Zahidin Aida Zairani Mohd, Saim Aminuddin, Idrus Ruszymah BH (2014) Reconstruction of limbal stem cell deficient corneal surface with induced human bone marrow mesenchymal stem cells on amniotic membrane. *Transl Res* 163: 200–210. doi:10.1016/j.trsl.2013.11.004.

153. Roper-Hall MJ (1965) Thermal and chemical burns. *Trans Ophthalmol Soc U K* 85: 631–653.

154. de ROTTH A (1940) PLASTIC REPAIR OF CONJUNCTIVAL DEFECTS WITH FETAL MEMBRANES. *Archives of Ophthalmology* 23: 522–525. doi:10.1001/archopht.1940.00860130586006.

155. Rueda Juan, Zschoche Stefan, Komber Hartmut, Schmaljohann Dirk, Voit Brigitte (2005) Synthesis and Characterization of Thermoresponsive Graft Copolymers of NIPAAm and 2-Alkyl-2-oxazolines by the "Grafting from" Method. *Macromolecules* 38: 7330–7336. doi:10.1021/ma050570p.

156. Saghizadeh Mehrnoosh, Winkler Michael A, Kramerov Andrei A, Hemmati David M, Ghiam Chantelle A, Dimitrijevich Slobodan D, Sareen Dhruv, Ornelas Loren, Ghiasi Homayon, Brunken William J, Maguen Ezra, Rabinowitz Yaron S, Svendsen Clive N, Jirsova Katerina, Ljubimov Alexander V (2013) A Simple Alkaline Method for Decellularizing Human Amniotic Membrane for Cell Culture. Ed. Deepak Shukla. *PLoS ONE* 8: e79632. doi:10.1371/journal.pone.0079632.

157. Saichanma Sarawut, Bunyaratvej Ahnond, Sila-asna Monnipha (2012) In vitro transdifferentiation of corneal epithelial-like cells from human skin-derived precursor cells. *International Journal of Ophthalmology* 5: 158–163. doi:10.3980/j.issn.2222-3959.2012.02.08.

158. Sangwan VS, Basu S, MacNeil S, Balasubramanian D (2012) Simple limbal epithelial transplantation (SLET): a novel surgical technique for the treatment of unilateral limbal stem cell deficiency. Br J Ophthalmol 5;96(7):931-4. doi: 10.1136/bjophthalmol-2011-301164.

159. Sangwan Virender S, Matalia Himanshu P, Vemuganti Geeta K, Rao Gullapalli N (2004) Amniotic membrane transplantation for reconstruction of corneal epithelial surface in cases of partial limbal stem cell deficiency. *Indian J Ophthalmol* 52: 281–285.

160. Schermer A, Galvin S, Sun TT (1986) Differentiation-related expression of a major 64K corneal keratin in vivo and in culture suggests limbal location of corneal epithelial stem cells. *J. Cell Biol.* 103: 49–62.

161. Schild HG (1992) Poly(N-isopropylacrylamide): experiment, theory and application. *Progress in Polymer Science* 17: 163–249. doi:10.1016/0079-6700(92)90023-R.

162. Sehic Amer, Utheim Øygunn, Ommundsen Kristoffer, Utheim Tor (2015) Pre-Clinical Cell-Based Therapy for Limbal Stem Cell Deficiency. *Journal of Functional Biomaterials* 6: 863–888. doi:10.3390/jfb6030863.

163. Shapiro MS, Friend J, Thoft RA (1981) Corneal re-epithelialization from the conjunctiva. *Invest. Ophthalmol. Vis. Sci.* 21: 135–142.

164. Sharma A, Coles WH (1989) Kinetics of corneal epithelial maintenance and graft loss. A population balance model. *Invest. Ophthalmol. Vis. Sci.* 30: 1962–1971.

165. Shimizu Kazunori, Fujita Hideaki, Nagamori Eiji (2010) Oxygen plasma-treated thermoresponsive polymer surfaces for cell sheet engineering. *Biotechnol. Bioeng.* 106: 303–310. doi:10.1002/bit.22677.

166. Shimizu Kazunori, Ito Akira, Yoshida Tatsuro, Yamada Yoichi, Ueda Minoru, Honda Hiroyuki (2007) Bone tissue engineering with human mesenchymal stem cell sheets constructed using magnetite nanoparticles and magnetic force. *J. Biomed. Mater. Res. Part B Appl. Biomater.* 82: 471–480. doi:10.1002/jbm.b.30752.

167. Shortt Alex J, Secker Genevieve A, Munro Peter M, Khaw Peng T, Tuft Stephen J, Daniels Julie T (2007) Characterization of the limbal epithelial stem

cell niche: novel imaging techniques permit in vivo observation and targeted biopsy of limbal epithelial stem cells. *Stem Cells* 25: 1402–1409. doi:10.1634/stemcells.2006-0580.

168. Sidney Laura E, Branch Matthew J, Dua Harminder S, Hopkinson Andrew (2015) Effect of culture medium on propagation and phenotype of corneal stroma-derived stem cells. *Cytotherapy* 17: 1706–1722. doi:10.1016/j.jcyt.2015.08.003.
169. da Silva Ricardo MP, Mano João F, Reis Rui L (2007) Smart thermoresponsive coatings and surfaces for tissue engineering: switching cell-material boundaries. *Trends Biotechnol.* 25: 577–583.doi:10.1016/j.tibtech.2007.08.014.
170. Sitalakshmi G, Sudha B, Madhavan HN, Vinay S, Krishnakumar S, Mori Yuichi, Yoshioka Hiroshi, Abraham Samuel (2009) Ex vivo cultivation of corneal limbal epithelial cells in a thermoreversible polymer (Mebiol Gel) and their transplantation in rabbits: an animal model. *Tissue Eng Part A* 15: 407–415. doi:10.1089/ten.tea.2008.0041.
171. Skeens Heather M, Brooks Brian P, Holland Edward J (2011) Congenital aniridia variant: minimally abnormal irides with severe limbal stem cell deficiency. *Ophthalmology* 118: 1260–1264. doi:10.1016/j.ophtha.2010.11.021.
172. Solomon Abraham, Ellies Pierre, Anderson David F, Touhami Amel, Grueterich Martin, Espana Edgar M, Ti Seng-Ei, Goto Eiki, Feuer William J, Tseng Scheffer CG (2002) Long-term outcome of keratolimbal allograft with or without penetrating keratoplasty for total limbal stem cell deficiency. *Ophthalmology* 109: 1159–1166.

173. Sottile V, Jackson L, Jones Dr, Scotting P (2007) Adult mesenchymal stem cells: Differentiation potential and therapeutic applications. *Journal of Postgraduate Medicine* 53: 121. doi:10.4103/0022-3859.32215.

174. Stile RA, Healy KE (2001) Thermo-responsive peptide-modified hydrogels for tissue regeneration. *Biomacromolecules* 2: 185–194.

175. Stile Ranee A, Healy Kevin E (2002) Poly(N-isopropylacrylamide)-based semi-interpenetrating polymer networks for tissue engineering applications. 1. Effects of linear poly(acrylic acid) chains on phase behavior. *Biomacromolecules* 3: 591–600.

176. Sueblinvong Viranuj, Loi Roberto, Eisenhauer Philip L, Bernstein Ira M, Suratt Benjamin T, Spees Jeffrey L, Weiss Daniel J (2008) Derivation of lung epithelium from human cord blood-derived mesenchymal stem cells. *Am. J. Respir. Crit. Care Med.* 177: 701–711. doi:10.1164/rccm.200706-859OC.

177. Sun Tung-Tien, Lavker Robert M (2004) Corneal Epithelial Stem Cells: Past, Present, and Future. *Journal of Investigative Dermatology Symposium Proceedings* 9: 202–207. doi:10.1111/j.1087-0024.2004.09311.x.

178. Sun Yubing, Chen Christopher S, Fu Jianping (2012) Forcing stem cells to behave: a biophysical perspective of the cellular microenvironment. *Annu Rev Biophys* 41: 519–542. doi:10.1146/annurev-biophys-042910-155306.

179. Sweeney DF, Xie RZ, O'Leary DJ, Vannas A, Odell R, Schindhelm K, Cheng HY, Steele JG, Holden BA (1998) Nutritional requirements of the corneal epithelium and anterior stroma: clinical findings. *Invest. Ophthalmol. Vis. Sci.* 39: 284–291.

180. Taghiabadi Ehsan, Nasri Sima, Shafieyan Saeed, Firoozinezhad Sasan Jalili, Aghdami Nasser (2017) Fabrication and Characterization of Spongy Denuded Amniotic Membrane Based Scaffold for Tissue Engineering. *Cell J (Yakhteh)*. doi:10.22074/cellj.2015.493. http://celljournal.org/journal/article/abstract/493.

181. Tan DT, Ficker LA, Buckley RJ (1996) Limbal transplantation. *Ophthalmology* 103: 29–36.

182. Tan Donald TH, Dart John KG, Holland Edward J, Kinoshita Shigeru (2012) Corneal transplantation. *The Lancet* 379: 1749–1761. doi:10.1016/S0140-6736(12)60437-1.

183. Tang Z, Okano T (2014) Recent development of temperature-responsive surfaces and their application for cell sheet engineering. *Regenerative Biomaterials* 1: 91–102. doi:10.1093/rb/rbu011.

184. Tang Zhonglan, Akiyama Yoshikatsu, Okano Teruo (2012) Temperature-Responsive Polymer Modified Surface for Cell Sheet Engineering. *Polymers* 4: 1478–1498. doi:10.3390/polym4031478.

185. Terry MA (2000) The evolution of lamellar grafting techniques over twenty-five years. *Cornea* 19: 611–616.

186. Thoft RA, Friend J (1983) The X, Y, Z hypothesis of corneal epithelial maintenance. *Invest. Ophthalmol. Vis. Sci.* 24: 1442–1443.

187. Thoft RA, Friend J, Murphy HS (1979) Ocular surface epithelium and corneal vascularization in rabbits. I. The role of wounding. *Invest. Ophthalmol. Vis. Sci.* 18: 85–92.

188. Tseng SC (1989) Concept and application of limbal stem cells. *Eye (Lond)* 3 (Pt 2): 141–157. doi:10.1038/eye.1989.22.

189. Tseng SC (1996) Regulation and clinical implications of corneal epithelial stem cells. *Mol. Biol. Rep.* 23: 47–58.

190. Tseng SC (2001) Amniotic membrane transplantation for ocular surface reconstruction. *Biosci. Rep.* 21: 481–489.

191. Tseng Scheffer CG (1998) Amniotic Membrane Transplantation With or Without Limbal Allografts for Corneal Surface Reconstruction in Patients With Limbal Stem Cell Deficiency. *Archives of Ophthalmology* 116: 431. doi:10.1001/archopht.116.4.431.

192. Tsubota K, Satake Y, Ohyama M, Toda I, Takano Y, Ono M, Shinozaki N, Shimazaki J (1996) Surgical reconstruction of the ocular surface in advanced ocular cicatricial pemphigoid and Stevens-Johnson syndrome. *Am. J. Ophthalmol.* 122: 38–52.

193. Twaites Beverley R, de Las Heras Alarcón Carolina, Lavigne Matthieu, Saulnier Annabelle, Pennadam Sivanand S, Cunliffe David, Górecki Dariusz C, Alexander Cameron (2005) Thermoresponsive polymers as gene delivery vectors: cell viability, DNA transport and transfection studies. *J Control Release* 108: 472–483. doi:10.1016/j.jconrel.2005.08.009.

194. Utheim Tor Paaske, Utheim Øygunn Aass, Khan Qalb-E Saleem, Sehic Amer (2016) Culture of Oral Mucosal Epithelial Cells for the Purpose of Treating Limbal Stem Cell Deficiency. *J Funct Biomater* 7. doi:10.3390/jfb7010005.

195. Varghese Viji Mary, Raj Vidya, Sreenivasan K, Kumary TV (2010) In vitro cytocompatibility evaluation of a thermoresponsive NIPAAm-MMA copolymeric surface using L929 cells. *J Mater Sci Mater Med* 21: 1631–1639. doi:10.1007/s10856-010-3992-x.

196. Vashist Praveen, Gupta Noopur, Tandon Radhika, Gupta SanjeevK, Sreenivas V (2013) Burden of corneal blindness in India. *Indian Journal of Community Medicine* 38: 198. doi:10.4103/0970-0218.120153.

197. Venugopal Balu, Fernandez Francis B, Babu Suresh S, Harikrishnan VS, Varma Harikrishna, John Annie (2012) Adipogenesis on biphasic calcium phosphate using rat adipose-derived mesenchymal stem cells: In vitro and in vivo. *Journal of Biomedical Materials Research Part A* 100A: 1427–1437. doi:10.1002/jbm.a.34082.

198. Wang Shihua, Qu Xuebin, Zhao Robert (2012) Clinical applications of mesenchymal stem cells. *Journal of Hematology & Oncology* 5: 19. doi:10.1186/1756-8722-5-19.

199. Waring George O, Bourne William M, Edelhauser Henry F, Kenyon Kenneth R (1982) The Corneal Endothelium. *Ophthalmology* 89: 531–590. doi:10.1016/S0161-6420(82)34746-6.

200. Wei Xin, Yang Xue, Han Zhi-peng, Qu Fang-fang, Shao Li, Shi Yu-fang (2013) Mesenchymal stem cells: a new trend for cell therapy. *Acta Pharmacologica Sinica* 34: 747–754. doi:10.1038/aps.2013.50.

201. Wiesmann UN, DiDonato S, Herschkowitz NN (1975) Effect of chloroquine on cultured fibroblasts: release of lysosomal hydrolases and inhibition of their uptake. *Biochem. Biophys. Res. Commun.* 66: 1338–1343.

202. Wong Victor W, Gurtner Geoffrey C (2012) Tissue engineering for the management of chronic wounds: current concepts and future perspectives. *Exp. Dermatol.* 21: 729–734. doi:10.1111/j.1600-0625.2012.01542.x.

203. Yamato Masayuki, Okano Teruo (2004) Cell sheet engineering. *Materials Today* 7: 42–47. doi:10.1016/S1369-7021(04)00234-2.

204. Yang Xueyi, Moldovan Nicanor I, Zhao Qingmei, Mi Shengli, Zhou Zhenhui, Chen Dan, Gao Zhimin, Tong Dewen, Dou Zhongying (2008) Reconstruction of damaged cornea by autologous transplantation of epidermal adult stem cells. *Molecular Vision* 14: 1064–1070.

205. Yao Lin, Li Zhan-rong, Su Wen-ru, Li Yong-ping, Lin Miao-li, Zhang Wen-xin, Liu Yi, Wan Qian, Liang Dan (2012) Role of Mesenchymal Stem Cells on Cornea Wound Healing Induced by Acute Alkali Burn. Ed. Arto Urtti. *PLoS ONE* 7: e30842. doi:10.1371/journal.pone.0030842.

206. Yazdanpanah Ghasem, Jabbehdari Sayena, Djalilian Ali R (2017) Limbal and corneal epithelial homeostasis. *Curr Opin Ophthalmol* 28: 348–354. doi:10.1097/ICU.0000000000000378.

207. Yeung Sonia N, Lichtinger Alejandro, Kim Peter, Amiran Maoz D, Rootman David S (2012) Retrospective contralateral study comparing deep anterior lamellar keratoplasty with penetrating keratoplasty: a patient's perspective. *Canadian Journal of Ophthalmology / Journal Canadien d'Ophtalmologie* 47: 360–364. doi:10.1016/j.jcjo.2012.04.002.

208. Yoon Jinny J (2014) Limbal stem cells: Central concepts of corneal epithelial homeostasis. *World Journal of Stem Cells* 6: 391. doi:10.4252/wjsc.v6.i4.391.

209. Yoshida Satoru, Shimmura Shigeto, Nagoshi Narihito, Fukuda Keiichi, Matsuzaki Yumi, Okano Hideyuki, Tsubota Kazuo (2006) Isolation of Multipotent Neural Crest-Derived Stem Cells from the Adult Mouse Cornea. *Stem Cells* 24: 2714–2722. doi:10.1634/stemcells.2006-0156.

210. Zhang Canwei, Du Liqun, Pang Kunpeng, Wu Xinyi (2017) Differentiation of human embryonic stem cells into corneal epithelial progenitor cells under defined conditions. Ed. Wei Li. *PLOS ONE* 12: e0183303. doi:10.1371/journal.pone.0183303.

211. Zhang Lianfeng, Bewick Mary, Lafrenie Robert M (2002) Role of Raf-1 and FAK in cell density-dependent regulation of integrin-dependent activation of MAP kinase. *Carcinogenesis* 23: 1251–1258.

212. Zhang Liying, Zou Dulei, Li Sanming, Wang Junqi, Qu Yangluowa, Ou Shangkun, Jia Changkai, Li Juan, He Hui, Liu Tingting, Yang Jie, Chen Yongxiong, Liu Zuguo, Li Wei (2016a) An Ultra-thin Amniotic Membrane as Carrier in Corneal Epithelium Tissue-Engineering. *Scientific Reports* 6. doi:10.1038/srep21021. http://www.nature.com/articles/srep21021.

213. Zhang Liyun, Coulson-Thomas Vivien Jane, Ferreira Tarsis Gesteira, Kao Winston WY (2015) Mesenchymal stem cells for treating ocular surface diseases. *BMC Ophthalmology* 15. doi:10.1186/s12886-015-0138-4. http://bmcophthalmol.biomedcentral.com/articles/10.1186/s12886-015-0138-4.

214. Zhang Yuan, Sun Hong, Liu Yongsong, Chen Shuangling, Cai Subo, Zhu Yingting, Guo Ping (2016b) The Limbal Epithelial Progenitors in the Limbal Niche Environment. *International Journal of Medical Sciences* 13: 835–840. doi:10.7150/ijms.16563.

215. Zuk Patricia A, Zhu Min, Ashjian Peter, De Ugarte Daniel A, Huang Jerry I, Mizuno Hiroshi, Alfonso Zeni C, Fraser John K, Benhaim Prosper, Hedrick Marc H (2002) Human adipose tissue is a source of multipotent stem cells. *Mol. Biol. Cell* 13: 4279–4295. doi:10.1091/mbc.E02-02-0105.